CAGE - Centre for Arctic Gas Hydrate Environment and Climate Report Series, Volume 9 (2021)

To be cited as: Bünz, S. et al., 2021. AKMA-AKER-GReAT. In: CAGE - Centre for Arctic Gas Hydrate Environment and Climate Report Series, Volume 9 (2021).
DOI: https://doi.org/10.7557/cage.6677
Additional info at: https://septentrio.uit.no/index.php/cage/database

ISSN: 2703-9625
Publisher: Septentrio Academic Publishing Tromsø Norway

UiT The Arctic University of Norway

R/V Kronprins Håkon
22-05-21 to 09-06-21
Longyearbyen – Tromsø

CAGE-21-1 Cruise Report

AKMA-AKER-GReaT

Co-Chief scientist: Stefan Bünz & Giuliana Panieri
Capt. R/V: Johnny Peder Hansen
Report prepared by: Stefan Bünz & Giuliana Panieri
With contributions by cruise participants

DOI:

Keywords:

Methane, Arctic, Gas hydrate, Methane seepage, Biogeochemical processes, Education, Outreach, Seafloor imaging

Front image:

RV Kronprins Håkon in front of Prins Karls Foreland.

Contents

1. PARTICIPANT LIST

Leg 1 (22-30.05.2021)

Stefan Bünz	CAGE, UiT	Chief Scientist
Giuliana Panieri	CAGE, UiT	Co-Chief Scientist, PI AKMA, Micropaleontology
Sunil Vadakkepuliyambatta	CAGE, UiT	Acoustics, survey planning, data management
Dimitri Kalenitchenko	CAGE, UiT	Microbiology
Francesca Vulcano	UiB	Microbiology
Kate Waghorn	CAGE, UiT	Heat flow, Coring
Claudio Argentino	CAGE, UiT	Pore water geochemistry, coring
Stormer Alexander Jensen	CAGE, UiT	Engineer, Coring, Heat Flow, Tow Cam
Matteus Lindgren	CAGE, UiT	Pore water geochemistry, coring
Alessandra Savini	UniMiB	ROV imaging
Christine Lockwood-Ireland	CAGE, UiT	GReAT student
Marie Stetzler	CAGE, UiT	GReAT student
Griselda Ortiz	CAGE, UiT	GReAT student
Maximillian Weber	IG, UiT	GReAT student
Cornelia Mentzoni Binde	CAGE, UiT	GReAT student
Sig Vågenes	NORMAR, UiB	ROV Operations
Jörn Patrick Meyer	IMR	ROV Operations
William Skjold	IMR	ROV Operations

Leg 2 (30.05-09.06.2021)

Stefan Bünz	CAGE, UiT	Chief Scientist
Giuliana Panieri	CAGE, UiT	Co-Chief Scientist, PI AKMA, Micropaleontology
Sunil Vadakkepuliyambatta	CAGE, UiT	Acoustics, survey planning, data management
Claudio Argentino	CAGE, UiT	Pore water geochemistry, coring
Matteus Lindgren	CAGE, UiT	Pore water geochemistry, coring
Kate Waghorn	CAGE, UiT	Heat flow, Coring
Stormer Alexander Jensen	CAGE, UiT	Engineer, Coring, Heat Flow, Tow Cam
Renate Paulsen	IG, UiT	GReAT student
Andreas H. Hagset	IG, UiT	GReAT student
Carmen Braun	IG, UiT	GReAT student
Przemyslaw Domel	CAGE, UiT	GReAT student
Julian Janocha	IG, UiT	GReAT student
Marie Bulinova	IG, UiT	GReAT student
Sofia Ramalho	UAveiro	Marine Ecology
Luca Fallati	UniMiB	Mapping, photomosaicking
Sig Vågenes	NORMAR, UiB	ROV Operations
Jörn Patrick Meyer	IMR	ROV Operations
William Skjold	IMR	ROV Operations

CAGE: Centre for Arctic Gas Hydrate, Environment and Climate
UiT: Arctic University of Norway
UiB: University of Bergen, Norway
UniMiB: University of Milan--Bicocca
UoA: University of Aveiro, Portugal
NORMAR, UiB: Norwegian Marine Robotics Facility, University of Bergen
IMR: Institute of Marine Research

Leg 1 group photo in front of the Ægir 6000 ROV.

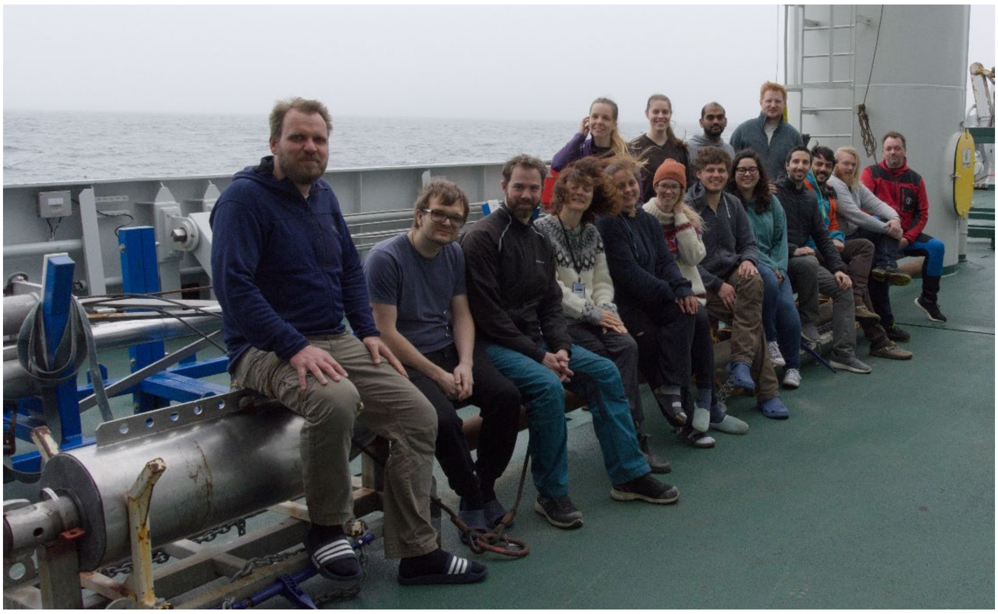
Leg 2 group photo sitting on the gravity corer.

2. INTRODUCTION AND OBJECTIVES

The research expedition cruise CAGE21-1 is a major component of the project AKMA and it is organized under the helm of the Norwegian Centre of Excellence for Arctic Gas Hydrate, Environment and Climate, CAGE at UiT The Arctic University of Norway in Tromsø. CAGE investigates Arctic gas hydrate and methane seepage systems to better understand the effects they may have on our oceans, ecosystems and global climate.

The CAGE21-1 cruise is fully supported through externally funded projects:

- AKMA - Advancing Knowledge of Methane in the Arctic (NFR INTPART programme)
- "The subsurface plumbing system" is a research project funded by Aker BP Norge

INTPART-AKMA is a collaborative project including scientists from UiT - The Arctic University of Norway in Tromsø and Woods Hole Oceanographic Institution (WHOI) in USA. Its aim is to advance collective knowledge about methane activity in the seabed, on the seafloor and in the ocean in Arctic regions. The Arctic regions are particularly vulnerable to the effects of climate changes, and methane is a highly effective climate changing gas when it reaches the atmosphere. Students from Norwegian and American institutions will have the opportunity to attend ship-based expeditions, attend courses and partake in exchanges with AKMA.

The project "The subsurface plumbing system" is a research project funded by Aker BP Norge with focus on the Leirdjupet Fault Complex in the SW Barents Sea. The main aim of the research project is a better understanding of the fluid flow system (sources, traps, seals and pathways) and the origin of the gas that is actively seeping into the water column at the Leirdjupet Fault Complex on the western flank of the Fingerdjupet Basin.

The CAGE21-1 cruise targets several methane seepage systems from shallow shelf environments to the deep sea, on the Svalbard continental and the Barents Sea margins (Figure 1

- Prins Karls Foreland (Superstation 1)
- Vestnesa Ridge (Superstation 2)
- Svyatogor Ridge (Superstation 4)
- Leirdjupet Fault Complex (Superstation 5)
- Håkon Mosby Mud Volcano (Superstation 6)

The main instrument used during this cruise is the Ægir 6000 ROV, a remotely operated vehicle from the Norwegian Marine Robotics Facility, University of Bergen. The overall goal of cruise CAGE21-1 therefore is to utilize the ROV in order to provide guided video imagery and to study methane seepage systems. Scientific problems that are to be addressed in the key target areas include the structure, seafloor expression and geological setting of gas seepage features, the quantification of methane concentrations in surface sediments and water column above, the occurrence of gas hydrates, benthic and microbial community studies, analyses of gas and pore water geochemistry and the periodicity and duration of gas seepage. In addition to sampling work from the ROV, we carried out sediment coring, heat flow and oceanographic (CTD, water sampling) studies and acoustic mapping (multi and single beam) from the ship.

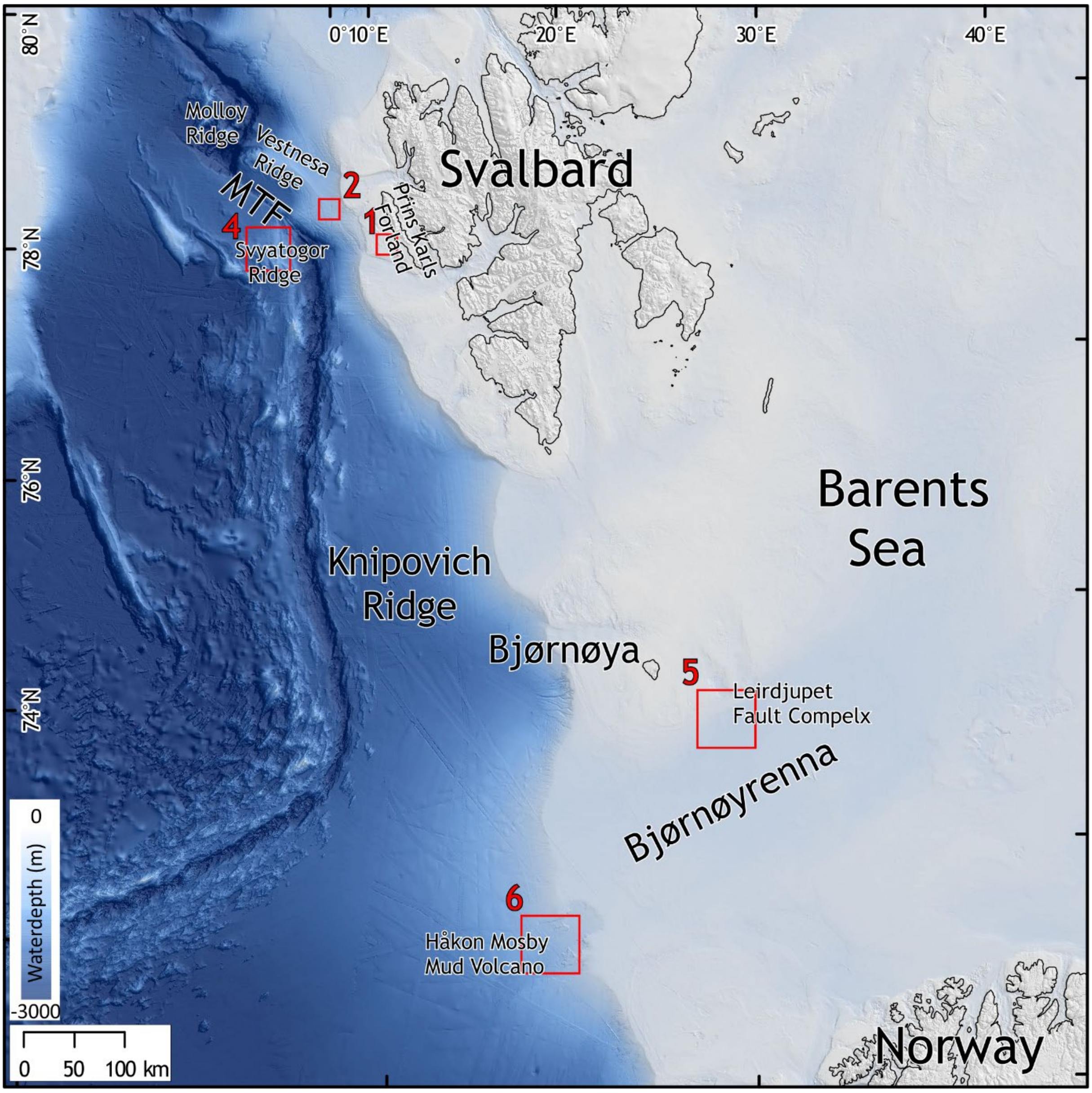

Figure 1: Overview map of the different working areas, named in the report "Superstations" (red number indicates the Superstations number).

3. GEOLOGICAL SETTING OF THE WORKING AREAS

3.1 PRINS KARLS FORELAND (SUPERSTATION 1)

Prins Karls Foreland is a small and elongated island on the western flank of the Svalbard archipelago. The island and its western submersed bank areas belongs to the West Spitsbergen fold-and-thrust belt, a system of complex horst and graben structures, which are comprised of a late-Tertiary wedge of sediments. It formed along the transform plate boundary between Greenland and the western Barents Sea during Paleocene-Eocene breakup in the northern North Atlantic. The Hornsund fault zone forms the western termination of the fold and thrust belt. This fault zone runs along the whole western Svalbard margin and has been associated with numerous active gas seepage areas. One of CAGE's major study sites is located just west of Prins Karls Foreland in 80-100 m water depth. Intense gas flaring has been observed over multiple years. More recently, satellite images revealed the presence of oil slicks on the sea surface at this location.

3.2 WEST-SVALBARD CONTINENTAL SLOPE, VESTNESA RIDGE (SUPERSTATION 2)

The Vestnesa Ridge is a ~100 km long sediment drift developed on <20 Ma oceanic crust on the western continental slope of Svalbard (Engen et al., 2008; Hustoft et al., 2009). It is an elongated ridge, oriented SE-NW in the eastern part and bends E-W towards the western part. It is comprised of contourite, turbidite, and hemipelagic sediments over 2 km thick (Vogt et al., 1994). Situated at water depths of over 1000 m, the Vestnesa Ridge hosts extensive fluid flow and gas hydrate systems (Bünz et al., 2012). Previous surveys by CAGE discovered a fluid flow system on the continental slope of West Svalbard at around 900 m water depth, characterized by a N-S oriented elongated depression at the seafloor (CAGE 15-5 and CAGE16-6 cruise report). Located at the eastern termination of Vestnesa Ridge, it has a length of ~3 km and exhibit subsurface acoustic anomalies piercing the sediment overburden (CAGE 16-6 cruise report). Carbonate crusts and chemosynthetic organisms have been documented during CAGE cruises (Panieri et al., 2017), gas hydrates have been sampled from this depression during CAGE 15-2 and CAGE17-5 cruise, and pore pressure measurements indicate that the fluid flow system in the area is presently active (Sultan et al., 2020).

3.3 SVYATOGOR RIDGE (SUPERSTATION 4)

The Svyatogor Ridge is a sediment drift atop the inside corner high of the Knipovich Ridge – Molloy Transform Fault intersection (RTI). The RTI inside corner high is underlain by a detachment fault accommodating spreading on the Knipovich Ridge. In this area, Johnson et al., 2015 and Waghorn et al., 2018, 2020 hypothesize a contribution from abiotic methane to the gas hydrate system. South of the Svyatogor Ridge is a paleo-transform fault which, during its period of activity, contributed to tectonic deformation of the crust and overlying sedimentary sequences at the southern end of the Svyatogor Ridge (Crane et al., 1991). Areas with exhumed mantle are of interest as the hydration of olivine produces H_2, which may in turn react with CO_2 on a metallic catalytic surface to produce abiotic methane (Etiope and Sherwood-Lollar, 2013). Inside corners of mid-ocean ridge-transform fault intersections are the predominant oceanic setting where abiotic methane is recognized (i.e. Lost City Hydrothermal Field, Mid-Atlantic; Kelley et al., 2005). During CAGE expeditions in 2018, seismic data showed that two ridges southwest of the Svyatogor Ridge had oceanic crust subcropping and one of the ridges had a BSR reflection in the sedimentary sequence above the crust subcrop (Waghorn et al., 2020). During CAGE21-1, we explore these two ridges in order to understand fluid cycling associated with Oceanic Transform Faults.

3.4 LEIRDJUPET FAULT COMPLEX (SUPERSTATION 5)

The Leirdjupet Fault Complex is a Late Jurassic to Early Cretaceous ~N-S striking extensional fault complex separating the Bjørnøya Basin from the Fingerdjupet Sub-Basin, Southwest Barents Sea(Serck et al., 2017). The horst between the Bjørnøya Basin and Fingerdjupet Sub-Basin is called the Ringsel Ridge. Most of the extension here occurred during the Late Jurassic and Early Cretaceous although there has been reactivation of extension through this region of the Barents Sea during the Aptian. Both the Bjørnøya Basin and Fingerdjupet Sub-Basin have Berriasian-Tithonian (Jurassic-Cretaceous boundary) and Barremian (Early Cretaceous) bright anomalies indicating hydrocarbon – likely gas of a thermogenic origin (NPD; Argentino et al., 2021). Faulting and reactivation along the Leirdjupet Fault Complex and subsequent glacial erosion has exposed these sequences subcropping at URU – the regional unconformity marking the level of glacial erosion across the Barents Sea. Associated with both the Leirdjupet Fault Complex and the approximate strike of subcropping hydrocarbon-rich sequences. Prior expeditions in the area have indicated gas seepage in associated with the Ringsel Ridge and following the Leirdjupet Fault Complex/sub-cropping sequences.

3.5 HÅKON MOSBY MUD VOLCANO (SUPERSTATION 6)

The Håkon Mosby Mud Volcano is located within a large slide scar (Bjørnøyrenna Slide; Late Pleistocene; Laberg and Vorren, 1993) at the termination of the Bjørnøyrenna Trough Mouth Fan. The sedimentary sequences in the area are approximately 6 km thick overlying oceanic crust (~35 Ma; Faleide et al., 1996). The root zone of this mud volcano is in Pliocene (~5 Ma) terrigeneous sediments and fluid composition data, along with the presence of gas hydrate and cold seep ecosystem indicate a gas component to the fluid remobilizing sediment here (Milkov et al., 2004; Pape et al., 2011). The Håkon Mosby Mud Volcano is approximately 1.4 km in diameter and covers 1.2 square km, with a ~15 m high relief above the seafloor (Milkov et al., 2004).

4. NARRATIVE OF THE CRUISE

Note: Given times in this narrative are local times. Log sheets are in UTC. ROV Dives are logged and can be found in the respective sections below.

All the education and outreach activities done during the cruise are reported in Chapter 13 "Education and Outreach".

Saturday, 22nd May

Official start of AKMA-AKER-GReAT expedition, scientific party comes on board at 10:00. Mobilization of equipment. Scientific teams set up laboratories. The ROV team from Bergen started to mobilize the ROV already a day ahead. Nonetheless, they will have to use much of Saturday and Sunday to finish mobilization.

Sunday, 23rd May

Continuation of mobilization and preparation of laboratories. We depart from Longyearbyen late in the evening.

Monday, 24th May

Arrival at Prins Karls Foreland working area at 09:00. We immediately spot the oil slick on the surface of the ocean. The working boat is deployed to take wipes at the surface slick, 3 samples are taken. CTD cast at 10:15. ROV Dive 1 commenced at 11:00 for visual survey. We discover several bacterial mats and several places with gas and oil seepage. ROV Dive 2 commenced at 17:00 taking along the gas sampler and sediment sampler. A CTD survey finishes our first visit to this site. Shortly before midnight, we depart to the continental slope north of Knipovich Ridge. Weather is favorable, winds increasing slightly over the day.

Tuesday, 25th May

Arrival at superstation #2 at 07:00, an elongated depression showing ample indications of past and possible still active seepage. Heat flow survey at 04:00. ROV Dive 3 commenced at 09:00 and lasted until 16:00 taking several sediment samples and carbonate rocks. CTD station and box core taken between18:30 and 20:00. Completed heat flow survey in this area with two more stations before departure to Molloy Transform and Svyatogor Ridge.

Wednesday, 26th May

Acquired two more heat flow stations on transit to Svyatogor Ridge. ROV Dive 4 commenced at 09:00 targeting two or three very prominent pockmark structures on the ridge crest. Dive concluded at 11:00 and we continue to slightly further south to aim at potentially outcropping basement structures. Increasing winds, elevated wave heights and occurrences of sea ice make the transit slightly difficult. ROV Dive 5 commenced at 14:30 on a basement structure that may be associated with a suspected paleo transform. The Dive did not find any outcropping basement but discovered a number of areas with bacterial mats and tubeworms on the flank of the basement structure in areas with very little sediment cover. Dive finished at around 19:00. A CTD cast completes the day before a short transit to the Svyatogor ridge crest.

Thursday, 27th May

Two gravity cores are taken during the night. ROV Dive 6 commenced at 08:30 taking sediment sampler along for sampling of the bacterial mats. Dive completed at 15:00. Dive 7 started at 16:00

and finished shortly after 20:00 inspecting another basement high slightly further south. We conducted a heat flow survey across the two basement structures during the night.

Friday, 28th May

The 15th heat flow station finished at 13:00. In the meantime, the ROV is refitted with a camera setup for acquiring a photomosaic at Svyatogor Ridge. ROV Dive 8 started at 15:00 acquiring micro bathymetry and a photomosaic at the basement structure where several patches of bacteria and other microorganisms (mostly tubeworms and gastropods) had been discovered. The Dive finished at 21:00. Two more gravity cores acquired to complete the scientific work on this day.

Saturday, 29th May

Re-did a heat flow station to fill a small gap in the survey of the previous night. Return to the slope north of Knipovich Ridge. ROV Dive 9 commenced at 09:15 to acquire microbathymetry and a photomosaic at the north-eastern corner of the elongated depression. Here, several carbonate mounds and bacterial mats indicate past and active seepage. Then focused shifted to another mound structure in the centre of the depression where cruise CAGE17-5 had recovered significant amounts of gas hydrates in a gravity core. The ROV was again equipped with sampling gear. Dive 10 started at 15:15 and took several carbonate crusts. Attempts to find and sample gas hydrates were unsuccessful. The Dive was finished at 20:00. This completed the work for Leg 1 of this cruise. We headed back to Longyearbyen for a change of scientific personnel on Sunday the 30th.

Sunday, 30th May

Arrival in Longyearbyen early in the morning at 07:30. The first student team and a few of the senior scientists leave the ship and other students and personnel join our expedition. We depart from Longyearbyen again at 22:00.

Monday, 31st May

Arrival at Prins Karls Foreland site at 05:00. We took 4 gravity cores, one of them empty, the other with recovery up to 1 m. ROV Dive 11 at 09:30 acquired a photomosaic along a transect with several gas and oil seepage locations and finished at 11:30. ROV changed to sampling setup and Dive 12 commenced at 12:30 taking several push and blade cores. The Dive is completed at 14:30 and we head out to the superstation 2 on the continental slope north of Knipovich Ridge. We sampled several carbonate crusts, push and blade cores at the small mound structure in the center of the elongated depression. This completes the work on the western Svalbard Margin. With a bad weather front coming in, we make our way southward trying to stay ahead of the weather.

Tuesday, 1st June

On transit to Storfjorden where aimed to pick up an OBS from UiB that was not responding on release command during an earlier cruise in 2020.

Wednesday, 2nd June

Arrival at OBS location in northern part of Storfjorden at 03:00. ROV Dive 14 commenced for the recovery operation at 03:20. The OBS was found after a short search in only 150 m water depth and subsequently successfully recovered by the ROV. We then continue our journey southward towards the Leirdjupet Fault complex in the SW Barents Sea. We took a CTD station in Sørkapp Basin during transit at 19:15.

Thursday, 3rd June

We arrived at Leirdjupet Fault complex at 06:30 and start with CTD. ROV Dive 15 commenced at 08:40 and collected a gas sample and 4 push cores at the southern vent sites. ROV Dive 16 followed up with acquisition of a photomosaic and sampling of two blade cores. For ROV Dive 17 at 18:30 we moved to the northern site, a small depression where we acquired microbathymetry and a quick visual inspection before the Dive finished at 20:00. One gravity core was taken afterwards but weather conditions did not allow other work to be done during the night. So we just ran a multibeam survey to expand bathymetric coverage.

Friday, 4th June

ROV Dive 18 commenced at 08:30 acquiring a photomosaic in a depression, where active gas seepage had been identified. Dive 19 started at 14:40 and acquired several gas samples and carbonate crusts. Attempts to sample sediment were not successful as the subsurface around the seeps was extremely hard, mostly carbonate. The Dive finished at 17:00. Harsh weather conditions persisted throughout the day. However, we were able to complete a CTD survey of 7 stations across the gas seepage site and then further expanded on multibeam coverage.

Saturday, 5th June

ROV Dive 20 commenced at 08:40 and carried a setup of cameras and checkerboard in order to determine bubble size, number of bubbles and bubble rising speed. For Dive 21 we moved back to the southern seep sites and acquired several push cores. The short Dive finished quickly and was followed by Dive 22 that acquired 2 additional blade cores. Work at Leirdjupet Fault complex concluded at 16:00 and we steamed further south to our last working are, the Håkon Mosby mud volcano (HMMV).

Sunday, 6th June

We arrived at HMMV at 09:00 in the morning. ROV Dive 23 commenced at 10:00 and acquired 2 lines of microbathymetry and several sediment samples (push and blade cores) along a transect from SE to NW crossing several different seafloor environments. The Dive finished at 17:15. A multi core, a box core and a CTD were acquired until the end of the day.

Monday, 7th June

During the night we acquired 3 gravity corers with up to 5 m recovery. ROV Dive 24 started at 09:15 and expanded the microbathymetry coverage with additional 2 lines providing almost full coverage of the main crater. Subsequently, we continued the sampling transect with additional sediment samples. Samples were brought up after a short Dive. ROV Dive 25 commenced at 12:00 and sampled two pieces of carbonate crust and 4 additional push cores. The Dive also gave some excellent visual material of the activity of this underwater mud volcano. We took two more gravity cores until the end of the day.

Tuesday, 8th June

Early in the night, we finally tested the new tow-camera setup on the multicorer. For the most part the technology seemed to work well, however, the whole setup of cameras and lighting requires fine-tuning. The last ROV Dive 26 started at 09:00 and acquired a photomosaic over areas with enhanced activity of HMMV. The Dive finished at 13:00. We steam towards Tromsø for the end of the cruise.

Wednesday, 9th June

Arrival in Tromsø at 07:00. End of cruise.

5. SCIENTIFIC EQUIPMENT

5.1 HYDROACOUSTIC SYSTEMS

The hydroacoustic systems onboard RV Kronprins Håkon can be operated simultaneously, where a dedicated software intelligently manages transducer pings to avoid interferences. In-ice operations only allow using acoustic systems that are mounted in the so-called Arctic tank, an ice window in the hull of the ship, where sea ice can slide along without damaging any transducers during ice breaking. However, ice operations make data acquisition more prone to noise.

Among the hydroacoustic systems, the following were used extensively during the CAGE 21-1 cruise:

- Simrad Kongsberg EA 600 – 12kHz single beam echosounder
- Simrad Kongsberg EM 710 multibeam echosounder
- Simrad Kongsberg EM 302 multibeam echosounder and SBP 300 Sub-Bottom Profiler

5.1.1 Simrad Kongsberg EA 600 –12kHz single beam ecosounder

The EA 600 single beam echosounder operates up to four high power transceivers simultaneously. Available frequencies span from 12 to 710 kHz. A variety of highly efficient transducers is available to suit all your operational needs from extreme shallow water to a depth of 11.000 meters. Major applications of this echosounder is to identify the depth and finding high-reflective objects in the water column, e.g. gas bubbles.

5.1.2 Simrad Kongsberg EM 710 multibeam echosounder

The EM710 multibeam echosounder is a high to very high-resolution seabed mapping system which operates at sonar frequencies in the 70-100 kHz range. The system is mounted on the port drop keel of Kronprins Haakon and is particularly suited for swath bathymetry surveys up to 800 m water depth. The system sends out 400 beams at an angle of upto 700 on each side (1400 coverage in total). In order to achieve a high-density of beams the system was used at an angle of 600 on each side. There are options to adjust the beam spacing, either equiangular or equidistant. There is an additional high-density mode to achieve higher sounding density by reducing the acoustic footprint. During the CAGE21-1 cruise, the system was run on high-density equidistant mode. In addition, EM710 also allows recording of water column backscatter data. This is particularly useful in identifying gas bubbles in the water column. New CTD data were acquired at each study area to update the water velocity used by the EM710 system.

5.1.3 Simrad Kongsberg EM 302 multibeam echosounder and SBP 300 Sub-Bottom Profiler

The EM 302 multibeam echo sounder has an operating frequency of 30 kHz and is designed to perform seabed mapping with high resolution and accuracy to a maximum depth of more than 7000 m. Beam focusing is applied both during reception and transmission. EM 302 is equipped with a function to reduce the transmission power in order to avoid hurting mammals if they are close by.

The system has up to 432 soundings per swath with pointing angles automatically adjusted according to achievable coverage or operator defined limits. With dual swath (two swaths per ping) the transmit fan is duplicated and transmitted with a small difference in along-track tilt. The applied tilt takes into account depth, coverage and vessel speed to give a constant sounding separation along track. In dual swath mode, 2 swaths are generated per ping cycle, with up to 864 soundings. The beam spacing is equidistant or equiangular.

The transmit fan is split in several individual sectors with independent active steering. This allows stabilization, which compensates for the vessel movements: yaw, pitch and roll. Each transmit sector has individual beam focusing.

In conjunction with a separate low frequency transmit transducer, the EM 302 may optionally be able to deliver sub-bottom profiling capabilities with a very narrow beamwidth. This system is known as the SBP 300 sub-bottom profiler. During this cruise, the SBP was operated constantly with a chirp pulse of 50 ms and frequency bandwidth of 2.5 – 6.5 kHz.

The EM 302 (including the SBP 300) is mounted in the ice window in the bottom hull of the vessel. During ice breaking, ice sliding beneath and along the ice window significantly affect the acquisition leading to high noise levels and false measurements.

During the cruise, the multibeam bathymetry data was processed and cleaned using QPS Qimera Software. Initial grid surfaces with a resolution of between 10-20 m were produced for the perimeter of the study areas.

5.2 ATTRIBUTED SENSORS

5.2.1 GPS/Navigation, Motion Reference Unit

RV Kronprins Håkon uses a Kongsberg Seapath 330-5 system, an integrated global navigation satellite system (GNSS), using the GPS, GLONASS, Galileo or Beidou signals and inertial measurements to provide high quality results for applications including hydrographic surveying, dredging, oceanographic research, seismic work etc. This Seapath system includes a 5th generation MRU motion sensor package, providing up to 0.008° RMS roll and pitch accuracy. This accuracy is achieved by the use of accurate linear accelometers and unique MEMS type angular rate gyros.

5.2.2 USBL HiPaP

RV Kronprins Håkon is equipped with a HIPAP 501 Acoustic Underwater Positioning and Navigation System. ROV, tow-cam, heat flow probe and partly also coring equipment were outfitted with a HiPaP beacon for exact positioning information on the seafloor. The HiPAP 501 system operates with the transducer mounted on the hull to allow the transducer to be lowered some meters below the hull of the vessel. A transceiver unit containing transmitter, preamplifiers and beam forming electronics is mounted close to the hull unit. The HiPAP 501 system has a spherical transducer with several hundred elements covering the whole sphere under the vessel. The system will dynamically control the beam, so it is always pointing towards the transponder. The transponder may be moving, and roll, pitch and yaw affect the vessel itself. Data from roll/pitch sensors are used to roll and pitch compensate the position.

The Super Short Base Line (SSBL) principle has the obvious advantage that it only requires installation of one hull mounted transducer and one subsea transponder to establish a three-dimensional position of the transponder. An SSBL system is measuring the horizontal and vertical angles together with the range to the transponder. An error in the angle measurement causes the position error to be a function of the range to the transponder. To obtain better position accuracy in deep water with an SSBL system it is necessary to increase the angle measurement accuracy. The frequency band of the HiPaP 501 is 21 - 31 kHz and the operating range is 1 - 5000 m. The range detection accuracy is given as 0.02 m assuming free sight between transducer and transponder, no or very little noise in the water column and no error from heading/roll/pitch sensor. We recognized interference between HiPaP and multibeam EM 302 systems due to usage of similar frequency bands.

For most operations at the seafloor, EM 302 acquisition was stopped, leading to more stable positioning of the USBL transponder.

5.3 CTD

Physical and chemical measurements are measured in the water column from a CTD/rosette. The CTD model is a Seabird SBE 911 plus mounted on a 12 10-liters Niskin bottles carousel. The CTD (conductivity, temperature, depth) sensor records physical (conductivity, temperature, P-wave velocity, pressure for depth calculation) and chemical properties (fluorescence/chlorophyll, O2 concentration, turbidity) vertically through the water column.

5.4 SEDIMENT CORING

5.4.1. Gravity corer

The gravity corer is one of the most useful tools for the collection of marine sediment (Figure 2). The gravity corer consists of a 6m long iron barrel with iron weights attached on top of it. The whole apparatus weighs close to 2 tons. The gravity corer has an inner diameter of 11cm. A plastic liner with outer diameter of 11cm and inner diameter of 10 cm is inserted into the steel barrel. During the coring operation, a core catcher and core cutter is attached to the lower end of the gravity corer. Core catcher keeps the sediments from falling out of the core, whereas core cutter helps the penetration of the core into the sediments.

The gravity corer lies on deck and during operation is lifted vertically with a winch and the gravity corer is lowered to around 20m away from the seabed. When at the chosen core location, the gravity corer is dropped. When the gravity corer is lifted from the seabed and is brought to deck, the core catcher and core cutter are sampled first, if there are sediments present in them. Then, the plastic liner is taken out, cleaned, cut to 1meter sections, and labeled. Cores are then sectioned and eventually sampled for pore water, biogeochemistry, microbiology, methane content, and micropaleontology.

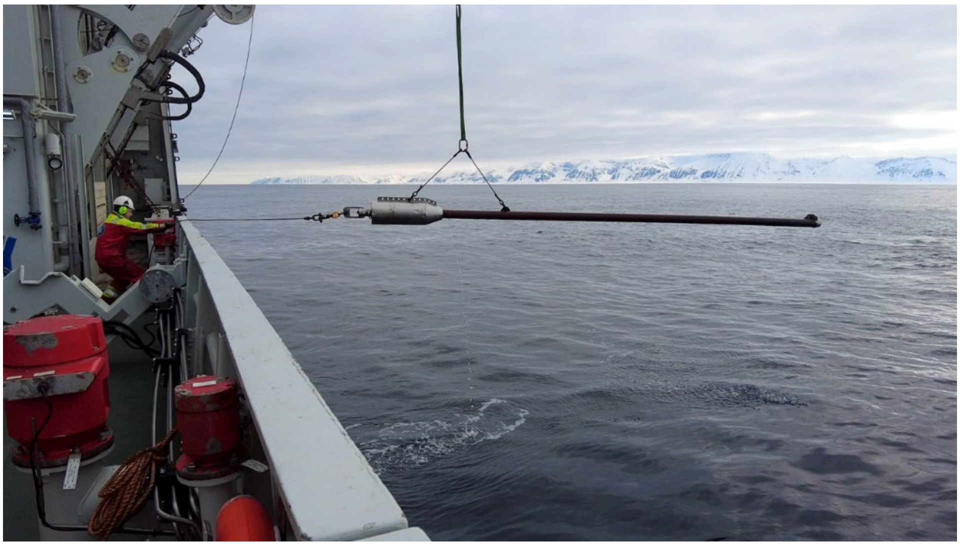

Figure 2: Gravity corer deploying

5.4.2 Box corer

The box corer is a marine geological sampling tool for soft sediment. It consists of a stainless steel sampling box (Figure 3) to contain a surface sediment block. It is deployed from the vessel with a wire and it is suitable for any water depth. It is designed for a minimum of disturbance of the sediment surface by bow wave effects which is important for quantitative investigations of the benthos micro- to macrofauna, geochemical processes, sampling of bottom water or sedimentology. Once the sediment is recovered onboard, the sediment box can be detached from the frame and taken to a laboratory for subsampling and further analysis.

Figure 3: Box corer full of sediment ready to be processed

5.5. HEAT FLOW PROBE

The heat flow probe is used to measure in situ thermal gradients and the thermal conductivity of the sediments. The Fielax Heat Flow Probe FLX-T015SM (Figure 4) consists of 22 thermistors (temperature sensors) distributed along a 6 m sensor string and a heating wire. The sensors are spaced 25 cm apart and is designed for a temperature range of -2 to 60°C, with a resolution of 1 mK and accuracy of 2mK after calibration. The probe weighs ~1100 kg and can penetrate up to 6 m of sediments, in water depths up to 6000 m. The head section of the probe contains a data acquisition and power supply unit.

The data acquisition unit records the data from the sensor string and initiates the heat pulse of the probe. The unit also comprises a high-resolution pressure/temperature sensor (PT100) and can measure the tilt and vertical acceleration of the probe. The configuration of the probe involves definition of stability requirements prior to heat pulse generation, based on pressures recorded by PT100, the tilt and vertical acceleration of the probe. Temperatures recorded by PT100 are used to calibrate the thermistors on the sensor string. The thermal gradients are calculated based on temperatures measured by the thermistors, whereas in situ thermal conductivity is estimated based on temperature decay as a function of time following heat pulse generation. Processing and quality control of the recorded data was done using the Fellow software from Fielax.

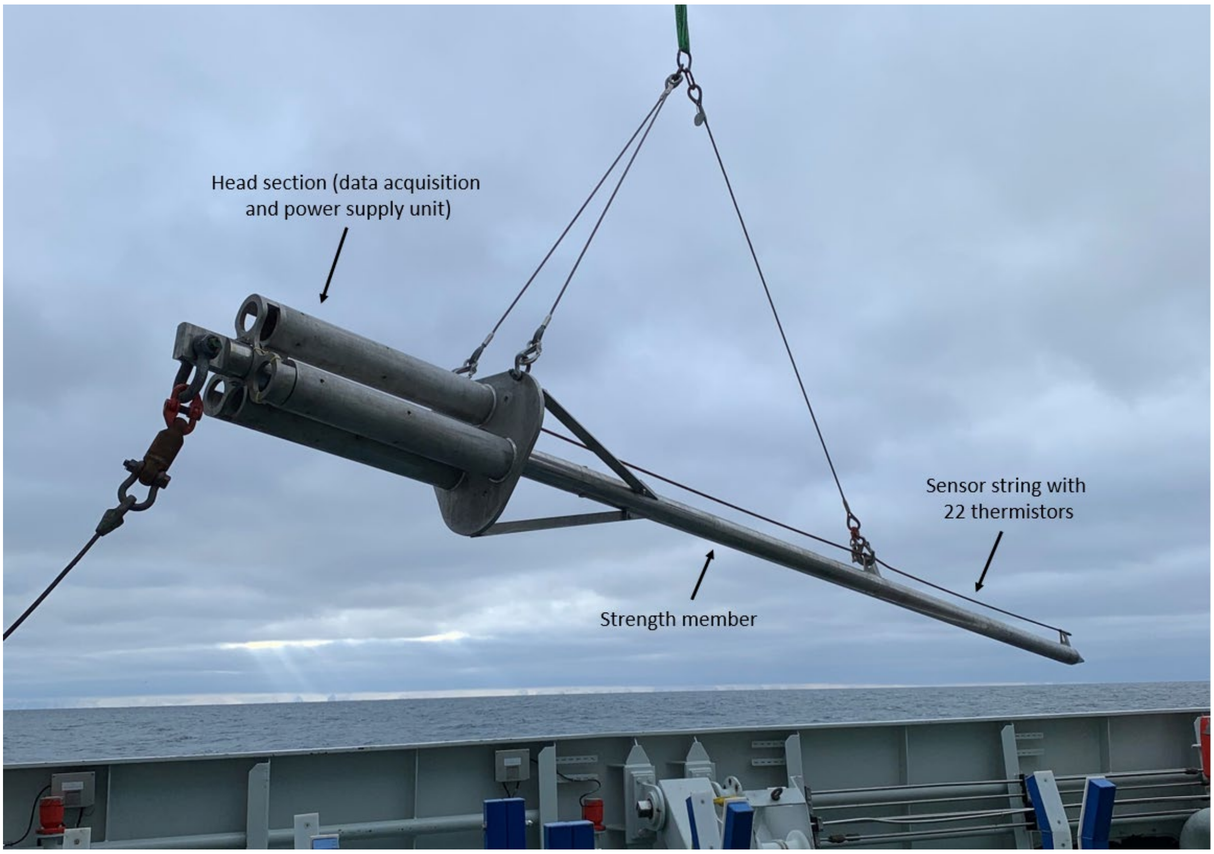

Figure 4 The Fielax heat flow probe being deployed from RV Kronprins Haakon during the CAGE21-1 cruise

5.6 DEEP-TOW CAMERA SYSTEM

The deep-tow camera system is a modification to the CAGE multicorer tool, that allows capture of images and videos from the multicorer during towing entire instrumentation behind the vessel (Figure 5). It consists of a pair of "wings" that are extending out from the front ant the back of multicorer frame and allows for ample space for mounting the cameras, lights and batteries. The system was co-designed with Woods Hole Oceanographic Institute in the U.S.

Batteries are placed in a box and attached to a shelf on the front 'wing' (in a big orange box). Data-link box, providing communication with cameras and lights, is kept in in a black housing on the top of the back 'wing' structure. To improve hydrodynamic shape and positioning during towing, two 130 x 61 cm fins are attached to the sides of the back wing, giving it a better hydrodynamic shape for the towing.

In the front of the system, on the front "wing", live feed camera is mounted pointing at the bottom at 45-degree angle (Figure 6). Two point lights, located on the both sides of it, provide necessary light.

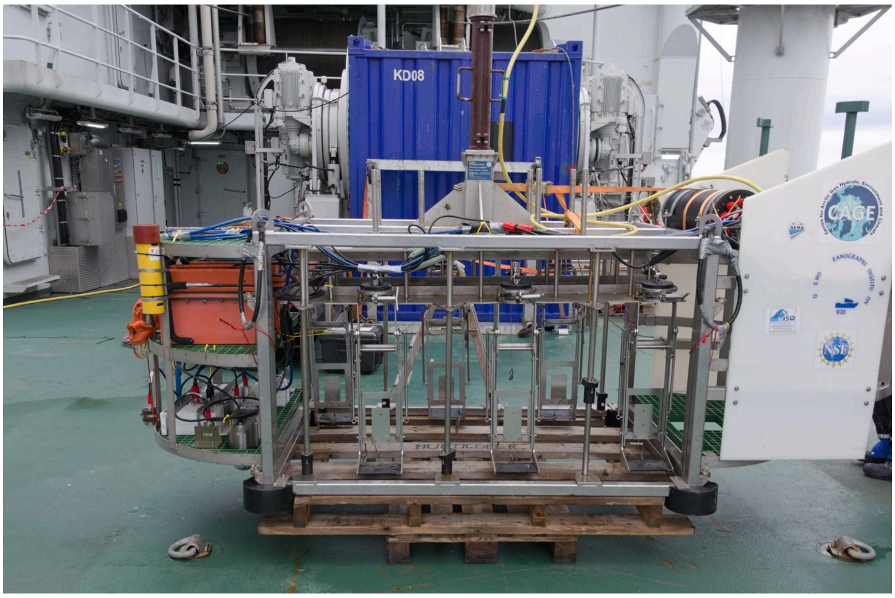

Figure 5: CAGE Deep-tow camera system in preparation for test deployment during CAGE21-1 cruise.

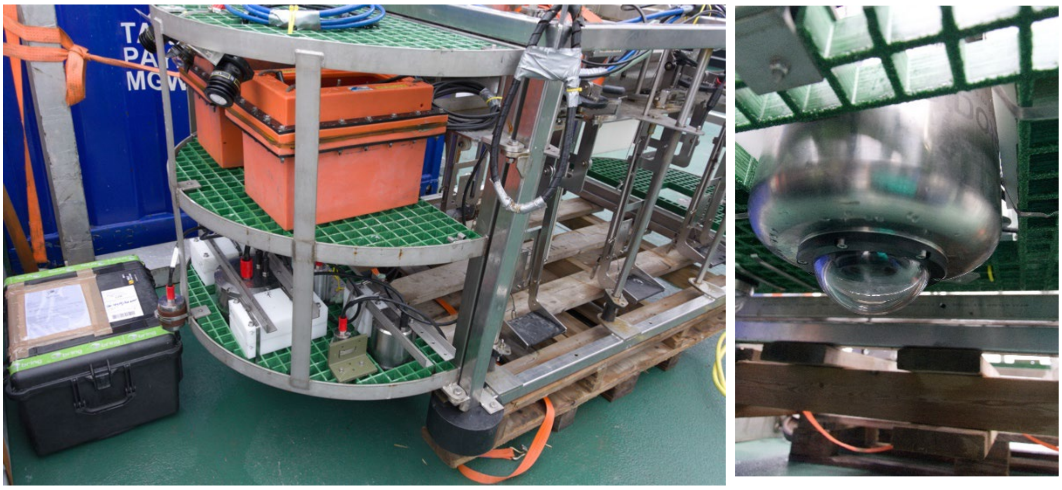

Figure 6: Front of the Deep-tow camera system (on the left), showing front facing camera, bottom facing camera, strobe lights and a battery pack. A detailed view of the pressure housing holding Nikon D810 bottom-facing camera is on the left.

Bottom-facing camera is held in a pressure housing (Figure 6), and it consists of off-the-shelf photo components (Nikon D810). Housing is located in the middle of the front wing structure, pointing directly down. Two green lasers, separated by 20 cm are mounted on left and right side of the bottom-facing camera (one for each side). Strobe lights providing necessary illumination are mounted at the same wing, on both sides of the camera, a little further back. On additional light is mounted in front of the camera, at the leading edge of the entire frame.

All data is transformed in the real time by fiber optic cable that is connected to system from the deck (using a winch). We can control status of the strobe lights, recording mode of the cameras and take photos using bottom-facing camera on command.

5.7 ROV ÆGIR 6000

The ROV ÆGIR6000 is a SUPPORTER 2-type ROV from Kystdesign in Aksdal, Norway (Figure 7). The ROV has a total combined power of 115 Kw, a depth rating of 6000 m and is maneuvered by 7 thrusters. Its dimensions are (LxBxH) 2,75 m x 1,7 m x 1,65 m and it weighs 3600 kg in air. The ROV can carry a payload of 400 kg and has two strong manipulators arms. 8 HD and composite video camera inputs provide full vision of operation and partly have zoom and focus capability. The lighting capacity includes ten dimmable lights and has a maximum total load of 2300W. The SUPPORTER 2 can accommodate up to 24 additional hydraulic tooling functions, up to 21 additional survey sensors and 8 camera connectors. All hydraulic functions are proportionally controlled, and all electrical power supplies are ground fault monitored. The ROV control system offers a variety of auto-functions like AutoPOS and AutoTRACK capabilities. The control pod and telemetry system for survey operations works via up to 6 fibre optic cables. The umbilical able on RV Kronprins Håkon provides 4 fiber optic cables. In addition to the video feed, the system is capable of supporting several additional communication channels both serial and Ethernet.

Figure 7 The ROV Ægir6000 is a Kystdesign Supporter ROV rated to 6000 m water depth.

The ROV is equipped with an EM 2040 multibeam echo sounder for deep water multibeam mapping of the near bottom sounding environment in great detail. The basic EM 2040 has a transmit transducer, a receive transducer, a processing unit and a deck-side processing computer. The EM2040 operates at 200 - 400KHz, with 400 beams in single-swath mode offering 0.4 x 0.7 degree angular resolution. A swath angle of up to 140 degrees can be reached providing a maximum coverage of 4 to 5 times the water depth. During the cruise, the maximum swath width was varied between 50 and 70 degrees on either side in order to improve data quality, reduce the amount of noisy data at the outer beams.

The ROV is equipped with a large drawer to store sample material during dives. A large basket was used to bring sample containers to the seafloor and back up using the A-Frame from the hangar at mid-ship position. That limits the times the ROV has to dive up and down and hence, saves considerable time. Aside from the manipulator arms that provide the opportunity to take direct carbonate or rock samples, the ROV ÆGIR6000 also offers a number of sampling tools, most prominently the push coring device that can take up to 60 cm long sediment cores with a diameter of 8 cm (Figure 8). Another device is the blade corer; it is 34 cm long and can sample a volume of sediment with a larger rectangular area of approximately 20x12 cm (Figure 8). The push cores are placed in the hull of the ROV during the entire dive, while the blade core container is held by one of the ROV arm during descent and ascent. When the ROV reaches the bottom, the blade cores container is placed on the seabed while the Dive is ongoing. The blade corer frame has an automatic closing mechanism at the bottom to avoid sample loss. Push core and blade core liners are pre-drilled for pore water sampling with a resolution of 1-2 cm. The push cores are of fiber glass, 60 cm long with a diameter of 8 cm. The blade cores are manually winded up before hand, and when placed on the seafloor the ROV will push them into the sediment and release a pin that makes the blades closing. This traps the sediments in the core and the whole core becomes sealed.

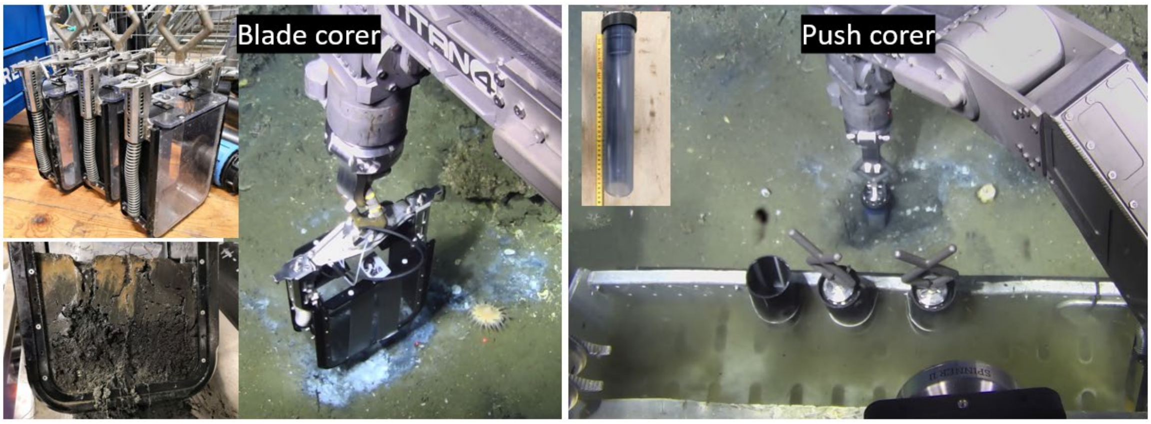

Figure 8 Blade corer (on the left) and push cores (on the right). The sampling tools are moved by the manipulators of the Ægir ROV. The blade corer has a closing system which prevents sample loss upon recovery and makes it a good sampling tool for fine to coarse sediment. The push coring works fine in clayey "sticky" sediments, but it is inappropriate for sampling of coarser sediments.

6. SAMPLING EVENTS

All sampling events are tabularized in the Appendix. There is also a table that provides details on processing and sub-sampling of sediment cores.

6.1 WATER COLUMN STUDIES

At chosen depths, the Niskin bottles sample water for methane concentrations analysis, using the headspace method described by Magen et al. (2014). This method consists of filling a 100ml glas flask up to the top with sampled water and adding 1 ml of 1 molar NaOH solution to it, in order to "poison" the sample. This prevents methane oxidizing bacteria from further consuming dissolved methane and thereby biasing concentrations. In the laboratory back on shore 5 ml N2 will be added to the headspace of these flasks. Dissolved CH4 present in the water sample will then diffuse into the headspace, which can be measured with a Gas Chromatographer. This technique helps understanding the vertical profile of CH4 concentrations in the water column. Water column properties (temperature, salinity and fluorescence) were measured at each new superstation, independently of water sampling.

6.1.1 Water column fluxes:

Ten samples coming from the superstation 2 (CTD sta0223) at 5, 10, 20, 40, 50, 60, 90, 120, 500 and bottom –10 m depth have been collected from the Niskin bottles. A volume of 2-3 L were sampled and filtered through a 0.45 µm Acetate cellulose membrane. Once the samples have been filtered, the filters have been rinsed with distilled water buffered with ammonia (5 ‰) and oven dried at 60°C.

6.2 MARINE GEOLOGY

The complete list of all sediment samples collected during the expedition are reported in the Appendix. In addition, table 1 lists all ROV-based sediment samples with indication of the sampling gear, namely pushcorers and bladecorers operated by Ægir ROV (Figure 8), as well as indication of the target analyses.

6.2.1. Sedimentology

Sediment grain size was assessed based on high-resolution ROV imagery of the seafloor (top layer) and visual inspection during push core and bladecore slicing. We prepared smear slides of the surface sediment of push cores collected in different areas and identified the main detrital and biogenic components using the optical microscope. X-ray fluorescence (XRF) core-scanning, a convenient non-destructive tool to rapidly assess elemental variations in grain size analyzes will be done once in the lab.

6.2.2. Pore water geochemistry

The push core and blade core liners were prepared by pre-drilling holes for pore water and gas sampling and covered with tape before deployment. The pore water sampling was conducted in cold storage (4 °C). The samples were obtained by inserting 5 cm long pre-wetted rhizons (0.15 µm mesh) into the pre-drilled holes from the top of the core to the bottom every 2 cm. A 10 ml syringe was attached to the rhizon with a wooden stopper inserted to create a vacuum. The first 0.2 ml of pore water was discarded immediately to flush out any potential distilled water that the rhizon filters were soaked in. The syringes were left for at least half an hour to collect the pore water. The pore water samples were divided in two: 1). 1 ml subsamples were transferred into 1.5 ml micro-tubes for dissolved inorganic carbon (DIC) analysis. 25 µl of mercuric chloride (HgCl2) was added to stop the microbial processes and the subsamples were stored at 4 °C. 2) The rest of the samples (0.5 ml-5 ml) was transferred into Eppendorfs and stored at -20 °C for sulphate analysis. Samples for strontium isotope analysis were collected from gravity core CAGE21-1-KH-04-GC-03. 10 µl of ultrapure nitric acid were added to lower the pH to < 2 and were stored at 4 °C. A total of 150, 117 and 7 sub-samples were prepared for sulphate, DIC and Sr during Leg I. 87, 201, 26 sub samples were prepared for sulphate, DIC and Sr, respectively, during Leg II.

6.2.3 Gas geochemistry

Bulk sediment samples (5 ml) were extracted for methane headspace analysis from sediment cores (push cores from ROV and gravity cores) using a syringe without the luer tip. The samples were transferred into glass vials prepped with 5 ml of NaOH (1 M) to stop microbial activity, plugged with a rubber septa, sealed with aluminum crimp caps and shaken, then stored at 4 °C. We collected a total of 26 gas samples during Leg 1 and 16 during Leg 2.

6.2.4 Rock sampling

During ROV operations we noticed a lot of large rock pieces in Svyatogor – on the seafloor near sites where seismic data indicates oceanic crustal rock outcropping or subcropping. Due to the interest in what rock type, and therefore minerals compose the oceanic crust at Svyatogor Ridge and environs, we collected some rock samples with the ROV. Visual inspection of the rock samples on board indicated a sedimentary origin (two greywackes and one coarse-grained lithified sandy limestone with many fossil shells). Therefore, these rocks were most likely deposited as Ice-Rafted Debris (IRD) and not indicative of the subsurface geology at the site.

In addtion, methane-derived authigenic carbonates were collected with the ROV in various locations. The methane-derived authigenic carbonates were washed with fresh water to remove any salt residue on carbonate surface. Samples were wrapped in aluminum foil and bubble wrap, labelled, and stored at -20°C.

6.2.5 Oil sampling

The Oil Spill Sampling kit (Figure 9) provided by Fugro has several different containers depending on the amount of fluid. Several syringes and smaller glass bottles can be used, when there is a big enough volume to extract. In the case of a thin oil slick on a water surface, a special membrane can be used which will catch in potential hydrocarbons. The membrane can be attached on the telescope rod and then be dipped into the water (Figure 10). The membrane will be then put into a glass bottle and afterwards into a plastic container to protect it from being shattered. A danger sign and normal labelling was attached on the sample, and it is ready to be send in for further analysis.

Figure 9 Material of the OIl Spill Sampling Kit (photo: Maximilian Weber)

:

Figure 10 Surface sampling for spilled oil with the special membrane attached on the telescope. (photo: Maximilian Weber, May 2021)

6.2.6 Heat Flow measurements

During the CAGE21-1 cruise, in situ temperatures were measured at 7 stations, with a total of 21 successful penetrations. The main objective of the heat flow survey was to obtain high-resolution heat flow measurements on the Northern Knipovich Ridge, Molloy Transform and Svyatogor Ridge. Previous studies in the area have revealed areas with anomalous thermal gradients and low thermal conductivities coinciding with fluid flow indications in seismic data, possibly indicating the presence of gas and active fluid flow.

The heat flow probe was deployed after configuration, and lowered to the seafloor with a winch speed of ~1.0 m/s. The probe was kept stable in the sediments for 15-20 minutes, allowing stabilization of temperatures after temperature increase due to frictional heating during penetration. A heat pulse was then generated, and the probe kept in the sediments for another 15-20 minutes to allow temperature decay following heating. The probe was then pulled out of the sediments with a winch speed of ~0.2 m/s. Two transects of heat flow measurements (HF-05 and HF-06) were conducted using the 'Pogo-style' method, in which the probe was lifted ~100 m above the seafloor, initiating a new cycle, and moved to a nearby location ~500 m away for new heat flow measurements. For HF-05 and HF-06, this procedure was repeated 8 and 7 times, respectively.

During all measurements, the heat pulse (duration of 20 s) was set to release if the probe remained stable for 15-20 minutes, and the tilt was within 10° with fluctuations within 0.5°, and acceleration fluctuations within 0.01 g. The distance limit for activating the second heat pulse was set to 50 dbar for HF-01 and HF-02, 500 dbar for HF-03 and HF-04 and 100 dbar for HF-05, HF-06 and HF-07.

6.3 MARINE BIOLOGY

6.3.1 Microbiology

The aim of this sampling campaign was the reconstruction of metagenomes and identification of novel species of ANMEs, from cold seeps fueled by biotic and abiotic methane in arctic region around Svalbard (Superstation 1, 2 and 4) and from an oil slick offshore Western Svalbard (Superstation 1). In addition, we wanted to investigate the distribution of ANME across the SMTZ (Sulfate Methane Transition Zone) in sediments interested by methane fluxes compared to reference sites (Superstation 1, 2 and 4). Hence, sediments were collected with push cores and blade cores (Figure 13) operated by ÆGIR6000 TITAN4 arm (Table 1).

At Superstation 1 we collected two push cores from a microbial mat interested by gas and oil emission. At Superstation 2, we collected 3 push cores in the microbial mat, 3 in reference sediments and 2 push cores along the transect from reference to active site (Figure 11). Push cores were equipped with 50 cm long (10 cm diameter) liners. Blade cores were 30 cm x 20 cm x15 cm in size, approximately. The length of collected sediment cores varied between 20 cm to 40 cm, approximately. Two blade cores were also collected in microbial mat covered sediments. At Superstation 4 we collected material from active and reference sites and from sediments hosting communities of tube worms.

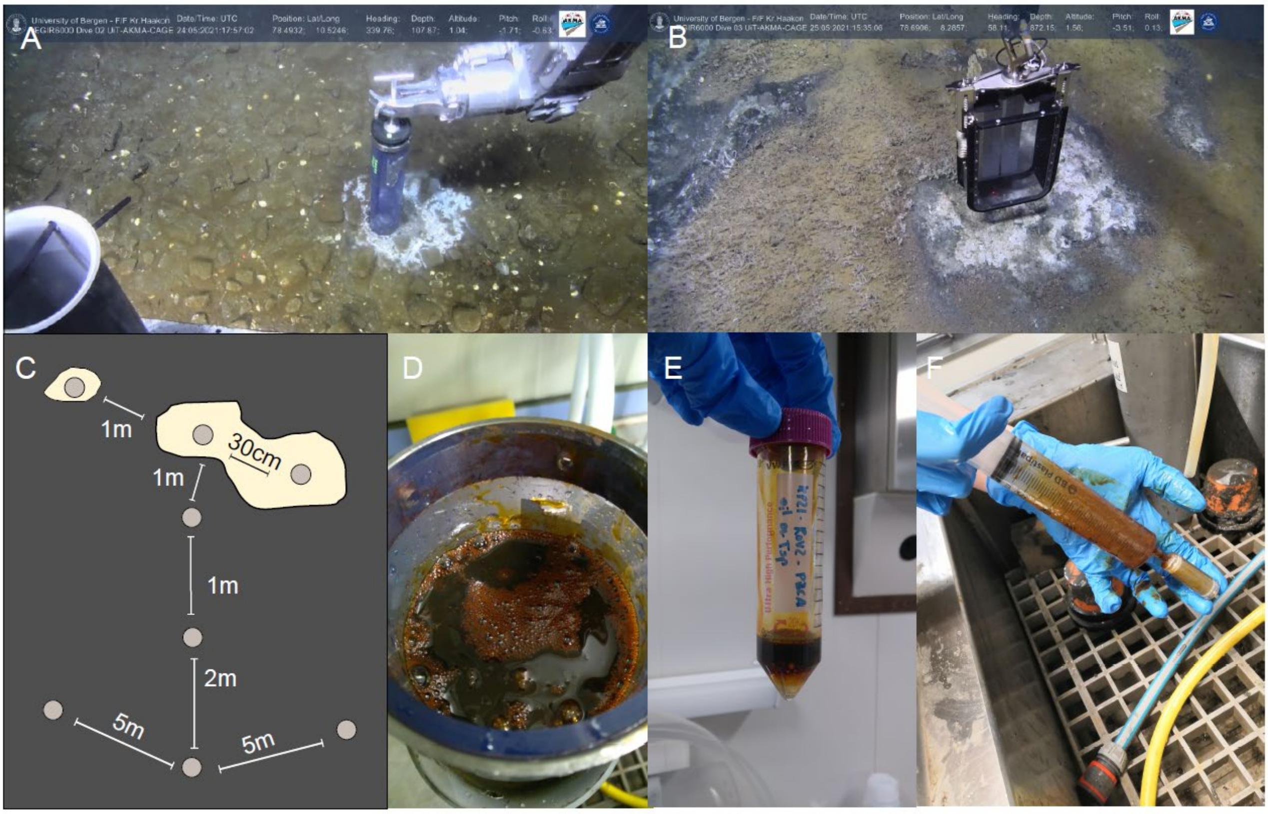

Figure 11 (A, B) Microbial mat covered sediments are sampled by the ÆGIR6000 TITAN4 with push cores and blade cores. (C) sampling strategy at Superstation 2; white marks represent the microbial mat; grey circles represent the push cores sampling location; approximative distances between sampling locations are indicated. (D, E, F (by Claudio Argentino)) Sampling of the push cores taken at Superstation 1.

On board, after collection of porewater, push cores were sampled for DNA extraction. Approximately 5-10 grams of material were collected every centimeter from top to bottom and stored at -80ºC on board. For blade cores, sediments were sampled at the seawater interface and every two centimeters and stored at -80ºC for DNA extraction.

Rocks above a microbial mat at Superstation 1 were also collected. Once on board, the surface was scraped to get the layer of microbial mat. For samples at Superstation 1, the oil floating at the surface of the push core was sampled (Figure 11) and bottom seawater from the push core was filtered in Sterivex syringes (0.2 µm Ø) for collection of microbes (Figure 11).

On shore, DNA will be extracted with a FastDNA™ Spin Kit for Soil (MP). Extracted DNA will be purified (AMPure Beads) and amplified with universal primers for 16S rRNA gene and sequenced with Ion Torrent technology. In addition, DNA extracted from selected layers will be sequenced with Illumina technology for metagenomes reconstruction.

Table 1: List of samples collected during Leg1.

Superstation	Dive #	Sample ID	Description	Porewater	DNA	CTG	DNA LifeGuard	Biomarker	
CAGE21-1-KH-01	Dive 1	RO1	Big rock on a microbial mat						
CAGE21-1-KH-01	Dive 1	RO2	Small rock on microbial mat						
CAGE21-1-KH-01	Dive 1	RO1	Surface (microbial mat)						
CAGE21-1-KH-01	Dive 1	RO2	Surface (microbial mat)						
CAGE21-1-KH-01	Dive 2	PC1	Oil on top of the push core						
CAGE21-1-KH-01	Dive 2	PC2	Oil on top of the push core						
CAGE21-1-KH-01	Dive 2	PC1	Filtered bottom water						
CAGE21-1-KH-01	Dive 2	PC2	Filtered bottom water						
CAGE21-1-KH-01	Dive 2	PC1	Microbial mat, gas and oil seepage	x	x	x	x		
CAGE21-1-KH-01	Dive 2	PC2	Microbial mat, gas and oil seepage (nest to PC1, same microbial mat)	x	x	x	x		
CAGE21-1-KH-02	Dive 3	PC1	Microbial mat 1		x				upside down, sampled for DNA only in the middle
CAGE21-1-KH-02	Dive 3	PC2	Microbial mat 1	x	x	x			
CAGE21-1-KH-02	Dive 3	PC3	Microbial mat 2	x	x	x			
CAGE21-1-KH-02	Dive 3	PC4	Reference 1	x	x	x			
CAGE21-1-KH-02	Dive 3	PC5	Transect 1	x					
CAGE21-1-KH-02	Dive 3	PC6	Transect 1						lost
CAGE21-1-KH-02	Dive 3	PC7	Reference 2	x	x				
CAGE21-1-KH-02	Dive 3	PC8	Reference 3	x	x				
CAGE21-1-KH-02	Dive 3	BC1	Microbial mat 3	x					fell upside down
CAGE21-1-KH-02	Dive 3	BC2	Microbial mat 4	x		x			
CAGE21-1-KH-04	Dive4	PC1							not sampled for microbiology
CAGE21-1-KH-04	Dive5	PC2	Microbial mat	x	x				
CAGE21-1-KH-04	Dive5	PC3	Tube worms	x	x	x			
CAGE21-1-KH-04	Dive6	PC4	Microbial mat	x	x	x	x	x	top, middle, bottom for biomarker
CAGE21-1-KH-04	Dive6	PC5	Sediments with tubeworms	x	x	x	x	x	top, middle, bottom for biomarker
CAGE21-1-KH-04	Dive6	PC6	Sediments with tubeworms	x					
CAGE21-1-KH-04	Dive6	PC7	Reference	x	x	x	x	x	top, middle, bottom for biomarker
	Dive6	BC1	half mat/half tubeworms	x	x				gradient destroyed, sampled one point for DNA
	Dive6	BC2	half tubeworms/ half reference	x	x				sampled in layers
CAGE21-1-KH-04	Dive 8	BC3	"dead" tubeworms	x	x	x			surface sampled for CTG, only tubes structures

6.3.2 Meio- and Macro-infauna

Sediments and the overlaying bottom water were collected in four seep areas, using either the Push cores (Ø 8cm) or the Blade Cores (32x25x10cm) deployed with the ROV Ægir6000 (Table 2). This sampling aimed to investigate the infauna diversity of the studied seep sites, namely the meiofaunal fraction (>32 µm) but also macrofauna fraction (>300 µm) at the Håkon Mosby Mud Volcano.

The samples collected for meiofauna studies will allow the quantification of meiofauna total density and support the comparisons between shallow and deep-water seeps in terms of nematodes biodiversity and community composition. Additionally, samples were also collected for subsequent molecular analyses. These analyses will be conducted at the University of Aveiro, Portugal.

In each seep area, three replicates' cores were collected in the "bacterial mat" micro-habitat and three replicates' cores at background sediments (as reference) for meiofaunal analyses, but also for the environmental characterization of the sediments. The overlaying water of each liner was removed and filtered over a sieve of 32 µm and for the selected cores in which geochemistry was also investigated, the pore-water was removed prior to core slicing. After the pore-water extraction was complete, each liner was sliced into 4 sediment depth layers (0-1cm, 1-2cm, 2-3cm and 3-5cm) and fixed in a formaldehyde (4%)/seawater solution for morphological analyses. For the cores where the sediment geochemistry (TOC, TIC, TN, grain size, sulfate content) and grain size analyses were also performed, ¼ of each sediment slice was kept in -20ºC. Additionally, at each superstation one Blade

Corer was also subsampled and sediments were preserved in 96% Ethanol solution for future molecular studies.

For the macro-infauna, sediment samples were collected in different micro-habitats at the Håkon Mosby Mud Volcano, namely in Siboglinid patches, bacterial mats and at the reference location, predominantly using the Blade Corer. The bulk samples were preserved in 96%Ethanol and will be processed at University of Bergen, Norway (UiB).

Table 2: List of sediment samples collected for meiofauna studies

Area	Superstation	Dive	Sample	Micro-Habitat	Water depth (m)	Preservation medium
Prins Karls Forland	KH01	Dive12	PusC-03	White Bacterial Mat	112.6	4% Formalin
	KH01	Dive12	PusC-05	White Bacterial Mat	113	4% Formalin
	KH01	Dive12	PusC-06	White Bacterial Mat	112.6	4% Formalin
	KH01	Dive12	BlaC-01	Background sediment	113	4% Formalin
	KH01	Dive12	BlaC-02	Background sediment	112.5	4% Formalin
North Knipovich Ridge	KH02	Dive13	PusC-09	Background sediment	877	4% Formalin
	KH02	Dive13	PusC-10	Background sediment	877	4% Formalin
	KH02	Dive13	PusC-11	White Bacterial Mat	874	4% Formalin
	KH02	Dive13	BlaC-03	White Bacterial Mat	872	4% Formalin + 96% Ethanol
	KH02	Dive13	BlaC-04	White Bacterial Mat	872	4% Formalin
Leirdjupet Fault Complex	KH05	Dive15	PusC-02	White Bacterial Mat	351	4% Formalin
	KH05	Dive15	PusC-03	White Bacterial Mat	350	4% Formalin
	KH05	Dive15	PusC-04	Background sediment	350	4% Formalin
	KH05	Dive16	BlaC-01	White Bacterial Mat	351	4% Formalin + 96% Ethanol
	KH05	Dive16	BlaC-02	Background sediment	352	4% Formalin
	KH05	Dive21	PusC-05	White Bacterial Mat	345	4% Formalin
	KH05	Dive21	PusC-06	White Bacterial Mat	345	4% Formalin
	KH05	Dive21	PusC-07	White Bacterial Mat	345	4% Formalin
	KH05	Dive21	PusC-08	Background sediment	344	4% Formalin
	KH05	DIve22	BlaC-03	White Bacterial Mat	344	4% Formalin + 96% Ethanol
	KH05	DIve22	BlaC-04	Background sediment	344	4% Formalin
Håkon Mosby Mud Volcano	KH06	Dive23	PusC-02	White Bacterial Mat (large)	1255	4% Formalin
	KH06	Dive23	PusC-03	White Bacterial Mat (large)	1255	4% Formalin
	KH06	Dive23	PusC-04	White Bacterial Mat (large)	1256	4% Formalin
	KH06	Dive24	PusC-07	Background sediment	1262	4% Formalin
	KH06	Dive24	PusC-08	Background sediment	1262	4% Formalin
	KH06	Dive24	PusC-09	Background sediment	1263	4% Formalin
	KH06	Dive25	PusC-11	White Bacterial Mat in the carbonate mound	1251	96% Ethanol
	KH06	Dive25	PusC-12	White Bacterial Mat in the carbonate mound	1251	96% Ethanol

6.3.3 Epifauna sampling

Opportunistic fauna sampling was conducted during the ROV Dives when recovering rock or carbonate rock samples, but also when large individuals were found during sediment coring (Figure 12, Table 3). The fauna collected was predominantly preserved in 96% to allow morphological identification and barcoding. The specimens will be processed at University of Bergen, Norway (UiB).

Figure 12 Examples of fauna observed on the surface of carbonate rocks. Left: visible Polychaete tubes (Serpulidae), ophiuroids (Ophiuroidea), echinoids (Echinoidea), sea anemones (actiniaria). Right: Sponges (Porifera) and polychaetes (Serpulidae).

Table 3: List of epibenthic fauna samples

Area	Superstation	Dive	Sample	Notes	Preservation medium
Prins Karls Forland	KH01	Dive 1	Rock	Sponge	96% Ethanol
	KH01	Dive 12	BlaC 1	Amphipoda and polychaeta	96% Ethanol
	KH01	Dive 12	BlaC 2	Ophiuroidea	96% Ethanol
	KH01	N/A	GC1	Top - Shell	-20C
	KH01	N/A	GC2	Shell	-20C
North Knipovich Ridge	KH02	Dive 13	BlaC 4	Polychaetes and Gastropoda	96% Ethanol
	KH02	Dive 13	BlaC 4	Gastropoda	96% Ethanol
	KH02	Dive 13	BlaC 4	Actiniaria	96% Ethanol
	KH02	Dive 13	BlaC 4	Surface sediments of microbial mat	Life Guard
	KH02	Dive 3	Carbonate rock	Echinoid	96% Ethanol
Svyatogor Ridge	KH04	Dive 05	PusC 2	Isopoda	96% Ethanol
	KH04	Dive 05	PusC 1	Siboglinid Polychaetes	96% Ethanol
	KH04	Dive 05	PusC 2	Gastropoda	96% Ethanol
	KH04	Dive 06	PusC 5	Siboglinid Polychaetes	96% Ethanol
	KH04	Dive 8	BlaC 1	Epifauna	96% Ethanol
	KH04	Dive 8	BlaC 1	Epifauna	Life Guard

Leirdjupet Fault Complex	KH05	Dive 19	Carbonate rock	Epifauna	96% Ethanol
	KH05	Dive 19	Carbonate rock	Epifauna	96% Ethanol
Håkon Mosby Mud Volcano	KH06	Dive 25	Litter item	Isopoda	96% Ethanol
	KH06	Dive 25	Carbonate rock	Sponge and Polychaetes	96% Ethanol
	KH06	Dive 25	PusC 12	Tubes	-20C
	KH06	N/A	Boxcore 1	Ophiuroidea	96% Ethanol

6.3.4. Micropaleontology

For the characterization of the living foraminiferal associations, sediment samples were collected from the uppermost pushcores or bladecores taken with the ROV Ægir. At each station, samples from 0-1 or 0-2 cm were treated with Cell Tracker Green (CTG), eDNA for benthic monitoring, and TEM for subsequent transmission electron microscope observations (see Table 'Details on processing and sub-sampling of sediment' in the Appendix for a reference to all samples for micropaleontology). For the study of living foraminiferal associations, refer to Methods chapter "Microfauna and Meiofauna".

The presence of foraminifera on the surface sediment has also been studied. A box core (BC01) (Figure 13) and a blade core (BlaC04) were collected at superstation 2 (NKR, 910 m water depth) and one blade core (BlaC06) at superstation 4 (Svyatogor ridge, 1900 m water depth).

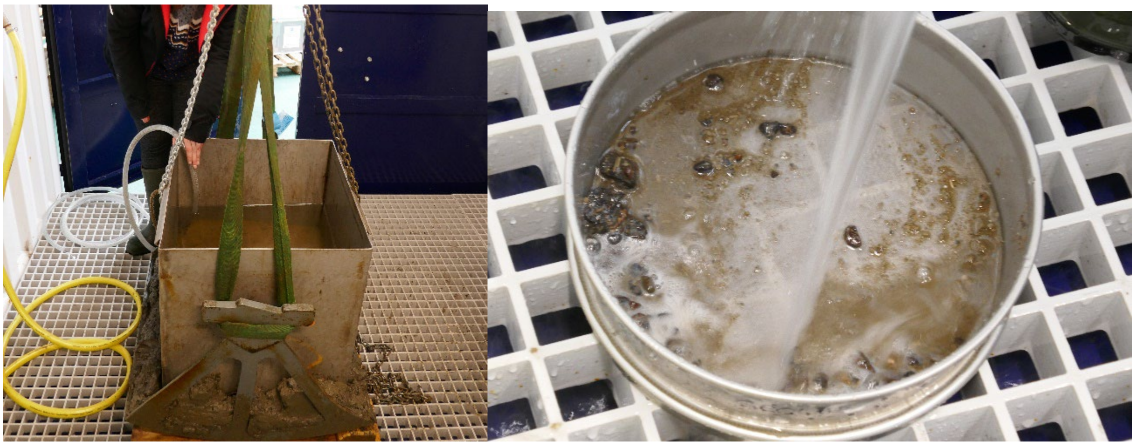

Figure 13 Box corer full of sediment and sediment being sieved for facilitate observations under the binocular microscope. Credits: Max Weber.

The upper centimeter was sampled by scraping the surface sediment with a spoon or spatula. Then, the sample was washed through a 100 um mesh size sieve with sea water and keep it wet and cold. Marine calcifiers (benthic and planktic foraminifera, and pteropods) were wet picked and photographed (Figure 14).

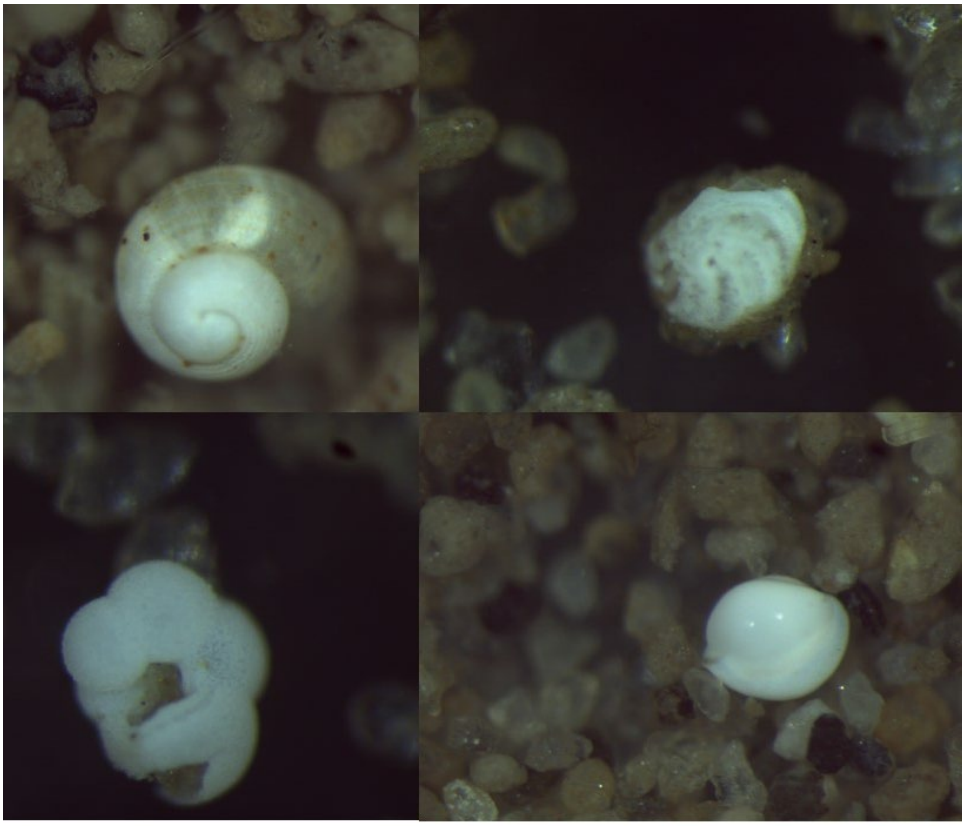

Figure 14 Marine calcifier: pteropods and foraminifera. Credits: Griselda Anglada-Ortiz

6.2.2.1 eDNA for benthic monitoring (0-2 cm depth only)

The protocol for sampling sediment eDNA for benthic monitoring according to ID-Gene ecodiagnostics, Campus Biotech, 15, av de Sécheron, 1202 Geneva, Switzerland was used for the determine the bioDiversity of foraminifera. Sediment was sampled using a sterilized spoon kept in a sterilized plastic bag, fixed with Life Guard TM (QIAGEN, ref. 12868-1000) solution for preserving eDNA, and stored at 5°C.

6.2.2.2 Cell Tracker Green - CTG labelling (0-1 cm depth only)

The samples used for CTG were treated with a method based on enzymatic reactions was used to distinguish living foraminifera (Bernhard et al., 2006; Pucci et al., 2009; Langlet et al., 2013, 2014). One milligram of Cell-Tracker™ Green (CTG 5 CMFDA: 5-chloromethylfluorescein diacetate) was dissolved in 1 mL of dimethylsulfoxide (DMSO) and diluted by 10 in situ sterile sea water. Samples were incubated for to 20-30 h in cold room without light in a solution of seawater, with a CTG final concentration of 1 micromol L-1. During this time, CTG passes through the cellular membrane of living organisms, and reaches the cytoplasm where hydrolysis with nonspecific esterases creates fluorogenic elements. After the death of the cell, esterases are decomposed in a few hours to some days at maximum, depending on environmental conditions, making the CTG method highly accurate to discriminate between living and dead organisms. After incubation, the samples were fixed in 96% ethanol and stored at 5°C.

6.2.2.3 TEM-staining (0-1 cm depth only)

A TEM solution of 10 ml glutaraldehyde (defrosted), 25 ml cacodylate buffer and 15 ml sterile seawater was prepared 1/2 hour prior to sampling under the fume hood. During subsampling, 20 ml (1/4 core slice, 1 cm thick) of sediment from 0-1 cm depth was transferred in a 60 or 100 ml HPDE bottle. We added the TEM solution until the bottle was almost full, we shook the bottle gently, sealed it with Parafilm, and stored at 5°C.

6.4. Deep-tow camera system

Currently, the deep-tow camera system is under continuous development and testing. Two test Dives were conducted on a SS6 (Håkon Mosby Mud Volcano). During the first test, on the 6th of June 2021, all systems operated as intended. We were able to control the lights, watch the video feed and take pictures of the seafloor using bottom-facing camera by sending a command. During the second test, on the 7th of June 2021, issue with bottom-facing camera was encountered – for some reason connection with it was very intermittent and no commands could be executed.

6.5 ROV photomosaics

A total of 26 ROV Dives were conducted with the ROV ÆGIR6000 during the CAGE 21-1 cruise, among which 6 Dives (DIVE08, 09, 11, 16, 18 and 26 – Table 8) were fully dedicated to collect video footage at a constant speed (0.1 kt) and distance from the seafloor (2 m) through a bottom-oriented camera and along planned adjacent and parallel track-lines, spaced 2 m from each other. The described procedure was performed to collect suitable data to implement photomosaic reconstruction of the seafloor in key areas. Seafloor photomosaic are planned to be provided applying Structure from Motion (SfM) techniques (a form of 3D photogrammetry) on frames extracted from the videos. Accurate ROV positioning obtained from the USBL system is critical for scaling and positioning the obtained photomosaic in the associated geographical context.

The high-resolution orthomosaics, realized from the processed images, allow us to reconstruct representative seafloor features of the sampled areas and figure out the spatial pattern characterizing the observed distribution of bacterial mats and detected macrofauna (i.e. tubeworms).

7. Preliminary observation and result: Prins Karls Foreland (Superstation 1)

Recent investigation of satellite images indicated oil slicks at the sea surface a few nm offshore Prins Karls Foreland over a period of several years. The main objective in this area was to confirm oil slicks at the sea surface from visual inspection and sampling, to identify the source of the oil at the seabed and to describe the sedimentary and microbial environment these oil seeps occur in. The oil slick was visible on satellite imagery on the 30th May (inset figure in Figure 15). When we visited this area on the following day, the oil slick could clearly be observed on the sea surface as a striping, glimmering pattern over a width of approximately 300-400 m. Four Dives with the ROV were conducted at this site (Figure 16, Figure 17) for visual surveys and sediment sampling. In addition, we collected two gravity cores and conducted a small CTD and water sampling survey.

Figure 15 Aerial view facing northwards showing the glimmering oil slick on the sea surface and RV Kronprins Håkon for scale. Lower right corner shows an example of the oil slick on satellite imagery from the 30th May, a day ahead before we investigated this site.

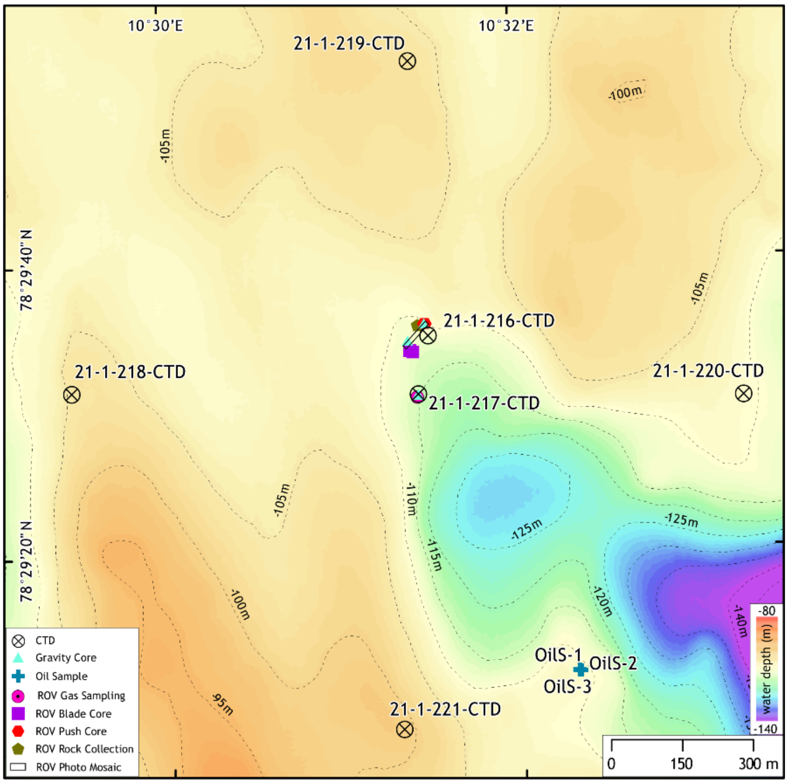

Figure 16: Map showing all stations at Prins Karls Foreland. Details of ROV Dives and sampling stations are shown in Figure 17.

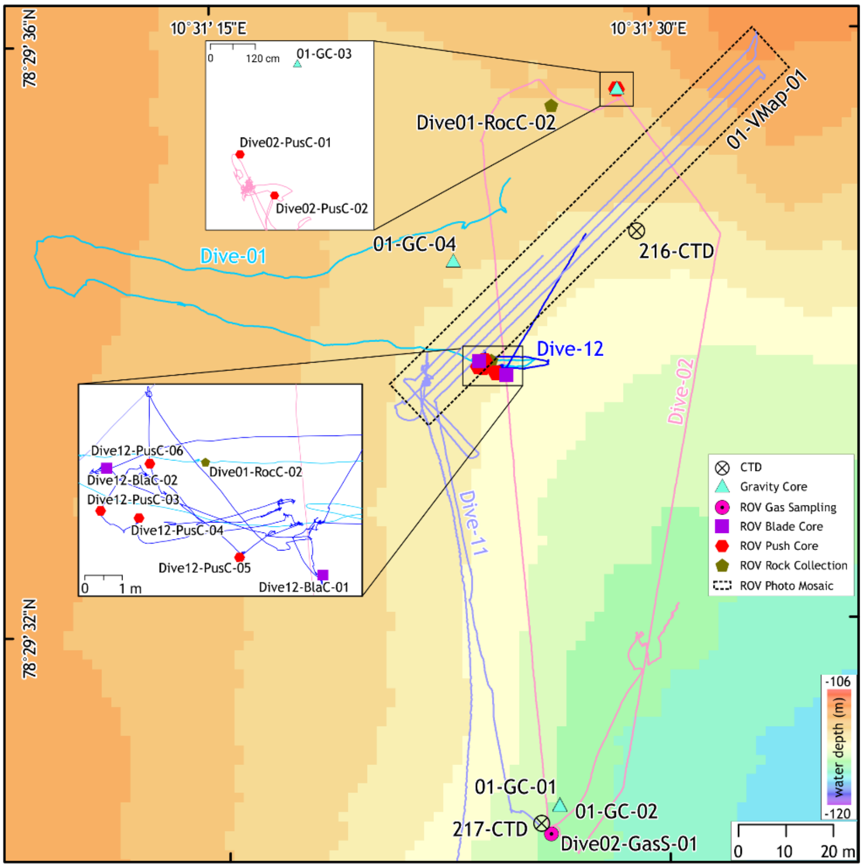

Figure 17: Map showing details of ROV tracks during Dives 1, 2 and 12 and sampling stations. The photo mosaic was acquired during Dive 11.

7.1 ROV visual surveys, Dive logs

During leg 1, two Dives (Dive 01 and Dive 02) were conducted at PKF in water depth of 105 – 120 m) (Figure 17). The aim of the Dives were to visually inspect the seafloor, identify locations of gas and oil seepage from the seafloor and take sediment and rock samples. The water is full of material in suspension raining down. The seafloor is showing a ground consisting of pebbles with the majority of them sub-angular (Figure 18, Figure 19). A minority of the pebbles/cobbles are sub-rounded. The gravel appears to be polymict. Rarely boulder size rocks are occurring on the seafloor. Finer material is located between the boulders, probably ice rafted debris (IRD) which are glaciomarine deposits. Roughly 5% of the seafloor is covered by organisms. The main part of the organisms is represented by shells/bivalves. The bivalves/shells are around 2 -4 cm. Rarely sea stars and urchins (regularia echinoidea) and anemones are visible. Several patches of white mats are visible coating the sediment. The mats range in size from 0.2 m up to 1.5 m in diameter and most likely of microbial/bacterial origin. Bubbles occasionally rise from the sports with the mats. The ROV arm is grabbing rock samples left side of the tray. After grabbing a rock black mud is mobilized (maybe anoxic conditions under the surface?).

White mat found with "black bubbles" (0.5-1 cm) ascending from it is interpreted to be the seeping oil. Another bacterial mat is found with oil bubbles emerging (12:37:26 UTC). Rock sample is taken at 12:44:00h UTC stored on the right side of the tray.

At 17:17:00 ROV has been lowered down to take two push cores and to collect oil and gas samples. At this site both oil bubbles and gas bubbles are emerging from the seafloor.

At 17:27:00 the gas sampler has been deployed at the sampling site. Oil bubbles are emerging into the gas collector (bubble catcher). At 17:55 push core 1 is obtained. Later also push core 2. It is unsure whether the gas sampler was able to retrieve the oil, but the push cores had oil in them, and the sediment was as well oil stained. During the night pore water and methane samples were collected from the cores and they were sliced every 1 cm and put into bags.

We returned to this site on the 31st May for ROV Dive 11 and Dive 12. Dive 11 acquired a photomosaic over the main seep area. Videos were acquired along 4 parallel transects (Table 8), 2 m spaced and 100 meters long, at a constant speed of 0.2 kn and altitude of roughly 2 meters, to obtain a field of view slightly larger than 2 m. Dive 12 collected additional push and blade core samples. Similar observations were made and there was again considerable marine snow in the water column as observed during the first leg. The seafloor was generally rocky with many clasts consistently covering ~30-60% of the seafloor, the sediments appeared to be fine grained, were mostly grey, with some phytodetrital cover. There were bacterial mats present. There were few anemones, sponges, sea stars, and brittle stars scattered throughout the area. There were a couple patches with abundant tube worms

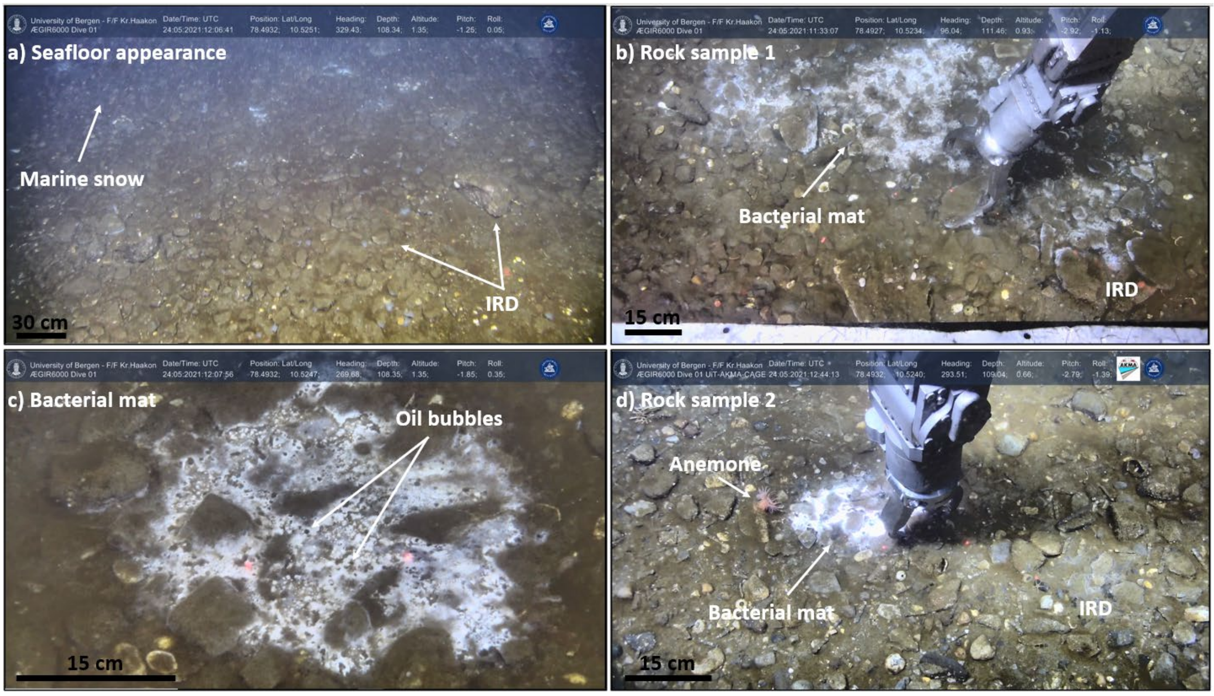

Figure 18: Screen shots of the ROV video feed showing a gravelly seafloor. Several patches of white microbial mats are visible coating the sediment. The mats range in size from 0.2 m up to 1.5 m in diameter.

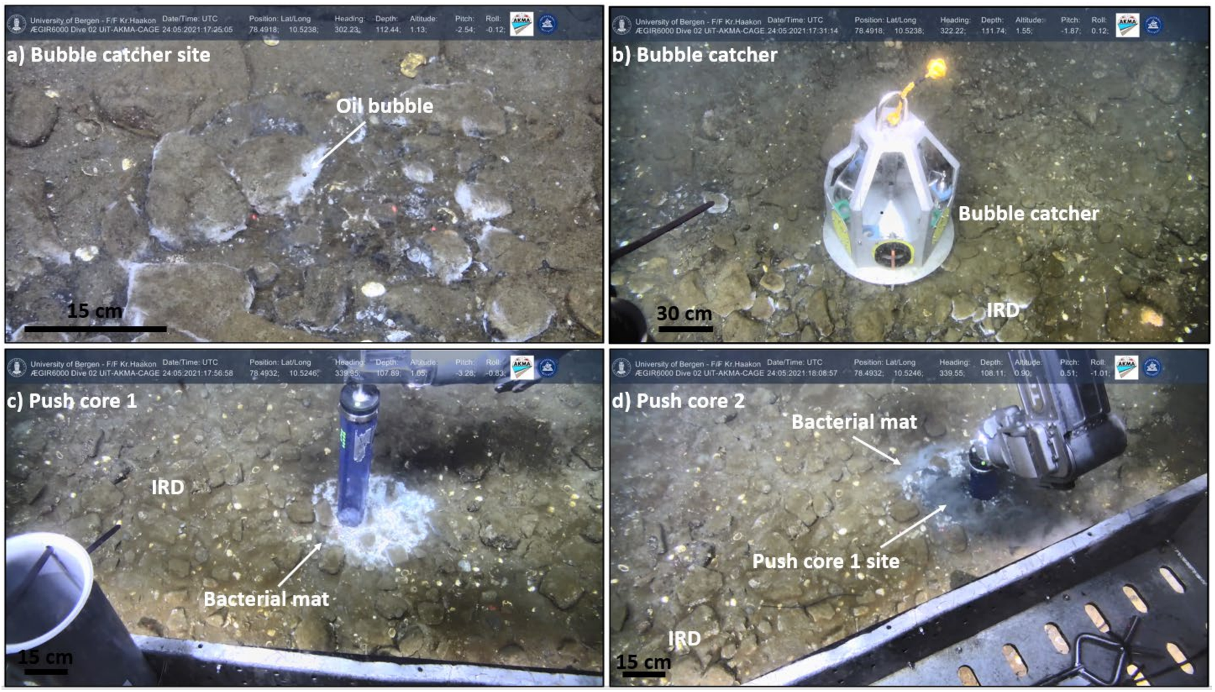

Figure 19: Screen shots of the ROV video feed showing oil seepage and sampling at Prins Karls Foreland.

7.2 Oceanography, water column

Five CTD casts with water sampling were carried out at Superstation 1 (offshore Prins Karls Foreland), around an oil seeping site, on the 24th of May. The first cast was taken at the location of the seep site.

Water from four further casts was sampled around this central site, forming a square where sampling stations are distant by 1 km from each other. It gives then the spatial distribution of CH4 concentrations around the oil and gas seep site investigated. This was undertaken at stations 217 to 221. No water sampling took place for the cast at station 216, only water column properties have been measured.

7.3 Oil sampling

A total of three membranes was used to sample the surface of the sea. The samples have been properly packed and labeled and sealed in plastic containers. The ROV obtained push cores on one of the seeping sites, where oil bubbles have been found. As the push cores reached the surface again and were taken into the lab, we saw that oil had accumulated on top of the water surface in the core liner (Figure 20). Several small oil samples have been taken with syringes into small glass bottles (Figure 21:). These samples are ready for further analysis.

Figure 20: Pushcore 01 with seeped oil covering the water surface in the push core liner. (Foto: Maximilian Weber)

Figure 21: Sampling of the seeped oil in pushcore 01 from Prins Karls Foreland (Foto: Maximilian Weber)

7.4 SEDIMENT SAMPLING, SEDIMENTOLOGY & MICROPALEONTOLOGY

We retrieved a total of 6 push cores (5 on microbial mats and 1 from a reference site). The cores from microbial mats had oil in the upper ~10 cm, where the core was also more clast-rich (mostly <1 cm). The sediments from the reference core had several small (<3 cm) clasts near the surface where the sediments were brown. Around 4 cm depth the sediments become grey and more clay-rich.

We also took two blade cores at this site, both from reference locations. They had some clasts (<3 cm) in the brown surface sediments, and in one core there was a transition immediately to grey clay-rich sediments around 5 cm below the surface, whereas in the second blade core, there were black sediments for about 5 cm between the transition from the brown sediments with clasts to the grey clay-rich sediments.

The sampling for micropaleontology aimed at obtaining both living and fossil foraminifera. The samples for investigating living benthic foraminifera were taken from the seafloor surface and preserved with Rose Bengal and CTG. The sampling and staining with Rose Bengal was done together with the sampling for meiofauna, and samples from the first 5 cm of sediments were taken. Details about number and interval of sediments taken are indicated in Table 'Details on processing and sub-sampling of sediment cores' in the Appendix.

7.5 PORE WATER AND GAS GEOCHEMISTRY

In total, we collected 18 samples for Dissolved Inorganic Carbon (DIC), 31 samples for sulfate, and 6 samples for headspace gas analyses. These will be further analyses in the laboratories at UiT. Detailed samples list available in table 'Details on processing and sub-sampling of sediment cores' in the Appendix.

7.6 MICROBIOLOGY

At Superstation 1 (JKF, 100m depth), patches of white microbial mat appeared scattered on the seabed, with a diameter of 10-30 cm and round shaped (Figure 22). Some of these patches were interested by gas bubbles emission, some by oil droplets (Figure 22) and some by both, supporting the hypothesis of a residing community of short or long chain anaerobic hydrocarbon degraders. The bottom seawater was rich in suspended particulate of organic matter.

Push cores from a patch of microbial mat from a gas/oil seepage were characterized by a black color at the top 4 to 10 cm. An oil layer also formed on top of the push cores, floating on bottom seawater. At higher depths, sediments had a clayish texture and light grey color.

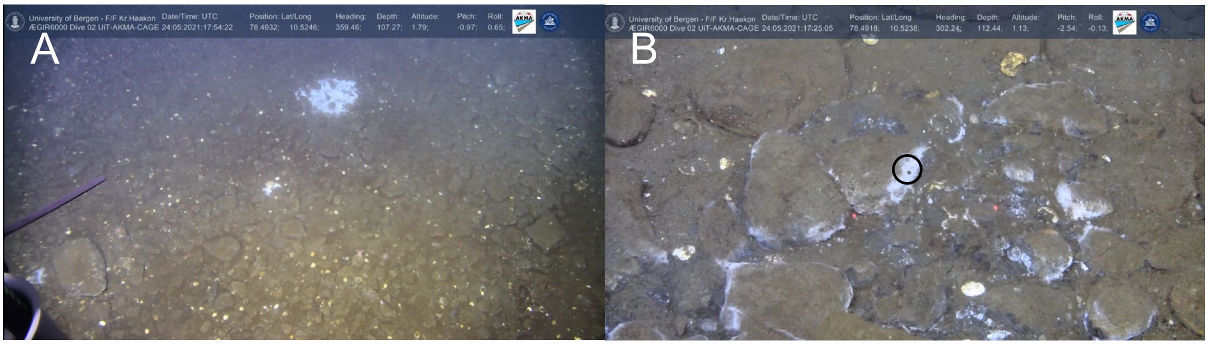

Figure 22: (A) Microbial mat at Superstation 1, sampled with push cores in Dive2. (B) An oil droplet released in the water column is indicated by a black circle.

7.7 MACROFAUNA

Overall, from the ROV dives we observed sparse bacterial mats and typically surrounded by common Arctic mega-epifaunal communities, living on coarse sediments and dead shell seafloor. Abundant presence of anemones (Actiniaria), large extensions tube-worm patches (possibly Sabellidae), but also presence of Alcyonacean corals (*Gersemia sp.*), diverse sponges (Porifera) species, as well various echinoderms (Asteroidea and Opiudoidea) and gastropods.

8. Preliminary observation and result: West-Svalbard continental slope, Vestnesa Ridge (Superstation 2)

Recent surveys conducted by CAGE have identified a fluid flow structure on the western continental margin of Svalbard in water depth of ~900 m between the onset of Vestnesa Ridge and the Knipovich mid-ocean Ridge (CAGE15-5, CAGE16-6 cruise reports) (Figure 23). This fluid flow feature is elongated in the N-S direction with an approximate length of 3 km, has a subtle depression and steep rim along its eastern rim. Pore pressure measurements indicated that this structure is an active feature, although observations of gas bubbles in the water column are missing (Sultan et al., 2020). Our ROV survey targeted hummocky structures at the NE margin of this elongated fluid flow feature and small depression in the center of it, where gas hydrates have been sampled during a previous CAGE cruise (CAGE17-5 cruise report).

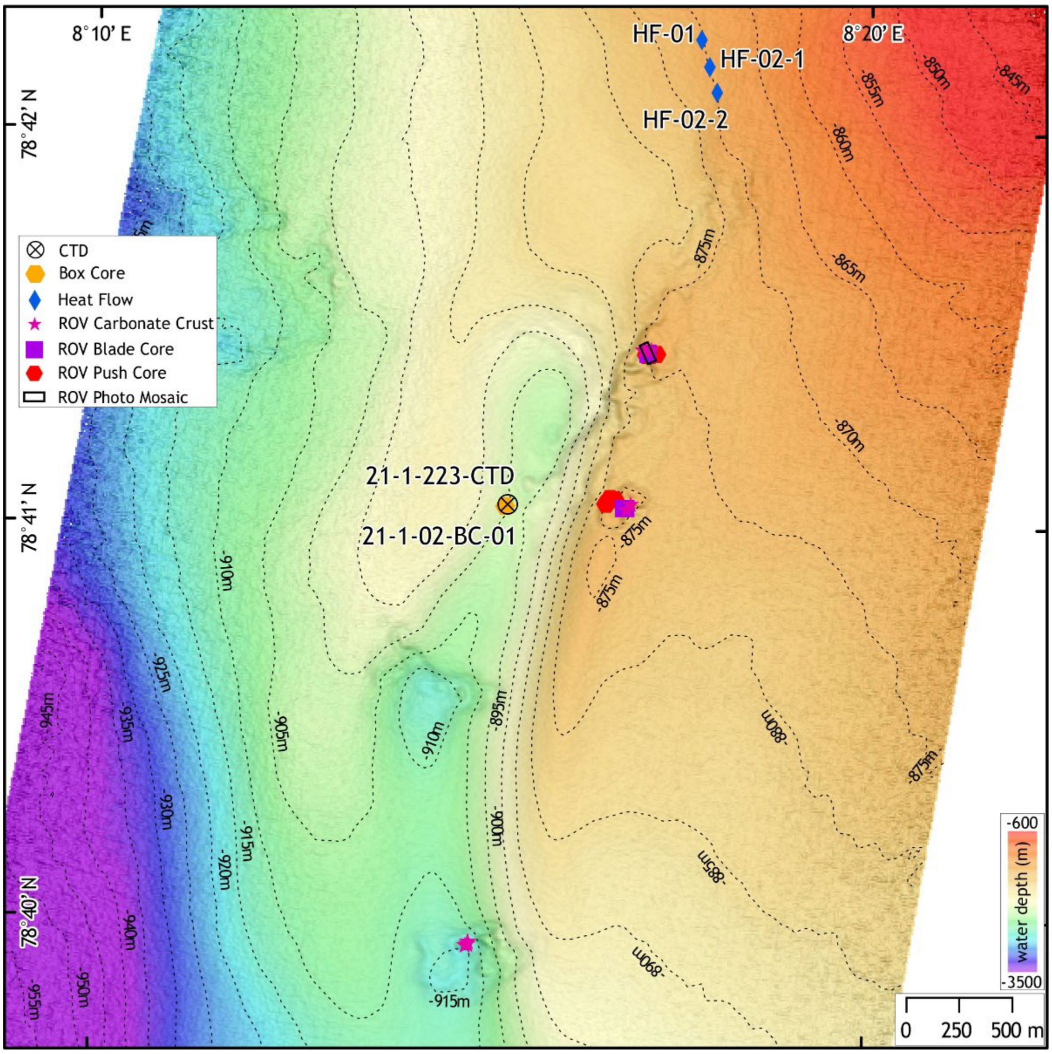

Figure 23: Map showing investigation at an elongated fluid flow feature on the western Svalbard margin

8.1 ROV VISUAL SURVEYS, DIVE LOGS

At this superstation, the ROV made 6 Dives (Figure 24 and Figure 25). We used the ROV to acquire multibeam bathymetry data and photomosaics of the area, as well as collect sediment samples with both push and blade cores.

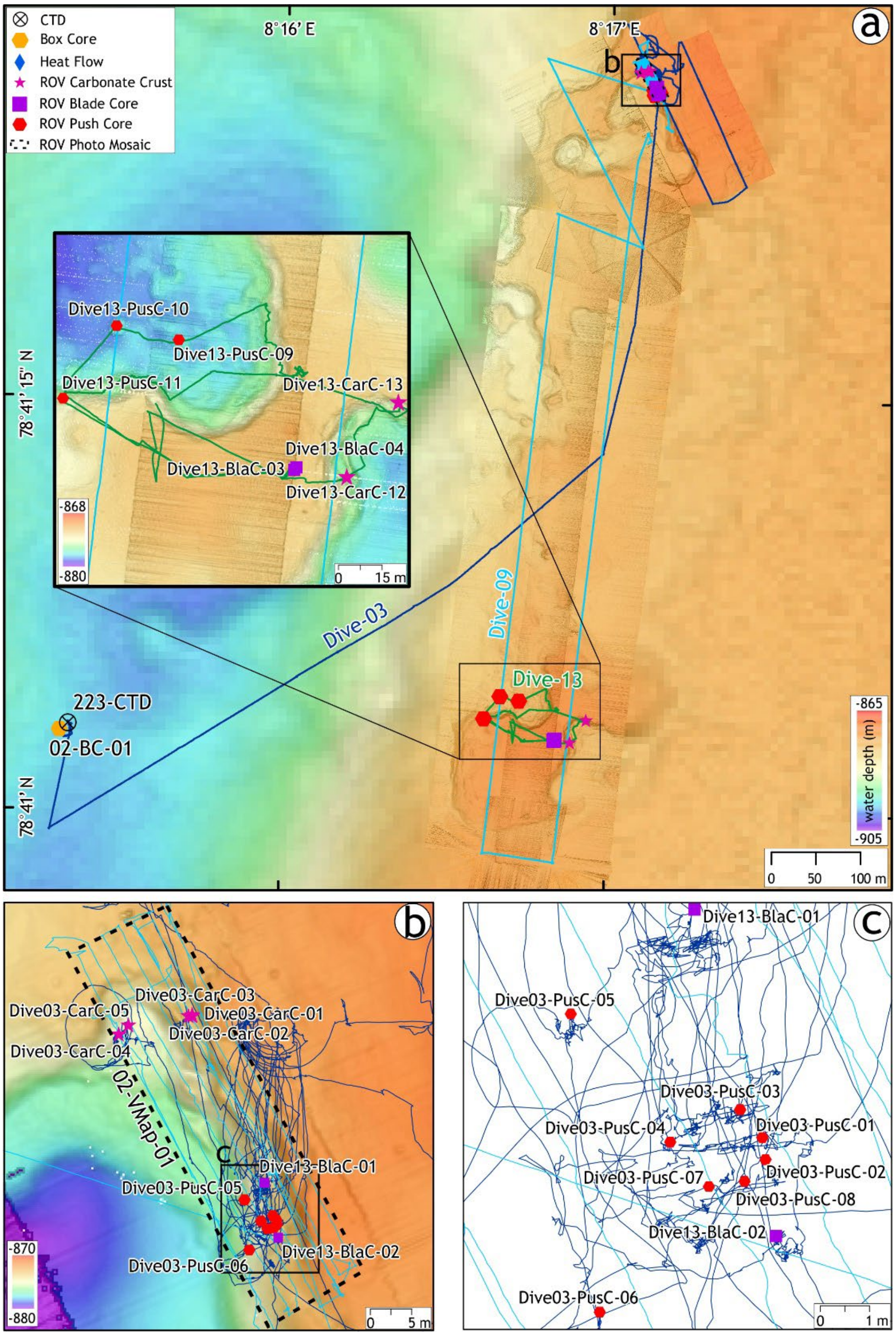

Figure 24: Map showing Dive tracks, sampling sites and area of photomosaic at the NE corner of a fluid flow feature on the western Svalbard continental slope.

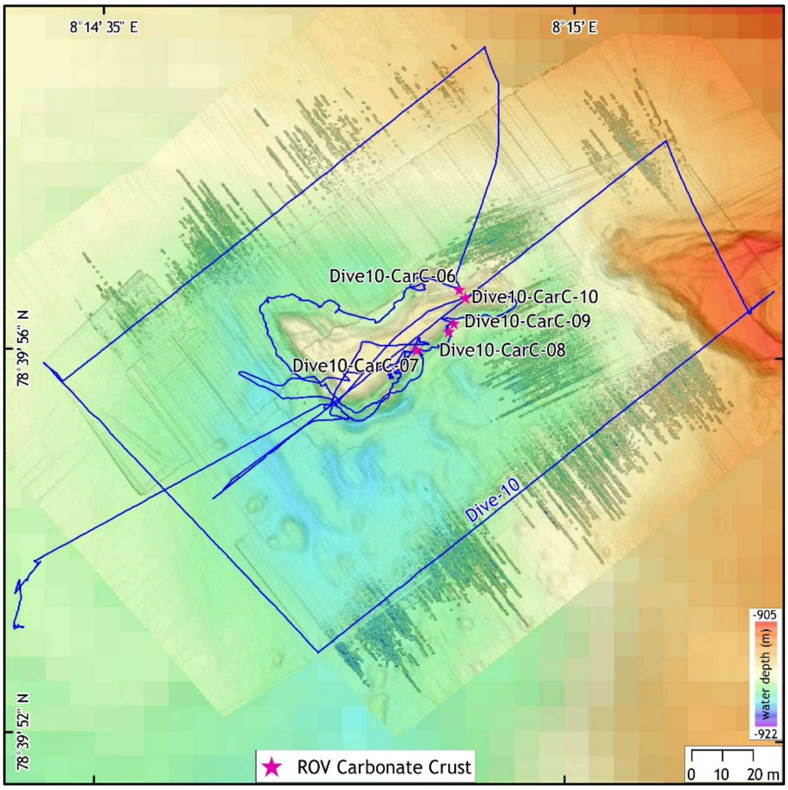

Figure 25: Map showing the central area of a small depression inside the elongated fluid flow feature.

At this station there was a lot of marine snow in the water column. The seafloor was predominately fine grey sediments (glaciomarine clay?) with greenish-brown phytodetrital cover, and clasts up to ~20 cm (Figure 26). There was a large area with carbonate crust at this superstation, and there were very few clasts in those areas, but otherwise the sediments were very fine grained with larger clasts ranging from ~5-30% coverage depending on the area.

In general, there were frequent bacterial mats (Figure 26), some anemones, sea stars, and brittle stars (some basket brittle stars, and others), and some sponges. We observed a few areas with tube worms, debris with attached sessile organisms and individuals of Arthropoda (sea spiders). No evident seep associated mega-epifauna near the bacterial mats. Fauna in the surroundings areas was sparsely distributed, including carnivore sponges *(Chondrocladia (Chondrocladia) grandis*), Alcyonacean *(Gersemia sp.)* and Pennatulacean *(Umbellula sp.)* corals, small pycnogonids and different species of Ophiuroidea and Asteroidea (including basket stars - Euryalidae).

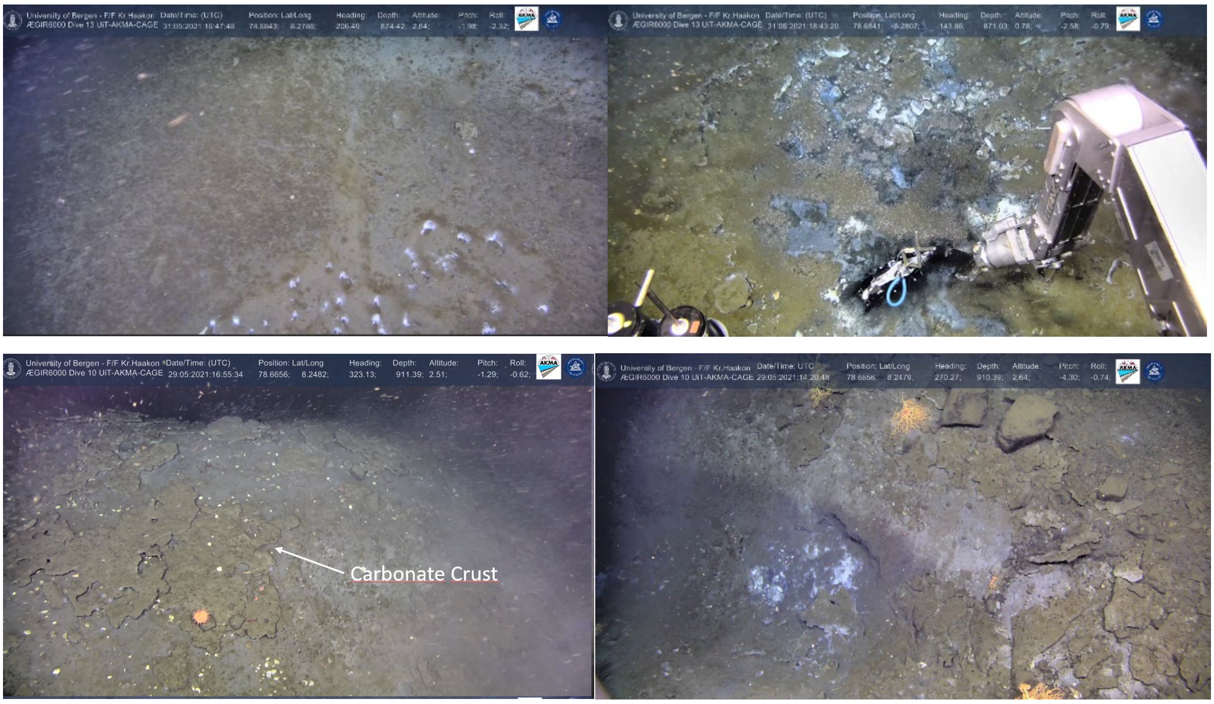

Figure 26: Stills from the ROV video feed showing the seafloor. Upper left: polychaete tubes, upper right: microbial mat; lower left: carbonate crusts; lower right: a small escarpment with carbonate crusts on top and bacterial mats on the flanks.

8.2 SEAFLOOR MAPPING AND PHOTOMOSAICKING

ROV-based multibeam micro-bathymetry was collected during DIVE03, DIVE09 and DIVE10 (Figure 24 and Figure 25). The northernmost area was initially surveyed during Dive 03 where a small escarpment was detected and densely sampled during the same Dive Two parallel multibeam lines, 40m spaced, approximately 200 m long and oriented from NW to SE, were acquired covering a total area of 0.02 km^2, from 870 to roughly 900 m of water depth. During DIVE09, the ROV-based multibeam survey was performed at 45 m of altitude. Two parallel, 60-m spaced multibeam lines, roughly NS oriented and 700 m long, were acquired at 0.5kn, as well as a shorter line, 130 m long and NW-SE oriented. The multibeam data was pre-processed on board, obtaining a DTM surface at 0.25x0.25m (grid cell size) of resolution.

Slightly south to the area covered by Dive 03 and Dive 09, an additional multibeam survey was performed at 45 m of altitude, where gas hydrates were sampled during the cruise CAGE17-5. Three parallel, 60-m spaced multibeam lines, SW-NE oriented and 170 m long, were acquired at 0.5kn, as well as a shorter line, 150 m long and NW-SE oriented. A total area of 0.04 km^2 was surveyed, from approximately 900 to 940 m water depth.

The small escarpment explored and mapped during DIVE03 were surveyed also using the central ROV camera (Dive 09), properly oriented toward the seafloor, in order obtain images suitable for applying SfM photomosaicing techniques. Videos were acquired along 7 parallel transects, 2 m spaced and roughly 100 meters long, at constant speed of 0.2 kn and altitude of 2 meters, in order to obtain a field of view slightly larger than 2 m.

8.3 OCEANOGRAPHY, WATER COLUMN

Only one CTD station was acquired at this superstation providing calibration for acoustic systems.

8.4 HEAT FLOW

21 heat flow measurements were carried out during this cruise (Figure 27). Heat flow data has been pre-processed and final processing will be done onshore. Preliminary results from measurements early in the cruise (HF-01 to HF-04) show a mean thermal conductivity on the western Svalbard margin fluid flow site of 1.576 W/mK at (HF-02-02) (Figure 28), and a relatively low 1.118 W/mK at Molloy Transform (HF-04). The mean thermal gradient based on HF-01 to HF-04 was 0.1204 K/m and the mean heat flow was 157.48 mW/m2. Stations HF-05 to HF-07 have yet to be processed.

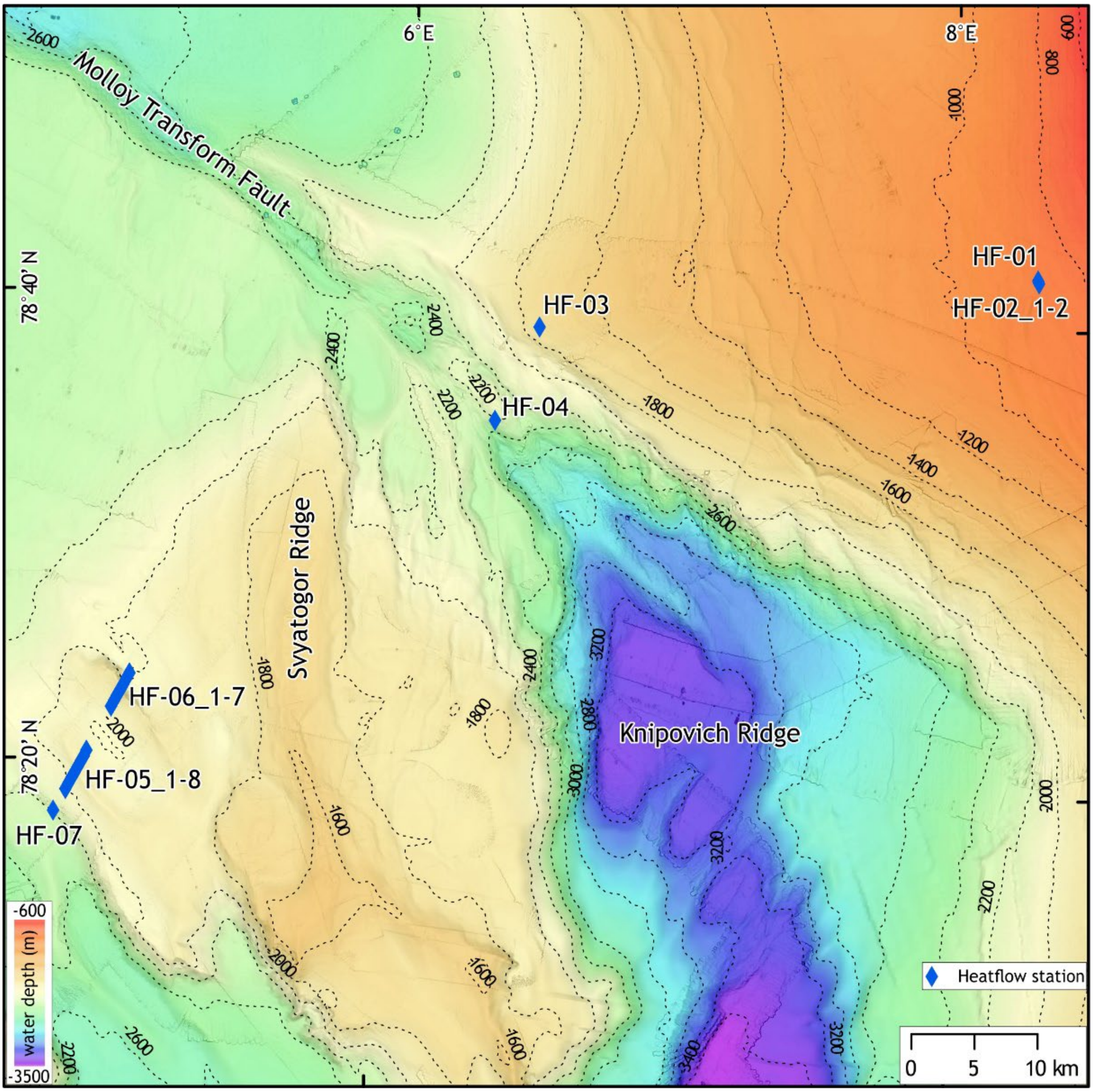

Figure 27: Heat flow stations conducted during this expedition.

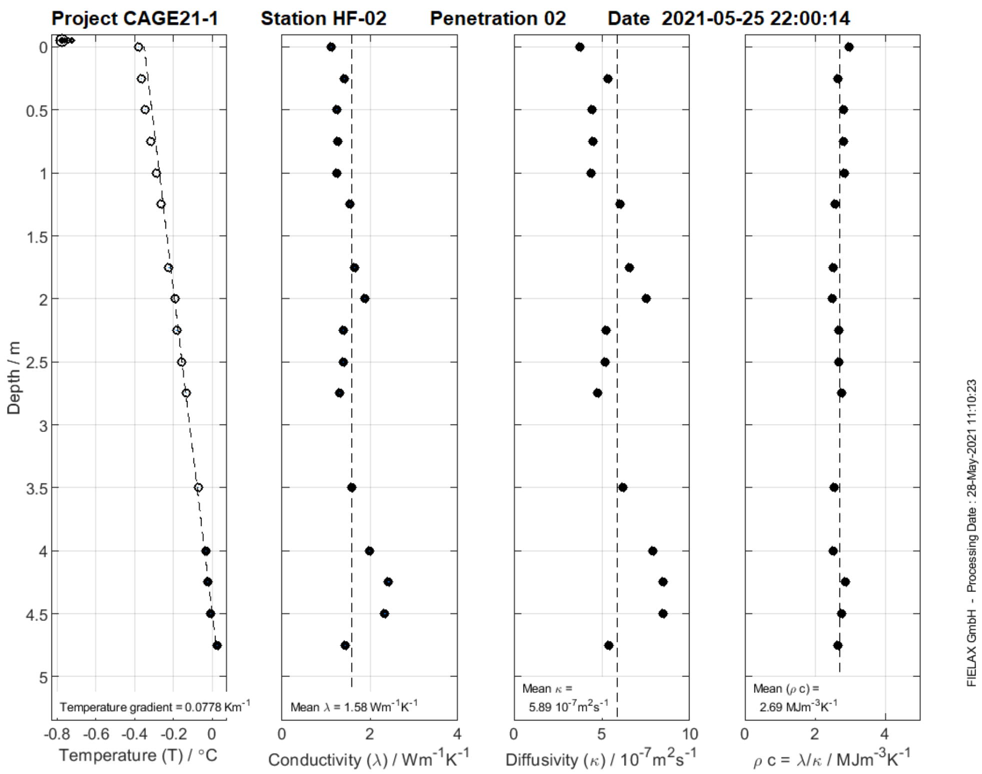

Figure 28: Plot of temperatures and thermal properties measured at station HF-02-02. Higher thermal conductivities are observed at 4.0 – 4.5 m below the seafloor.

8.5 SEDIMENT SAMPLING, SEDIMENTOLOGY & MICROPALEONTOLOGY

This area has been investigated during both legs of the cruise. In total in this area, we retrieved 11 push cores and 3 blade cores, some from the background are and some from bacterial mats of tube worm areas. The reference cores had brown, slightly sandy/silty surficial sediments with grey clay beginning at ca. 2 or 10 cm and continuing for the rest of the core. Two blade cores from leg 1 and two from leg 2 were retrieved, from microbial mats (Figure 29). The sediments in the blade cores were mostly fine grained, and entirely black indicating anoxic conditions very typical for an active seep environment.

Figure 29: KH02_Dive12-BlaC3 showing the black sediments.

At superstation 2, the surface sediment of the box core and the blade core were analyzed for marine calcifiers. After wet sieving (though 100 um mesh size) we observed abundant empty shells of benthic and planktic foraminifera. Planktic foraminifera appear to be smaller and more damaged than the benthic foraminifera. We also observed some dead pteropods (*Limacina retroversa*) (both in the box and blade core) and big gastropod that was not classified. Several samples were taken for micropaleontological analyses and the detailed list is provided in the Appendix.

8.6 PORE WATER AND GAS GEOCHEMISTRY

In total, we collected 38 samples to be measured for Dissolved Inorganic Carbon (DIC) and 44 for sulfate analyses. We also collected 3 sediment samples for headspace gas. All the samples taken will be further analyzed in the laboratories at UiT. Detailed samples list available in the Appendix.

8.7 METHANE-DERIVED AUTHIGENIC CARBONATES (MDAC)

MDAC samples were collected from 5-10 cm-thick carbonate slabs exposed on the seafloor (Figure 26). Samples consist of light grey carbonate dominated by a rather homogeneous micritic matrix (visible in fresh fractures created during sampling). The samples are dense and show isolated mm-sized cavities, not interconnected. We observed a circular conduit-like feature, 1.5 cm in diameter, representing a potential pathway for methane bubbles. MDAC are covered with serpulids and sponges. Two fossilized bivalves occur at the bottom of one carbonate slab; they are in “life position” perpendicular to the expected paleo-seafloor. A sample was collected from a pinnacle-like structures dominated by fossilized bivalves and located few meters away from the carbonate slabs.

8.8 MICROBIOLOGY

At superstation 2 (900m depth), patches of white microbial mat were observed along the edge of a cliff structure (Figure 26 and Figure 30A). Microbial mats were approximately 30-50 cm wide and in variable shapes. A blue/transparent microbial mat covered the sediments not far from seepage sites (Figure 30B). Probably the result of decomposition of dead organisms.

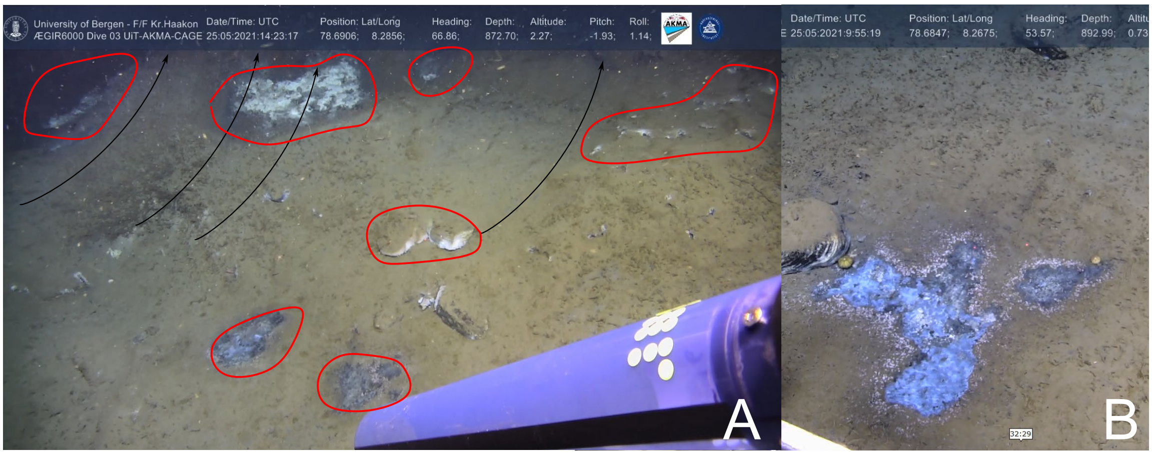

Figure 30: (A) Active sites along a cliff at Superstation 2; patches of microbial mat are indicated in red; black arrows represent the slope of the cliff approximately. (B) Blue microbial mat.

9. PRELIMINARY OBSERVATION AND RESULT: SVYATOGOR RIDGE (SUPERSTATION 4)

The Svyatogor Ridge is a sediment drift atop the inside corner high of the Knipovich Ridge – Molloy Transform Fault intersection (RTI). The RTI inside corner high is underlined by a detachment fault accommodating spreading on the Knipovich Ridge. In this area, Johnson et al. (2015) and Waghorn et al. (2018, 2020) hypothesize a contribution from abiotic methane to the gas hydrate system. South of the Svyatogor Ridge is a paleo-transform fault which, during its period of activity, contributed to tectonic deformation of the crust and overlying sedimentary sequences at the south ern end of the Svyatogor Ridge (Crane et al., 1991). The major aim of Dives and Heat Flow measurements in this area were to identify and sample evidence of past seepage activity in prominent pockmarks at the crest of Svyatogor Ridge and at supposed basement outcrop structures that delineate the hypothesized paleo-transform fault (Figure 31).

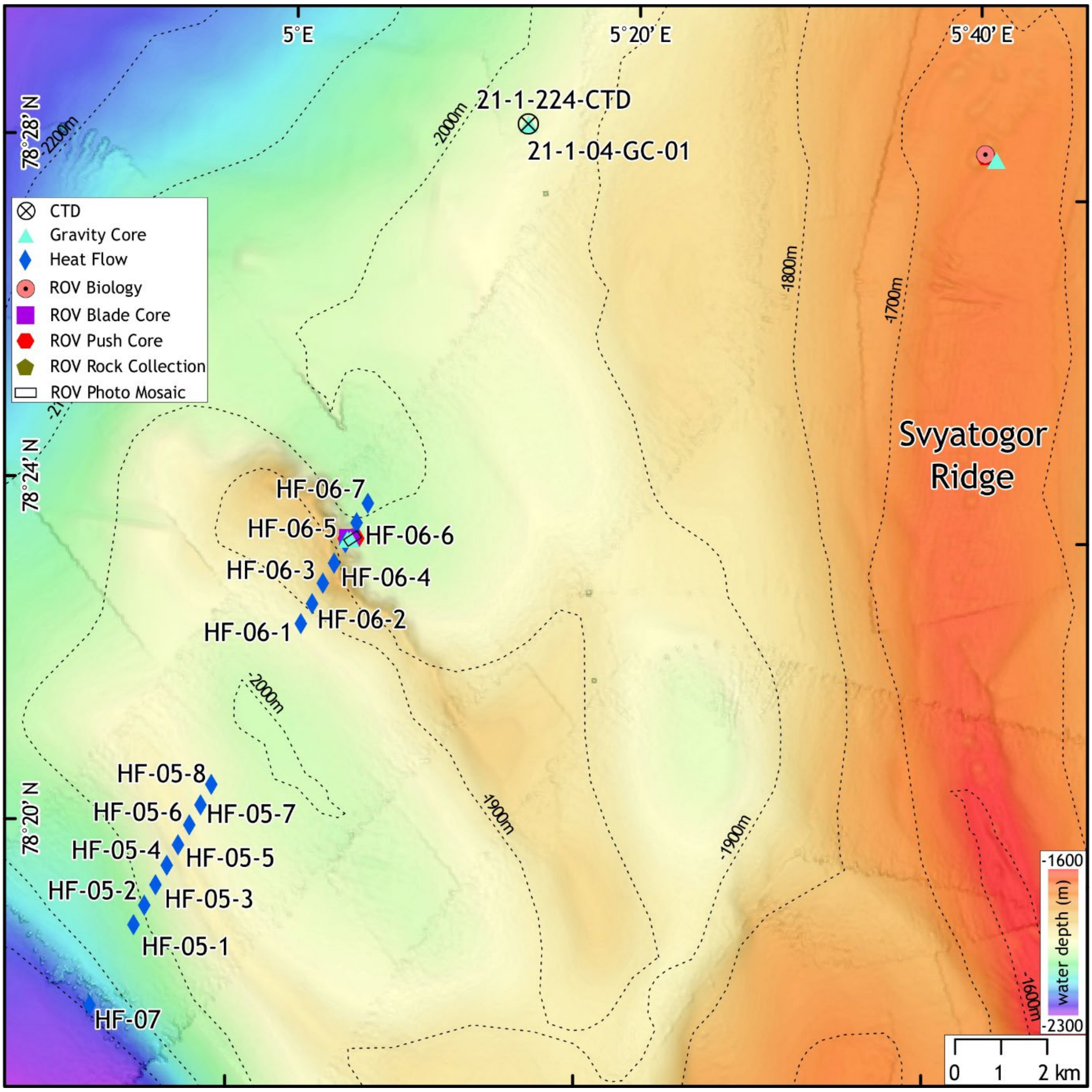

Figure 31: Map showing scientific stations in the Svyatogor Ridge area. A total of 5 Dives were conducted in this area. In addition, heat flow was measured across two prominent basement structures.

9.1 ROV VISUAL SURVEYS, DIVE LOGS

Dive 04 investigated some of the major pockmark structures on the Svyatogor Ridge (Figure 32). Here we were aiming to identify signs of past seepage activity, e.g. carbonate crusts, that could prove the hypothesis of the suspected abiotic origin of methane gas at Svyatogor Ridge.

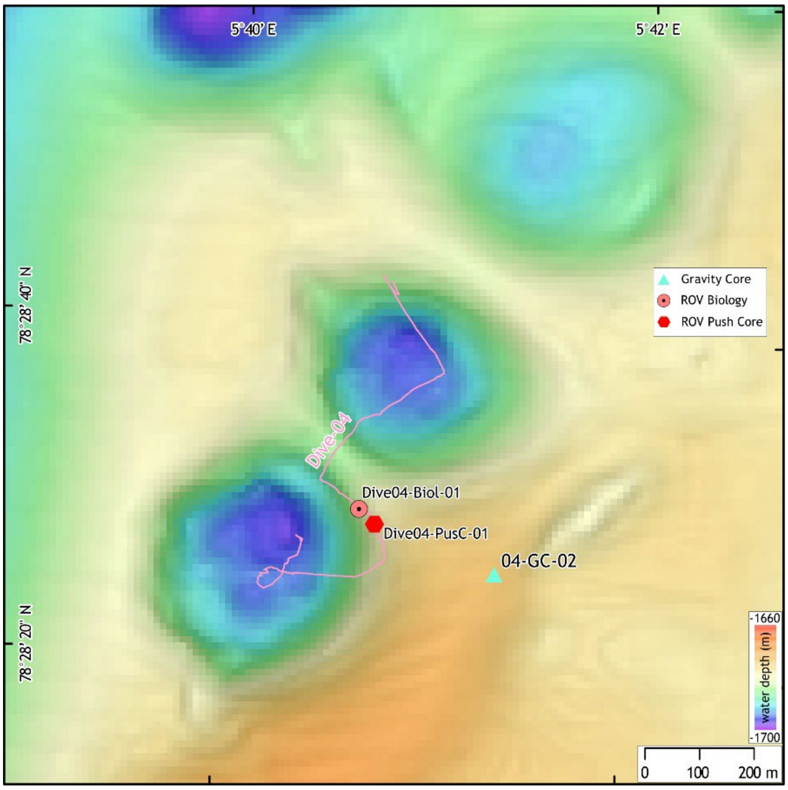

Figure 32: Two of the most prominent pockmark structures were visually inspected for any traces and signs of past seepage activity that may show a link to the hypothesized abiotic origin of the methane at Svyatogor Ridge (Johnson et al., 2015).

Water column is characterized by less evident marine snow and living organisms compared to previous sites. Seafloor consists of an overall fine sediment cover (mud) and is characterized by subtle, circle depressions covering approx. 25-40% of the seafloor in several places (Figure 33). Some of the depressions are associated with central burrows, some appear to be infilled with sediments. White shells or foraminifera are also observed on the seafloor. Both smaller (2-5 cm) and larger (30-50 cm) burrows are also observed, the latter likely produced by fish. Subangular rocks (most likely IRD) are distributed unevenly on the seafloor and some of them are colonized by sponges, anemones (2-5 cm high?) and other organisms. White crinoids (?) up to 5 cm in height and worms were also observed on the seafloor. In one area, several mounded structures with burrows and mini-sediment lobes of different colors (white to greyish) were observed. Possibly microbial origin, with evidence of bioturbation and expulsion of sediments on a small scale. One push core and one rock sample was taken during Dive 04 in this particular site (Figure 33).

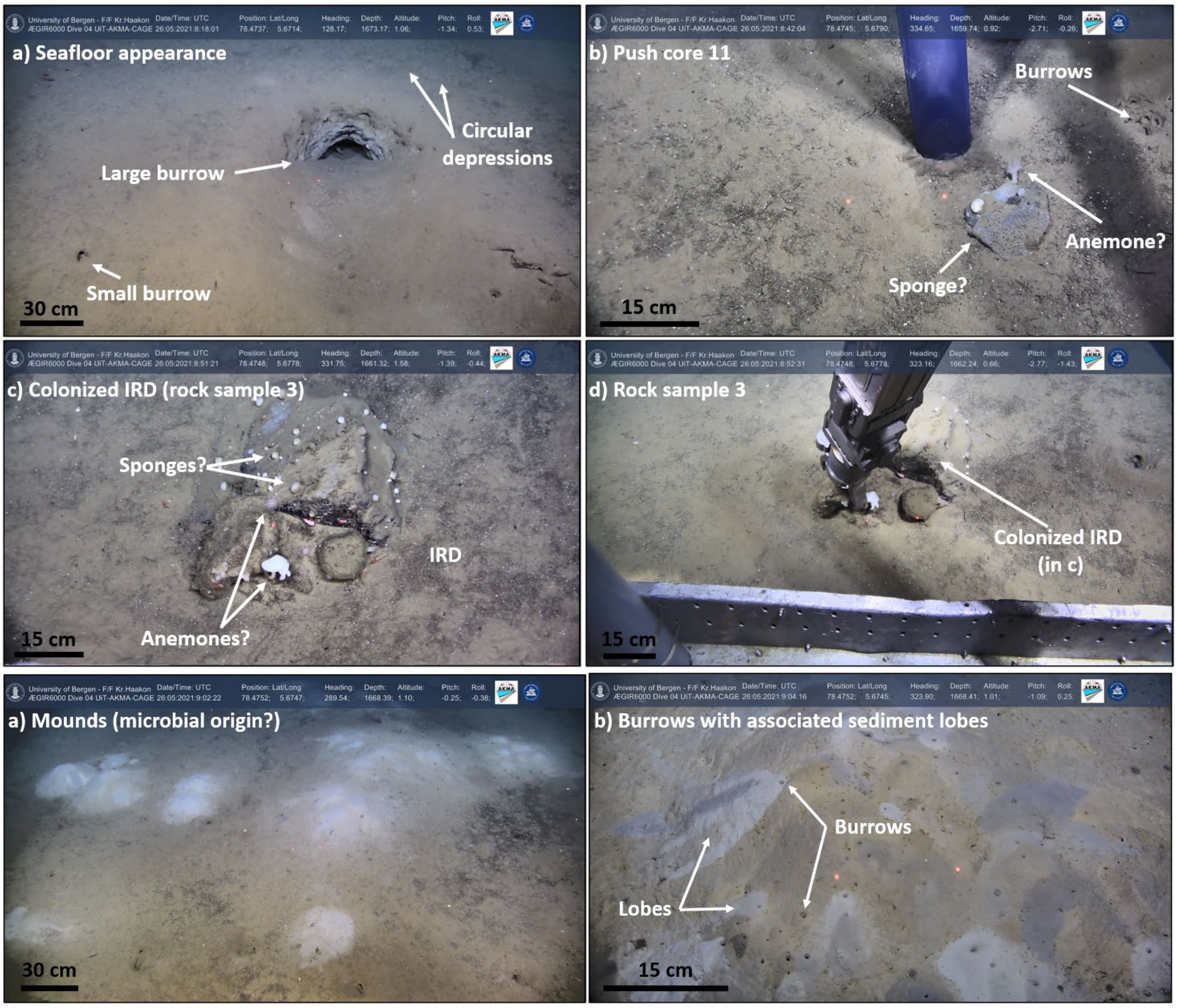

Figure 33: Images of the ROV video feed showing observations during Dive 04.

Dive 05 investigated a suspected basement outcrop, potentially associated with a paleo transform (Figure 34). The main goal was to sample basement rocks. However, the flank of the outcrop was covered with sediment and surprisingly showed significant biological activity. The seafloor appearance is similar to that observed during Dive 04, characterized by a fine sediment cover (mud), burrows (small and large) and circular depressions (Figure 35). White shells or foraminifera fragments are also observed on the seafloor. Rocks (IRD or crustal fragments?) are again distributed unevenly on the seafloor, some of them also colonized by organisms such as sponges. Mounds similar to those observed during Dive 04 also occur. Several white bacterial mats can also be observed; they could be sites of decomposition of surficial organic matter or indicate site of methane rising. One push core and two rock samples were taken during Dive 05.

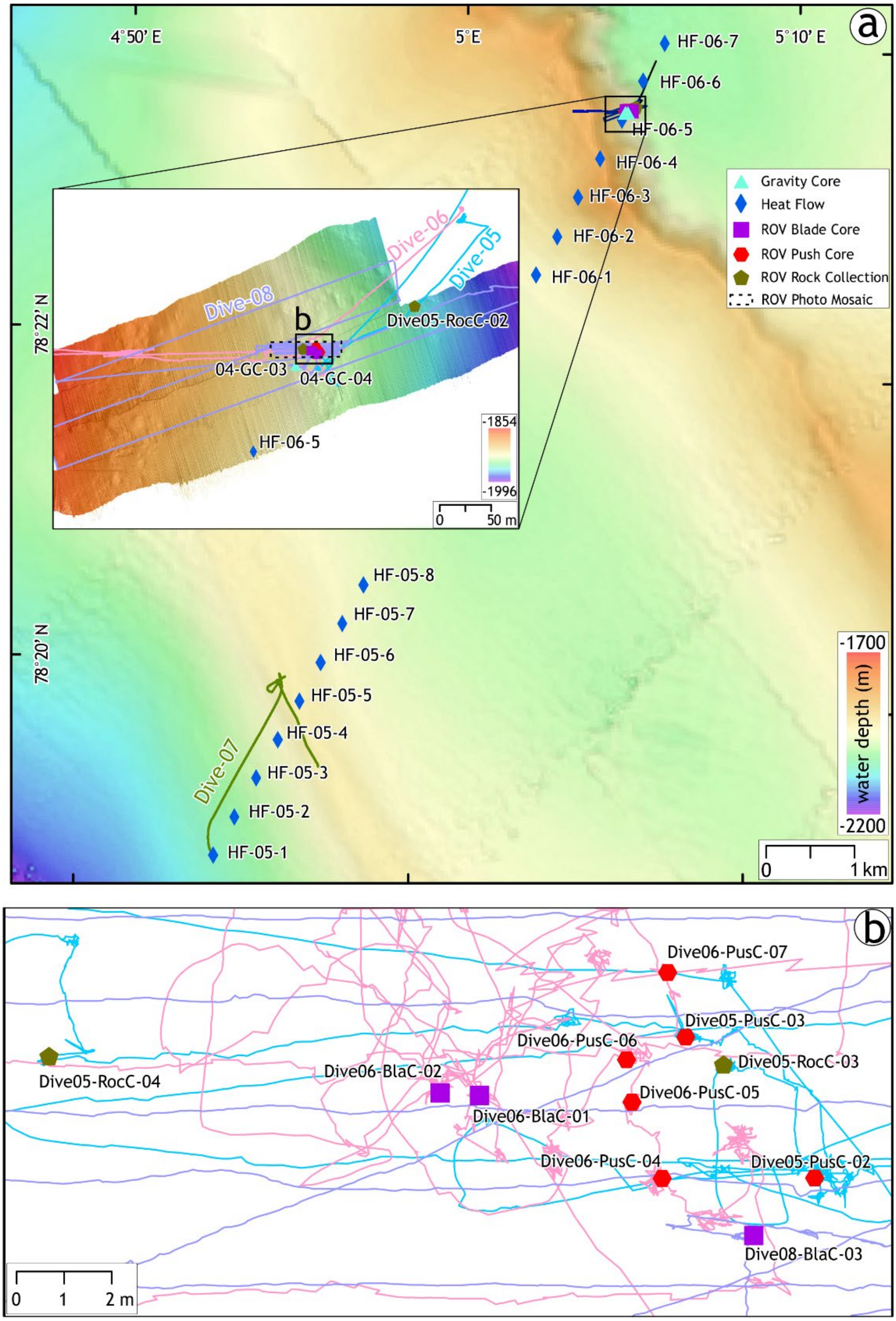

Figure 34: Overview of ROV Dives and samples at basement outcrops at Svyatogor Ridge.

Dive 06 went down to the same structure as Dive 05 and carried several additional push and blade cores for a systematic sampling of the bacterial mats (Figures 35 & 36). White material is scattered

(<5%) and could maybe be shell fragments or foraminifera. There are burrows with a diameter of approximately 1-2 cm sparsely distributed. Mounds built up by excavated material of organisms are visible. Several mats of microbes appear. The fauna of the seafloor comprises sea urchins, fish and other sediment excavating lifeforms (maybe some crustaceans). A special association worth mentioning is found in "forests" of tubeworms. There, white shrimps or amphipods, foraminifera and gastropods are living closely together with the tube worms. The seafloor shows regularly high amounts of fecal pellets.

Dive 07 investigated another but smoother basement outcrop a little further south (Figure 34). This structure has a larger sediment cover based on existing seismic data. General seafloor observations are similar to Dives 05 and 06. However, we did not observe any feature of note.

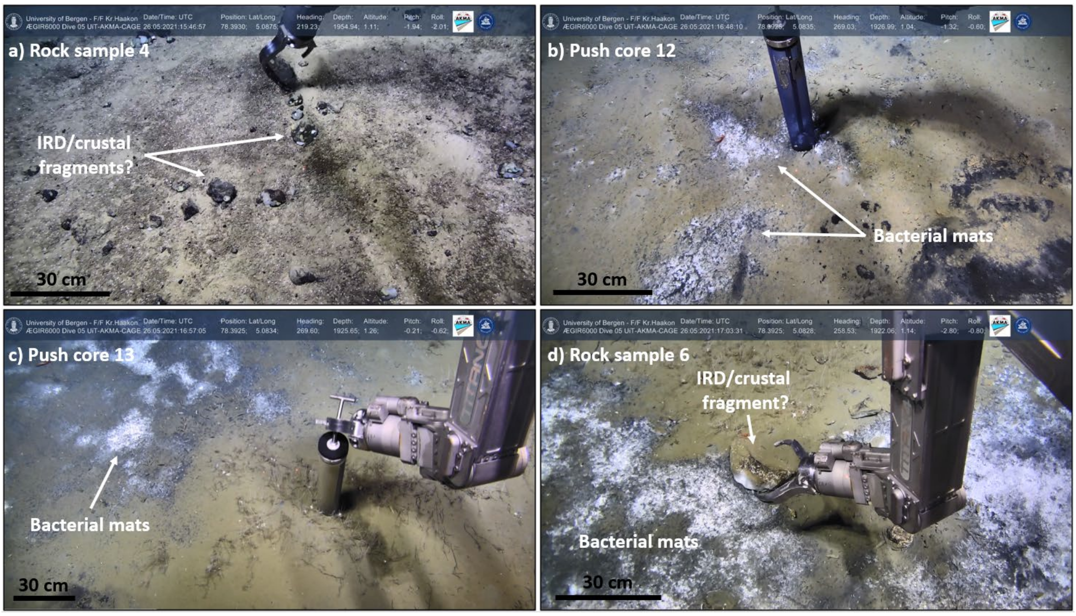

Figure 35: Dive 05 discovered several patches of bacterial mats and associated fauna on the flank of a basement outcrop with very thin sediment cover.

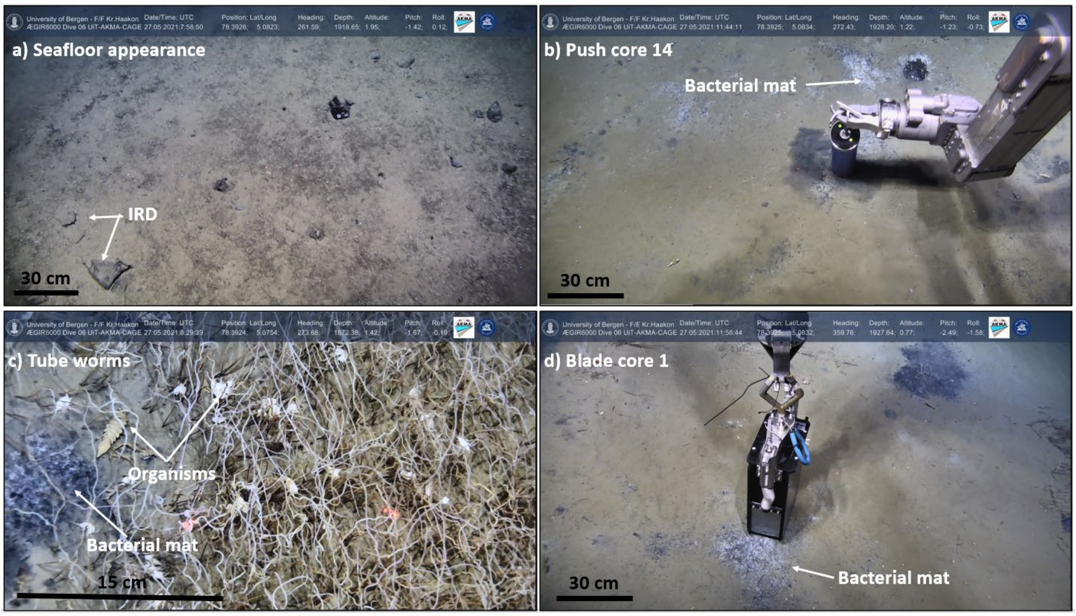

Figure 36: Seafloor observations during Dive 06.

9.2 SEAFLOOR MAPPING AND PHOTOMOSAICKING

During Dive 08 a ROV-based multibeam survey was performed at 20m of altitude, on the eastern flank of a NW-SE elongated crest of the Svyatogor Ridge, where Dive 05 and Dive 06 detected intriguing patches of bacterial mats and tubeworms (Figures 33 & 35). Three parallel, 40 m spaced multibeam lines, WSW to ENE oriented and between 350 and 500 m long, were acquired at 0.2 kn, covering a total area of 0.07 km^2, from approximately 1850 to 2000 m of water depth. During the same ROV Dive (Dive 08) a subarea was also surveyed through a downward looking camera to obtain suitable images to implement photomosaic and Structure from Motion (SfM) techniques. Videos were acquired at a constant speed of 0.2 kn and altitude of 2 meters, along 8 parallel transects, 2 m spaced and roughly 120 meters long, in order to obtain a field of view slightly larger than 2 m.

9.3 OCEANOGRAPHY, WATER COLUMN

A CTD was casted at Superstation 4 (Svyatogor Rige, station 224) for water column profiling (Figure 31).

9.4 HEAT FLOW

The highest mean thermal conductivity recorded at Svyatogor Ridge was at HF-06-05 (1.408 W/mK), and the lowest at HF-05-06 (1.207 W/mK). The mean thermal gradient based on HF-05 to HF-07 was 0.1244 K/m and the mean heat flow was 153.82 mW/m^2.

9.5 SEAFLOOR ROCK SAMPLING

During ROV operations we noticed a lot of large rock pieces on the seafloor near sites where seismic data indicates oceanic crustal rock outcropping or subcropping (Figure 33). Due to the interest in what rock type, and therefore minerals compose the oceanic crust at Svyatogor Ridge and environs, we collected some rock samples with the ROV. Visual inspection of the rock samples on board indicated a sedimentary origin (two greywackes and one coarse-grained lithified sandy limestone with many fossil shells). Therefore, these rocks were most likely deposited as Ice-Rafted Debris (IRD) and not indicative of the subsurface geology at the site.

9.6 SEDIMENT SAMPLING, SEDIMENTOLOGY & MICROPALEONTOLOGY

At superstation 4, the surface sediment of one blade core were analyzed for marine calcifiers. After wet sieving (though 100 microns mesh size) under the optical microscope we observed:

- Benthic foraminifera found attached to a tube worm (see picture from the cruise report).
- A potentially living benthic foraminifera was found in the sediment from the BlaC06 (preserved in the freezer at -80 C for DNA analyses)
- A gastropod (size ca 500 microns).

We could confirm that the shells observed during the ROV dives were foraminifera shells. They appear very shining when illuminated by the ROV lights and magnified under the lenses of the ROV camera and are clearly visible in the videos.

9.7 PORE WATER AND GAS GEOCHEMISTRY

In total, we collected 61 samples to be measured for Dissolved Inorganic Carbon (DIC) and 76 for sulfate analyses. We also collected 16 sediment samples for headspace gas. All the samples taken will be further analyzed in the laboratories at UiT. Detailed samples list available in the Appendix.

9.8 MICROBIOLOGY

At Superstation 4 wide areas with scattered microbial mats (20-50 cm diameter) were surrounded by circular outlines of tubeworms (Figure 37). Circular pattern without visible activity, perhaps extinct sites, were also scattered on the seabed.

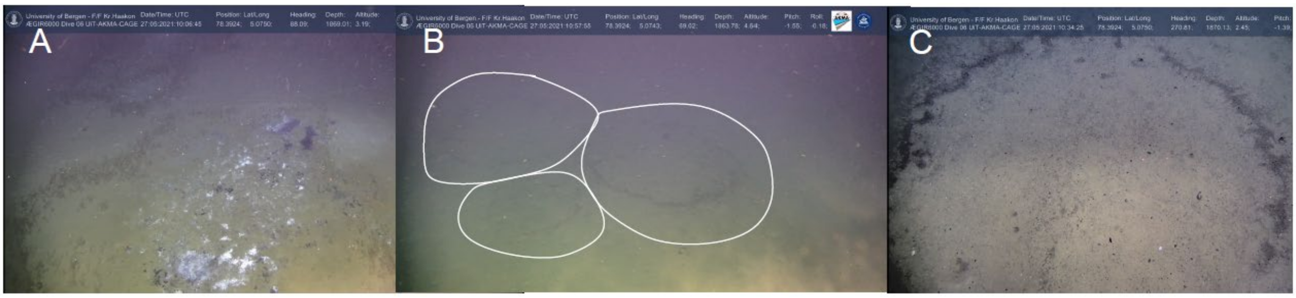

Figure 37: (A) Active sites, at Superstation 4. (B) Circular marks on the seafloor, highlighted by white lines. (C) Close up on one of the circular features at Superstation 4

Push cores taken from active methane cold seeps showed dark grey sediment throughout the core, while reference push cores appeared light grey and clayish. At the edge of a tube worms covered area, sediments taken with a blade corer did not show significant differences in color with adjacent reference sediments: a thin layer of brown oxic sediments (approximately 1-2cm) covered a 5 cm layer of black sediments (Figure 38). Deeper layers were characterized by a grey color.

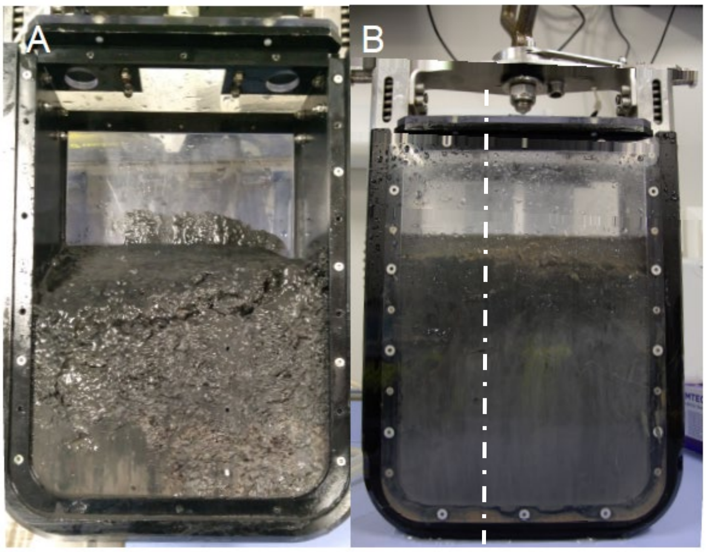

Figure 38: (A) Blade cores taken in a microbial mat covered area and (B) on the edge between tube worms hosting sediments and inactive sediments; the white dotted line indicates the separation between tube worms covered area and adjacent reference sediments.

9.9 MACROFAUNA

Overall, areas with soft sediment outside the active seepage site displayed commonly known fauna from similar depths in the region, including, stalked crinoids (*Bathycrinus cf. carpenterii*), Pandalidae shrimps, various sponges (Porifera; e.g., *Caulophacus arcticus*, including the carnivorous sponge, *Cladorhiza gelida*). Active seepage area was by opposition composed of known seep-associated fauna, including tube worm patches (*Sclerolinum contortum*), zoarcidae fishes, and Buccinidae gastropods (possibly *Mohnia sp.*), several species of Amphipods and isopods (species identification to be confirmed).

10. Preliminary observation and result: Leirdjupet Fault Complex (Superstation 5)

The Leirdjupet Fault complex is a fault system on the western flank of the Fingerdjupet basin (Figure 39). Active gas seepage was discovered here during a RV Helmer Hanssen cruise in 2017. Visual inspection using a tow camera confirmed gas bubbles from the seafloor and also showed other ample evidence of activity, e.g. bacterial mats and tube worms. The ROV related work focused on two targets in this area, a southern area, morphologically characterized by ploughmarks but showing considerable gas seepage during previous cruises, and a northern pockmark area, a large depression that also has shown gas seepage in its vicinity.

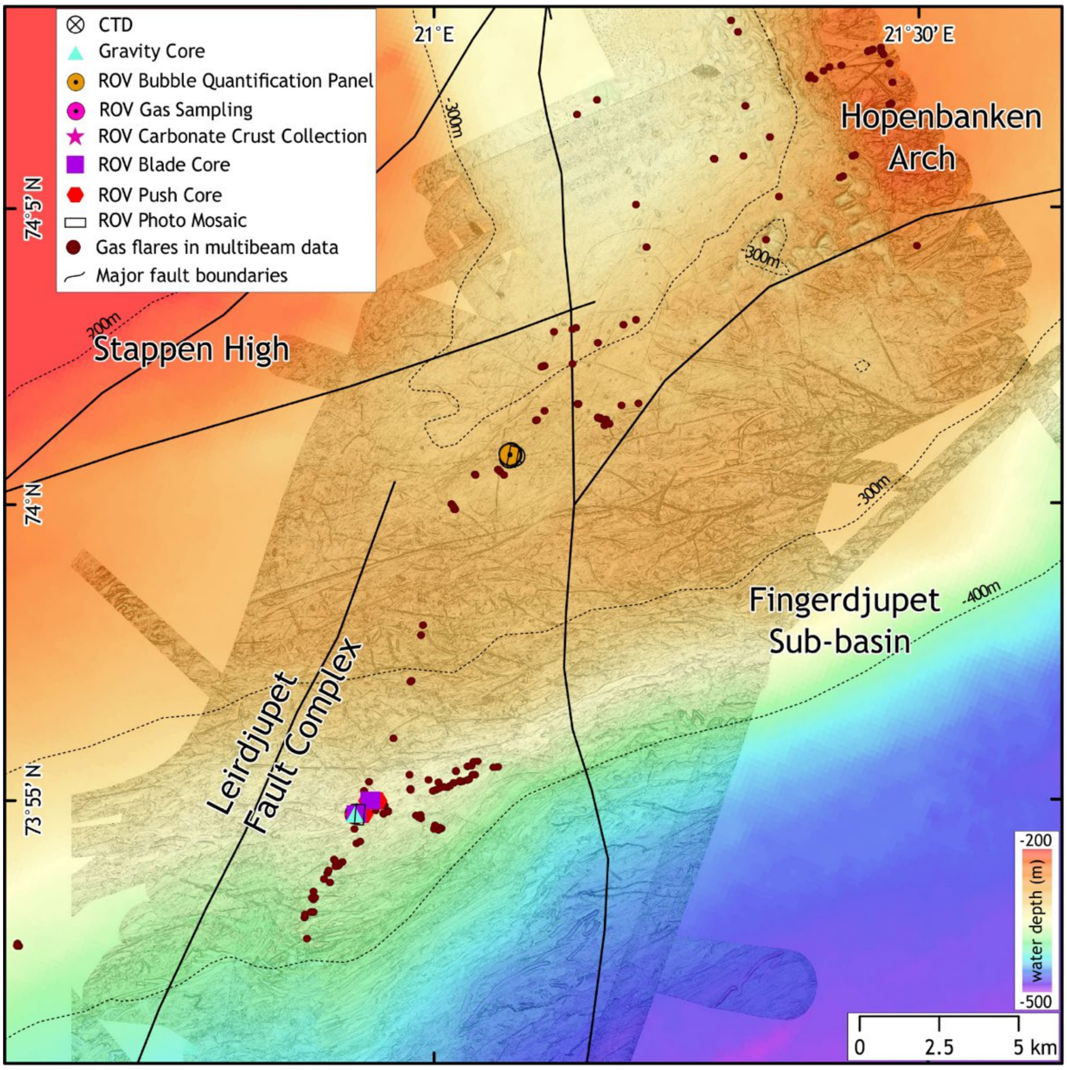

Figure 39: Overview of scientific work at the Leirdjupet Fault Complex.

10.1 ROV VISUAL SURVEYS, DIVE LOGS

8 ROV Dives (Dive 15, Dive 16, Dive 17, Dive 18, Dive 19, Dive 20, Dive 21, Dive 22) were performed at superstation 5 (Leirdjupet Fault Complex) (Figure 40 & 41).

Dive 15 at about 350 m of water depth, aimed at collecting sediment and sampling gas seepage (Figure 40). A total of 4 push cores were sampled. The seafloor appears muddy/sandy with smaller pebbles and shells, some of which are inhabited by anemones. Extensive occurrence of bacterial mats was also detected at the location where multicore sampling was done in 2018. Dive 15 was used to collect 1 gas sample and 4 push cores. The gas catcher was placed on top of a bacterial mat with gas seepage to sample the emitted gas. Furthermore 3 push core samples from bacterial mats were taken, although one of them was not successful. One reference push core was also collected outside the bacterial mats.

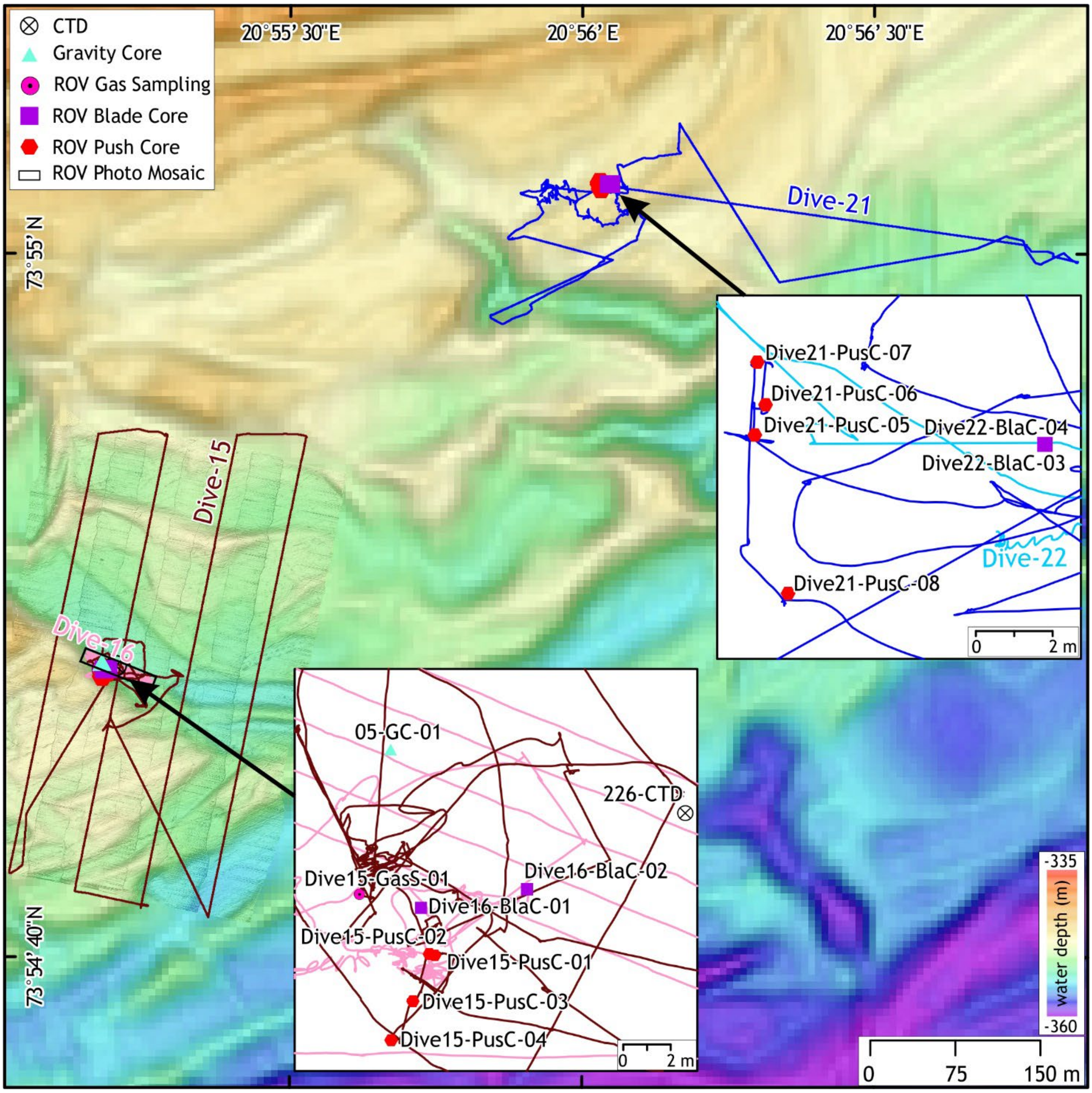

Figure 40: ROV track and sampling in the southern area, herein labelled as ploughmark area.

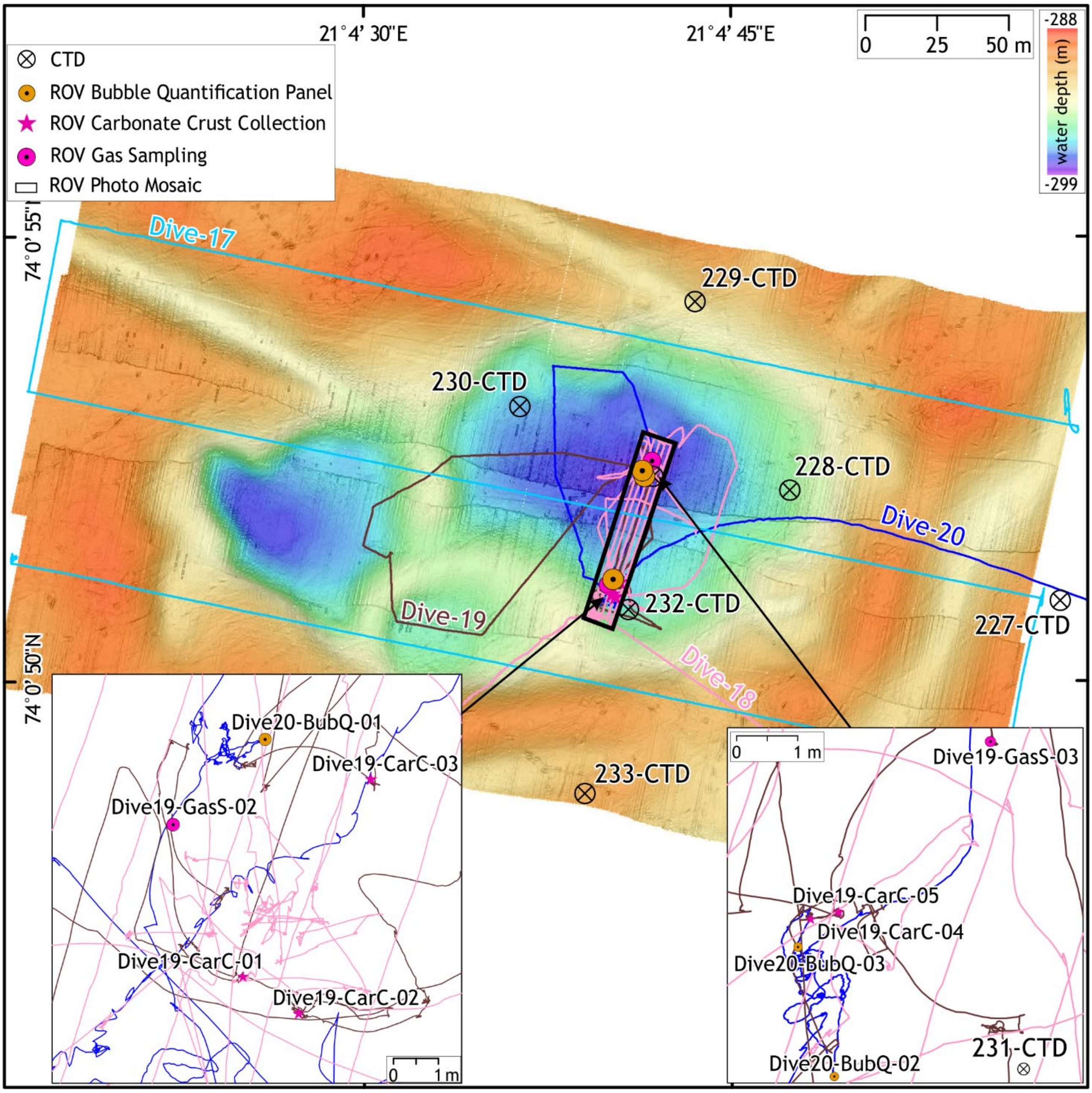

Figure 41: ROV track and sampling in the northern area, herein labelled as pockmark area.

Dive 16 performed at roughly 350 m of water depth (Figure 40), was aimed at acquiring video data suitable for seafloor photomosaic over the area sampled by Dive 15, that was typified by extensive bacterial mats. Videos were acquired using the ROV's mosaicking camera, adequately oriented toward the seafloor, to obtain images suitable for applying SfM techniques. The videos were acquired along 7 parallel transects, 2 m spaced and 100 meters long. The ROV was flying at a constant speed of 0.2 knt at roughly 2 meters of distance from the seafloor, to obtain a field of view slightly larger than 2 m, which ensures a good lateral overlap between the transects. After the successful acquisition of video data, 2 blade core samples were taken. The first blade core sampled a smaller bacterial mat which released gas during sampling. The second blade core sampled a reference area outside the bacterial mats. Dive 16 ended after sampling operations.

Dive 17 was dedicated to microbathymetry acquisition at the pockmark site (Figure 41).

Dive 18, performed at 295 m of water depth was dedicated to collect video for photomosaic and sampling (Figure 41). The seafloor looked covered by fine greyish sediment with carbonate crusts. The water column showed a lot of marine snow, which makes seeing the seafloor tricky in some places. A large part of the dive was spent near a carbonate crust where active gas seepage was visually detected. Carbonate crusts were generally characterised by abundant macrofauna (many fish, crabs, anemones etc were observed). An attempt for blade core sampling was made during the dive, but most likely because of the presence of extensive hard ground, the sampling was unsuccessful.

Dive 19, performed at 295 of water depth (same location of Dive 18), was aimed at sampling seafloor sediment (with push cores), carbonate crusts, and the escaping gas at selected sites using a gas sampler (Figure 41). The gas sampler was placed over a gas seepage site close to a relatively large carbonate crust, where also large anthropogenic trash was detected. Fragment of carbonate crusts were sampled in 2 places at the same location. The 3rd attempt to sample carbonate crust was not successful. The gas sampler was then moved to a second sampling site. During dive 19, 2 gas samples and 2 carbonate samples were thus collected. Moreover, some anthropogenic trash was collected and taken up to the ship.

Dive 20 was at the same site as Dive 18 (Figure 41). The objective was to use the checkerboard to estimate the size and velocity of the methane bubbles rising from the seafloor. The checkerboard was placed over gas seepage site that present large anthropogenic trash. We did a second attempt to measure the bubble size and we moved the checkerboard to a second sampling site. During the dive, we also picked up several pieces of plastic and other material from the seafloor.

Dive 21 was aimed at exploring the seafloor and sampling by push core (Figure 40). The seafloor was muddy and locally showed bacterial mats. Some of the bacterial mats had gas seeping from them and tubeworms living in the surroundings were also noticed. A large bacterial mat was sampled by 3 push cores. A 4th push core sample was then taken outside of that bacterial mat as a reference core.

Dive 22 was short and dedicated to sample with the blade core the same location of Dive 21 (Figure 40). Two blade core samples were successfully retrieved.

10.2 SEAFLOOR MAPPING AND PHOTOMOSAICKING

A multibeam survey was collected at SS5, Leirdjupet Fault Complex (Figure 42) in order to expand existing multibeam coverage. This survey is situated just outside the north-western boundary of the Fingerdjupet Subbasin, and between Stappen High and Hopenbanken Arch. Several features associated with gas flares such as pockmarks and depressions are present on the seafloor. On board the ship we processed a bathymetry map of the survey area with a resolution of 5m.

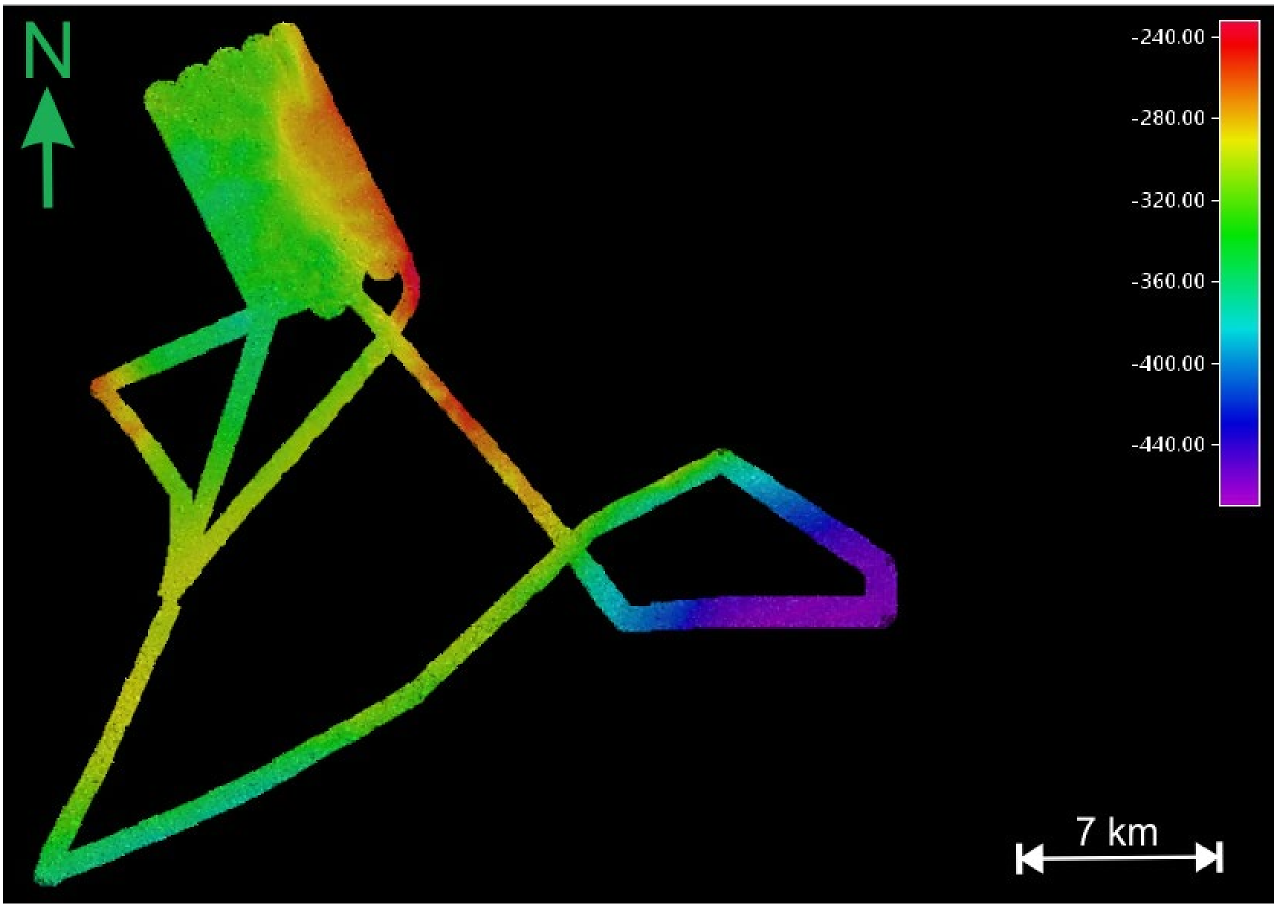

Figure 42: Bathymetric map generated from the multibeam data collected over SS5, Leirdjupet Fault Complex. The map has a 5 m resolution, making it possible to zoom in on small features. The vertical scale is in meters.

Video data for photomosaic were collected during Dive 16 and Dive 18. During both Dives videos were acquired using the downward looking ROV's mosaicking camera flying at a constant speed of 0.2 kn and an altitude of roughly 2 meters to obtain a field of view slightly larger than 2 m. Dive 16 collected a total of 7 parallel video transects, 2 m spaced and 100 meters long. Dive 18 collected 5 parallel video transects, 2 m spaced and 100 meters long and was located slightly further north, where carbonates crusts and methane bubbles emissions were sampled in Dive19.

10.3 OCEANOGRAPHY, WATER COLUMN

Preliminary results indicate that there are several gas flares and associated pockmarks situated at SS5. Studies investigating the source of these flare are ongoing, but we know (Argentino et al., 2021) that these are most likely sourced from a mixture of thermogenic and microbial degradation of organic matter. On board the ship we identified gas flares in the water column data of the multibeam dataset (Figure 43).

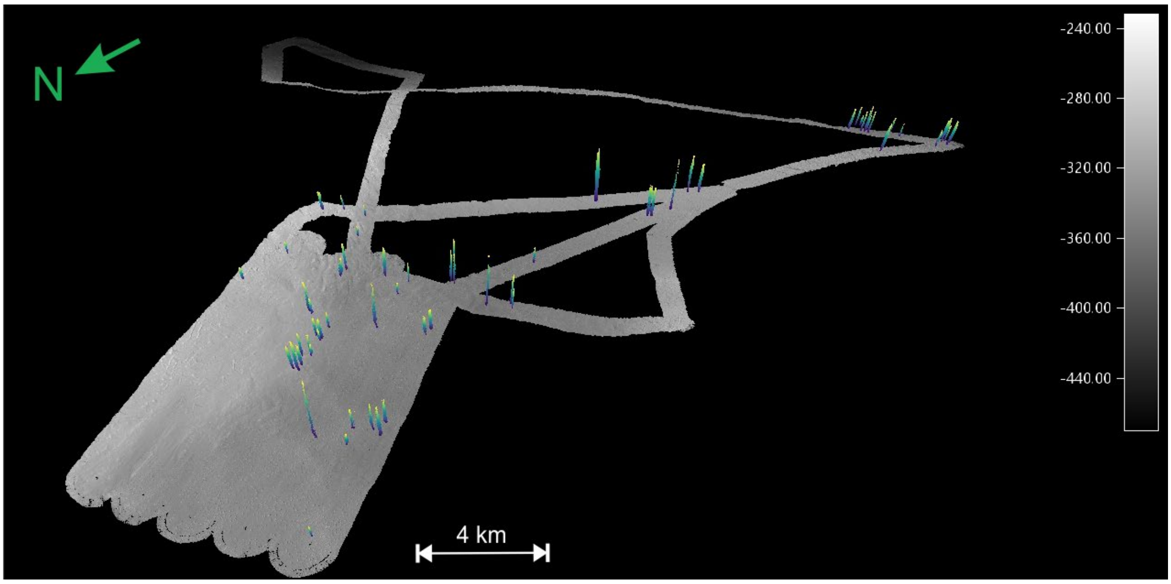

Figure 43: 3D map of the multibeam survey at SS5, highlighting the flares that were extracted from the raw multibeam data. The depth of the bathymetry map is indicated based on a grey scale (m). The mapped gas flares are displayed as vertical features in a colour scale from purple to yellow.

10.4 SEDIMENT SAMPLING, SEDIMENTOLOGY & MICROPALEONTOLOGY

We collected four push cores and two blade cores in this area (Figure 40). Of the push cores, three of them were from microbial mats. One had microbial mat remaining at the surface when opened and showed darker black sediments in the upper 2-3 cm (of one at least) and the bottom the sediment was mostly grey clay. The reference core had brownish sediments in the uppermost centimeter, black streaks in the sediments until 10 cm, and then grey clay below.

We also collected two blade cores, one from a microbial mat was black and gravelly sediments throughout. The reference core had siltier brown sediments in the upper 5 cm and then black sediments that were very sticky. The collected sediments are rich in ice-rafted debris. None of the samples were preliminary observed for micropaleontology.

10.5 PORE WATER AND GAS GEOCHEMISTRY

In total, we collected 47 samples to be measured for Dissolved Inorganic Carbon (DIC) and 66 for sulfate during 3 Dives. In this area, we collected a total of 2 headspace samples for gas geochemistry. The taken samples were stored at 4ºC and are further processed after arrival to Tromsø. Detailed samples list available in the Appendix.

10.6 METHANE-DERIVED AUTHIGENIC CARBONATES (MDAC)

The ROV manipulator arm took five carbonate samples at superstation 5. All five samples have irregular shape and have a high cavernous porosity. Sample 3 (Figure 44) is grey-brown and has very cylindrical porous conduits, a cavity (1 x 1 cm) and several black gravel inclusions up to 0,7 mm. There were two small brachiopods attached to this sample. Sample 2 is also grey to brown with several orange spots on its surface, probably due to the oxidation, and several white spots due to encrusting sponges of various sizes. It is 37 x 32 cm large and it has black gravel inclusions up to 0,7 mm large. The sample has large conduits and cavities and many channels. We could also observe aragonite crust in some areas of the carbonate. Many tubes with living serpulid polychaetas, burrows with several ophiuroids, two large anemones and several small anemones and one echinoid are attached to its surface. Sample number 5 is black on one side which can be due to partial burial in the black sediment of the sample in the seafloor (Figure 44, c). The upper side is brownish or grey. In between those sides, there is a microbial mat. This sample has many conduits. Largest cavity is 4 x 3 cm. It is highly porous (0,5 x 1-2 cm on average). Four small anemones (not removed) and one ophiuroid are attached to its surface.

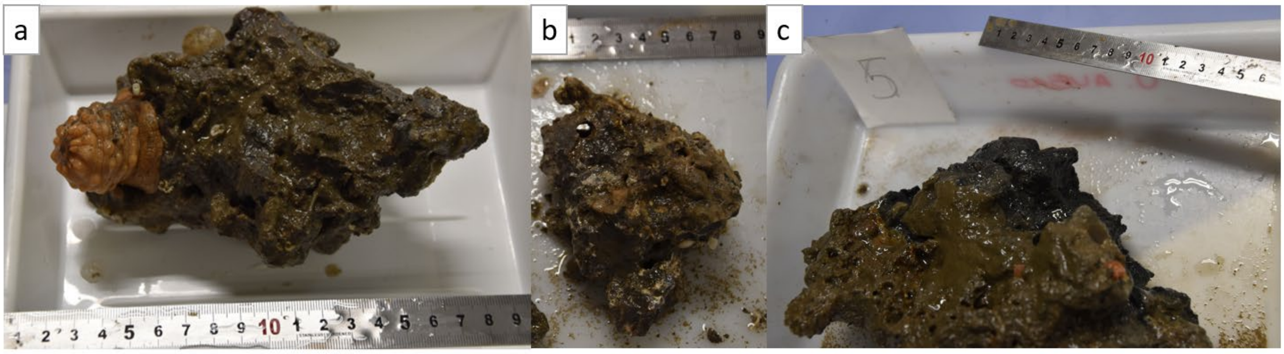

Figure 44: Samples taken with the ROV manipulator arm at superstation 5. Photo (a)- sample 2; photo (b) – sample 3; and photo (c)- sample 5.

10.7 MACROFAUNA

Overall, in both Leirdjupet Fault Complex sites, the mega-epifauna investigated was primarily composed of distinct species of anemones (Actiniaria). Carbonate crusts act as a substrate for copious amounts of Serpulidae polychaetes. Overall, the area displayed sparse presence of sponges (Porifera), Alcyonacean corals *(Gersemia sp.)*, small pycnogonids, ophiuroids and Pandalidae shrimps.

11. Preliminary observation and result: Håkon Mosby Mud Volcano (Superstation 6)

The Håkon Mosby mud volcano (HMMV) is a focused fluid/mud venting structure on the Bear Island Fan in water depth of about 1260 m (Figure 45). This mud volcano has been intensively studied over a decade ago. Recent activity was documented by long-term monitoring (Feseker et al., 2014). The seabed surface of HMMV is characterized by different biological and ecological environments and the main goal at HMMV was to sample 4 such environments for micropaleontological studies. Planning of ROV dives were guided by high-resolution (1 m grid cell size) bathymetry provided by the Woods Hole Oceanographic Institution who had acquired this data during a Maria S Merian expedition in 2010 (Boettius et al., 2013; Feseker et al., 2014). We repeated acquisition of bathymetry using the multibeam system mounted on the ROV.

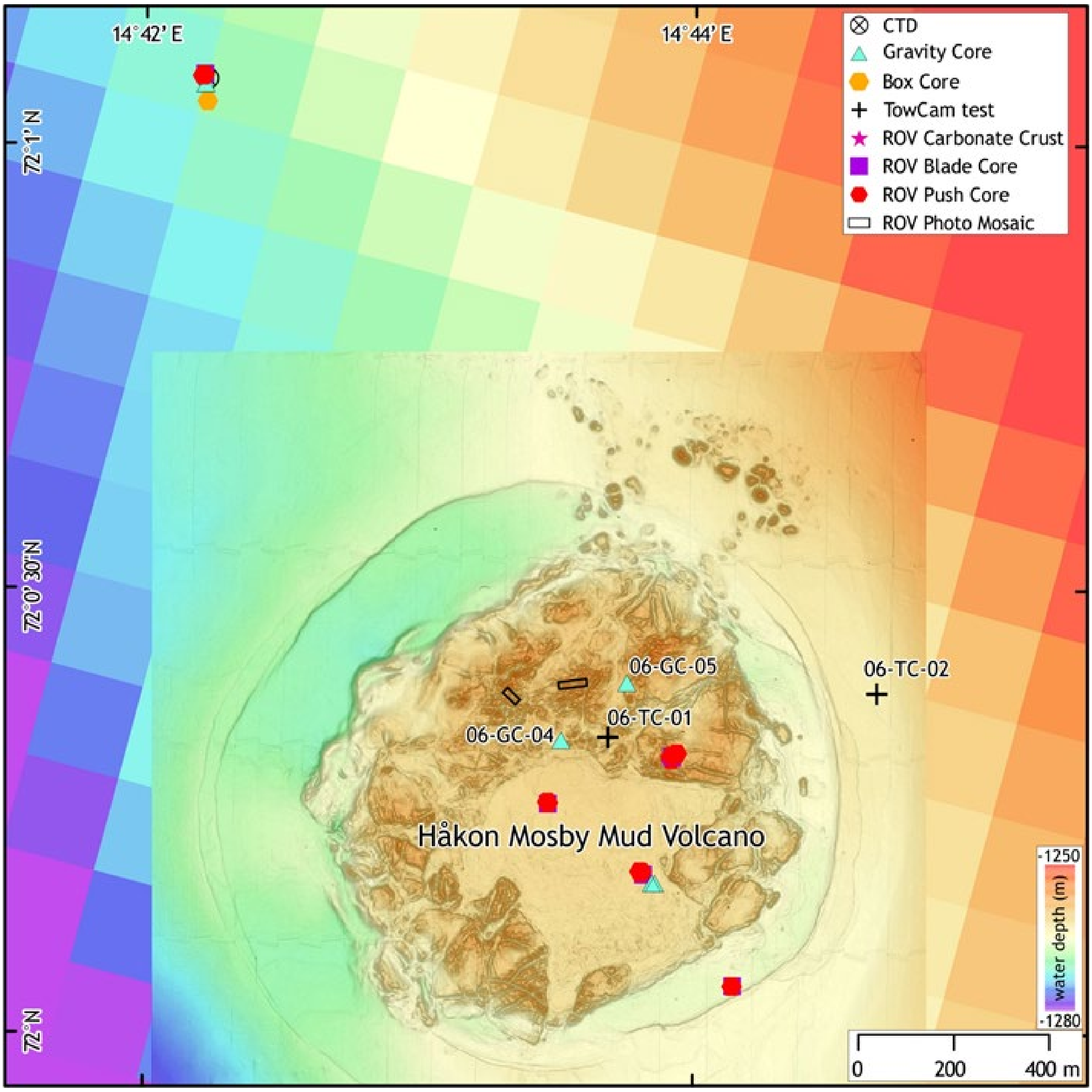

Figure 45: Overview of scientific work at Håkon Mosby Mud Volcano (HMMV). High-res bathymetry courtesy of Woods Hole Oceanographic Institution (Dana Yoerger) (Feseker et al., 2014).

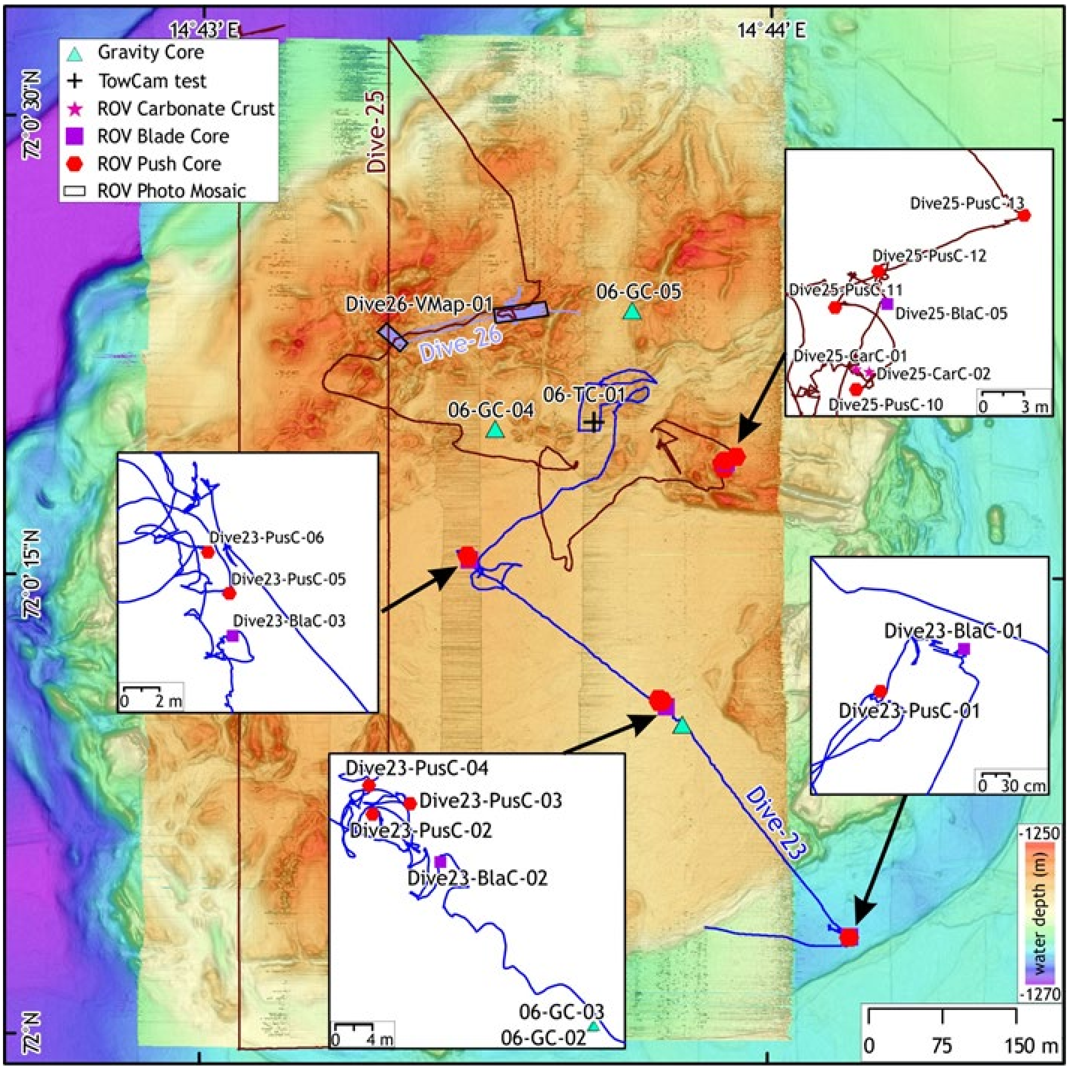

Figure 46: ROV Dive tracks and sampling locations.

11.1 ROV VISUAL SURVEYS, DIVE LOGS

At superstation 6, HMMV, the ROV did four dives (dive 23-26 – Figure 46). We used the ROV to acquire multibeam bathymetry data and photomosaic of the area, as well as to collect samples with both push cores and blade cores. In addition, some physical carbonate samples were collected.

The waters were clean with little influence of marine snow, and the seabed muddy with few clasts or input of coarser character. In areas where the mud volcano is less active (or has not been active in a long time) the seabed was covered with large bacterial mat, sometimes covering up to 70% of the seafloor. In addition, vast colonies of tubeworms were seen in between the bacterial mats. Several smaller fishes and many stingrays are living scattered around in the area. In some areas where the mud volcano is more active, there is up to 90% mud on the seabed.

11.2 SEAFLOOR MAPPING AND PHOTOMOSAICKING

Although a systematic multibeam survey was not scheduled at Superstation 6, the Simrad Kongsberg EM302 from the vessel acquired data continuously during cruise operations, over night and transit time. An area south of HMMV was mapped in much greater detail than available from existing data at UiT (Figure 47).

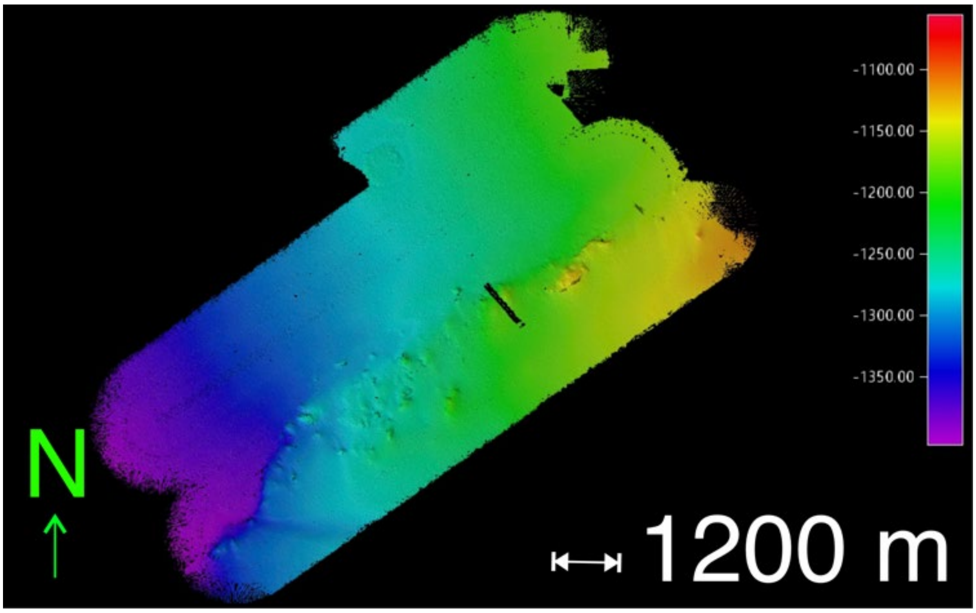

Figure 47: Multibeam lines covering parts of the Håkon Mosby mud volcano and the area bounding to the south. Vertical scale in meters.

An ROV-based multibeam survey was performed during Dive 23 and Dive 24 (Figure 46). During Dive 26, we surveyed two nearby areas in the central part of the Håkon Mosby Mud Volcano to collect video data suitable for seafloor photomosaic. The selected area is notable for the evidence of very recent eruptive activity. Indeed, in the previous Dive 24, we had the opportunity to record in real time the eruptive activity of the mud volcano from a minor fissure. The videos were acquired using the ROV's mosaicking camera, adequately oriented toward the seafloor. The first area was surveyed acquiring 6 parallel video transects, 1.8 m spaced and approximately 50 meters long. This area presented a complex seafloor morphology, and for this reason, we also added 3 transversal lines that crossed the central part of the main video transects. A small rounded depression, similar to a crater, was inspected during the second part of the dive. The video over this area was acquired along 5 parallel transects, 1.8 m spaced and approximately 30 meters long. The survey covered the spot with the observed mud eruptive event.

11.3 OCEANOGRAPHY, WATER COLUMN

A quick revision of the multibeam lines collected during transit, indicated that there was no apparent gas flaring in the area. This may be coupled with different geological aspects, but we should also note that the water depth is 1250 m in the area. Surprisingly, we observed fluid emissions during the last Dive at this site, when we observed suspended clays rising from a seafloor cavity within a feature similar to a canyon. The methane sensor on the ROV recorded an increase of methane in the water column.

11.4 SEDIMENT SAMPLING AND SEDIMENTOLOGY

We retrieved 13 push cores and 5 blade cores. Seven of the push cores were from microbial mats and two with tubeworms on the surface (Figures 46 and 48). The cores from the microbial mats were generally oozier in the upper 5 cm and higher in clay content with dark grey color compared to the cores taken on tubeworms and the reference cores. The sediments in these cores were generally more even throughout the whole core and with a distinct smell. The cores from the tubeworm field had a more brownish color in the top with 2-3 cm of oxic sediments and then a 5 to 10 cm transition to more grey and dark grey further down. No distinct smell are noticed from the tubeworm cores.

Four of the push cores were reference cores taken outside microbial mats. They did not show the dark grey and liquid type of sediments on the top compared to the microbial mats and were generally lighter in color. No clasts were observed in any of the cores. Three of the blade cores were taken on microbial mats and had a generally oozy and dark grey color throughout the whole core and with a distinct smell. Two of the blade cores were reference cores taken outside microbial mats. During the ROV dives we observed tiny whitish spot at the seafloor. After sample retrieval, observation under microscope of minor portion of seafloor sediment revealed that those were benthic foraminifera shells.

Figure 48: Push core taken on a tubeworm area shows brown oxygenated surface with tubeworms sticking out from the sediments

11.5 PORE WATER AND GAS GEOCHEMISTRY

At Håkon Mosby we collected a total of 116 samples for Dissolved Inorganic Carbon, 109 for sulfate analyses and 10 headspace samples for gas geochemistry (see list in Appendix). The samples were stored at 4ºC and are further processed after arrival to Tromsø.

11.6 METHANE-DERIVED AUTHIGENIC CARBONATES (MDAC)

We collected 2 carbonate samples exposed on the seafloor. Sample CAGE21-1-KH-06_Dive25-CarC-01 was collected from a 30 cm-tall pinnacular structure (Figure 49). Sample CAGE21-1-KH-06_Dive25-CarC-02 comes from a carbonate slab. Both samples are highly porous and have cavities (< 1 cm in diameter); they are poorly cemented and very brittle.

Figure 49: Close-up view of sample CAGE21-1-KH-06_Dive25-CarC-01.

11.7 MACROFAUNA

Mega-epifauna diversity of the area has been well described in past studies and similar observations were made during the AKMA surveys. Widespread distribution of bacterial mats and tubeworm patches (of both Oligobrachia haakonmosbiensis and Sclerolinum contortum); presence of other mega-epifaunal groups include Pygnogonids *(Colossendeis proboscide*), Zoarcidae fishes, Buccinidae gastropods, several species of Ophiuroids and anemones (Actinaria).

12. Preliminary observation and result: ROV ÆGIR6000 VIDEO MAPPING DIVES

Using photogrammetry underwater is still in an exploratory phase, and relatively few SfM surveys have been carried out in the deep-sea due to the difficulty of acquiring controlled images at depth with appropriate illumination. High performed work-class ROVs, such as the AEGIR6000 ROV, however, can collect suitable images and data. An experimental methodological protocol was therefore designed on board, focusing on defining (1) camera position and orientation, (2) intensity and coverage of lighting on the footage, (3) survey speed and altitude, and (4) appropriate overlap between adjacent lines, in accordance with the complexity and morphological attributes of the topography of the surveyed seabed.

Preliminary data processing on 5 of the 6 «video mapping» ROV dives (Dive 09, 11, 16, 18, 26), showed the extent to which the followed procedure was particularly critical to follow in order to obtain reliable results, which consist of a seamless high resolution (i.e.: sub centimetre) orthomosaic of the ROV surveyed areas and associated 3D models.

To implement data processing, one frame per second was extracted from each video footage, using VLC Media Player. The images were imported into Agisoft Photoscan Professional (v. 1.3.4.5067) applying the dedicated workflow for 3D reconstruction. High-quality dense clouds were created for each ROV transect. Dense clouds were subsequently georeferenced (based on the ultra-short baseline (USBL) ROV positioning system and data obtained from microbathymetry when available) and optimised for scale using information from ROV point lasers, spaced 14 cm apart, as a reference scale detected at multiple flat locations within each 3D reconstruction. The outputs were exported as digital elevation models (DEM) and orthomosaics at the highest resolution (predominantly ~ 1 mm per pixel).

Agisoft Photoscan Professional was not always able to achieve a successful alignment between photos from parallel transects, especially in the predominantly flat areas with low morphological complexity (i.e. Dive 16, 11, 18). Having the camera orthogonal to the subject is therefore not an absolute requirement for 3D reconstructions. Our results highlighted instead the need of consistent overlap between adjacent line (at least 40%) on flat regions and homogeneous illumination, to ensure good alignment of captured frames between all video transects. In addition, the sloping and complex topography typifying the seafloor mapped at the North Knipovich Ridge (Dive 09) and on the Håkon Mosby mud volcano (Dive 26), that prevented true nadir camera angle, showed the slightly angled ROV camera against the rugged topography was actually favourable for 3D reconstructions, as assessed from our preliminary 3D processing, that was particularly successful in these regions.

Both DTMs and orthomosaics obtained from our processing show to be integral to the understanding of the high lateral small-scale variability and complexity of cold seep systems, which represent a relevant knowledge gap in the understanding of their ecological functioning and of biogeochemical processes taking place on them.

13. EDUCATION and OUTREACH

13.1 Education

Onshore seminars

Prior the cruise, there was a two-day crash-course which covered the main topics of the AKMA project. The course was organized at UNIS in Longyearbyen, and the goal was to inform the participants of the main expedition objectives and the AKMA project. Scientists from the University of Tromsø provided physical lectures while the colleagues from WHOI (USA) provided digital lectures.

Onboard seminars

During both legs of the cruise, the education component of the 2021 AKMA Expedition continued with remote lectures from WHOI and lectures provided by scientists onboard. The topics covered were part of the AKMA scientific goals alongside methodologies used to collect data at sea. The seminars were organized during transits and evenings. Details about the seminars are provided in Table 1.

Hands-on experiments and work

Students onboard participated actively in the sampling operations and sample treatment. The operations onboard were presented and discussed during a science meeting each evening.

Student evaluation

At the end of the cruise, the students receive an evaluation form to be filled where they could assess the crash course done before the cruise and the lectures and practical activities onboard.

The questions in the student evaluation form are below:

1. *What did you like most about the AKMA cruise?*
2. *What did you like least about the AKMA cruise?*
3. *What topics (pertaining to AKMA) would you like covered in more depth?*
4. *Do you think there are any topics that we should develop more in practical/lab-based work?*
5. *How can the AKMA cruise be improved?*
6. *Do you think your educational background was enough to get the best out of the cruise? May you explain why?*

13.2 Outreach

POLARoid Project

Details are provided in the “Polaroid project” document

Virtual Expedition

In November 2020 G. Panieri, A. Savini and M. Lindgren were on board of KPH to collect the material for developing an interactive virtual expedition. The virtual environment focused primarily on the life and people aboard the research vessel. Crew members were filmed and interviewed, giving input on their respective role and duties onboard. The virtual cruise includes content (instrument description, purposes of samplings, data acquisition) in the 360° images and 360° videos of all the decks and laboratories and builds up tailored teaching material for students unable to physically access a research vessel.

Documentary

During the AKMA expedition Giuliana Panieri, Dimitri Kalenitchenko, and Sunil Vadakkepuliyambatta have filmed and provided interview for the PBS Permafrost Documentary produced by Blink Films. Blink Film is a BAFTA award-winning production company based in London and Ireland. Our programmes are known for their intelligence, warmth and creativity. The Documentary will be released in December 2021. The AKMA project will be acknowledge.

Student Outreach

As science communication is an increasingly valued skill for an Early Career Researcher, the AKMA Expedition tried to also cover an outreach aspect in the evaluation of the course. Therefore, the candidates onboard contributed a blog post or video for outreach. Everyone selected a topic related to the expedition The candidates were asked to target their contribution towards a ‘youth and general public’ audience, in both language use and writing style (for example, avoiding jargon and thinking about how to make a ‘mundane’ topic engaging through writing style). Some students opted to write about the science undertaken aboard the ship while others displayed other elements such as life aboard the ship or the cooperative nature of research expeditions. All blogs and videos will be uploaded to the website and other social media platforms over the course of the post-expedition period.

Example of the blog and video can be seen here: https://akma-project.com/expedition-blog

Social Media

We created short-form content for both Twitter and Instagram pertaining to discoveries and activities before, during and after the expedition. We posted content on daily, with Instagram stories and IGTV used for short movies (i.e. ROV launch) aimed to inform about general daily life aboard the Kronprins Haakon and scientific operations while twitter outreach was aimed towards parts the scientific community would find interest in. In the short term, we found Instagram has reached a younger generation (the school students participating in the Polaroid project, among others) and also other followers interested in polar research. Interaction with content on Twitter, alternatively, has been primarily users associated with Earth Science already, and predominantly Early Career Researchers. Our most viewed twitter post was 'Lending a (Mechanical) Hand' – regarding a blog post by PhD Candidate Przemeslaw Domel with 280 views (of the full tweet) within the first 12 hours, however people followed the link to the post only 6 times, whereas our post on World Ocean Day received less views but more users following the link to the post. Instagram requires 10,000 followers for full analytic services, so it is difficult to make statements about whether our posts are engaging users to read our material. Using specific hash tags (for example Arctic, or PolarScience, AKMA project, Arctic science, Expedition), we expand the number of non-following accounts that we reach.

2021 World Ocean day

To celebrate the 2021 World Ocean day, two videos were made. One video was uploaded on EGU and UiT website on June 8. The video was made during the second leg of the cruise and describes the operations and sampling activities onboard. Each participant was asked to write on a paper a short description of the operation in which she/he was involved and show it to the camera. Short explanatory captions (max 40 characters) were included in the video. The video was made by M. Bulinova (PhD student on board).

A second video was uploaded on YouTube, on 8 June at 10:00 am, as part of the material provided by the University of Milano bicocca for the second fully virtual celebration of United Nations World Oceans Day, on 8 June 2021, that highlight the theme of The Ocean: Life and Livelihoods (https://unworldoceansday.org/).

On this celebratory occasion, in the first year of the Decade of Ocean Science for Sustainable Development, students from Milano-Bicocca university and researchers shared, in short videos, their current activities related to the pursuit of the Sustainable Development Goals, and particularly SDG 14. This activity offers diverse perspectives from the field in different disciplines related to oceanic studies (https://unworldoceansday.org/events/milano-bicocca-studia-gli-oceani/). A. Savini produced the video.

Table 1. Education (yellow) and outreach (light blue) activities performed during the AKMA cruise

Date	Time	Speaker	Title
22nd	1800-1900	Maximilian Weber (IG student on board)	Geology of Svalbard
		Alessandra Savini (UniMiB, IT)	ROV imaging using ROV Ægir

	1600-1700	Claudio Argentino	Pore water chemistry and sampling techniques
	1800-1900	Claudio Argentino Giuliana Panieri, (CAGE UiT)	Everything you should know about Proxies
	1830-1930	Sunil Vadakkepuliyambatta (CAGE UiT)	Heat flow measurements
24th	2000-2100	Dan Fornari (WHOI, USA)	Mid-Ocean Ridges and seafloor mapping techniques
25th	1200-1300	Claudio Argentino and AKMA team with IESS High School, Reggio Emilia, IT	"Life on board" AKMA-Polaroid project
	2000-2100	Andy Bowen (WHOI, USA)	"Exploring the oceans with undersea robots"
27th	1400-1500	CAGE seminar in Tromsø NO	AKMA team presents the cruise
28th	1030-1130	Kate Waghorn and AKMA team with Giordano Bruno Institute, Medicina (BO), Italy	"Life on board" AKMA-Polaroid project
	1400-1500	Sunil Vadakkepuliyambatta and AKMA team with TRINT International school in Tromsø, NO	"Life on board" AKMA-Polaroid project
	1615 -1645	Giuliana Panieri, Invited talk, PaleoARC 2nd International Conference PalaeoArc Processes and Palaeo-environmental changes in the Arctic: from past to present	Tracing past methane emissions in the Arctic Ocean
	2000-2100	Joan Bernhard (WHOI, USA)	Fascinating foraminifera: chemocline adaptations and methods for study
30th	End of 1st Leg, start of 2nd Leg		
31st	2000-2100	Dan Fornari (WHOI, USA)	Mid-Ocean Ridges and seafloor mapping techniques
1st	1530-1700	Sofia Ramalho (Aveiro University, Portugal)	Meiofauna from Extreme Environments
		Luca Fallati (UniMib, Italy)	ROV structures from motion

		Sunil Vadakkepuliyambatta (CAGE, UiT)	Heat flow measurements
	2000-2100	Joan Bernhard (WHOI, USA)	Fascinating foraminifera: chemocline adaptations and methods for study
2nd	0900-1000	Dimitri Kalenitchenko from the school Lycée sacré Coeur, Tourcoing in France connected with the AKMA team on board	"Life on board" AKMA-Polaroid project
	1530-1700	Claudio Argentino Giuliana Panieri, (CAGE UiT)	Everything you should know about Proxies
		Kate Waghorn	Leirdjupet fault complex
	2000-2100	Andy Bowen (WHOI, USA)	Exploring the oceans with undersea robots
3rd	1100-1200	Dimitri Kalenitchenko from the school Giordano Bruno; medicina in Italy connected with the AKMA team on board	"Life on board" AKMA-Polaroid project
	2000-2100	Dan Fornari (WHOI, USA)	Mid-Ocean Ridges and seafloor mapping techniques
4th	1100-1200	Dimitri Kalenitchenko from the school Giordano Bruno, Medicina in Italy connected with the AKMA team on board	Dimitri Kalenitchenko from the school in Italy connected with the AKMA team on board
	1215-1315	Department of Geosciences UiT " Friday Seminar"	The AKMA team presents the cruise to the Department of Geosciences and NT Fak at UiT and to the Norwegian Research Council
	2000-2100	Marie-Anne Blanchet, (NPI, Tromsø, NO)	Marine mammals in Svalbard
7th	1330-1400	Chess Annual Meeting	The AKMA team presents the project and the cruise
8th		World Ocean Day	The AKMA team launch a blog and video to celebrate the World Ocean Day in European Geosciences Union EGU https://blogs.egu.eu/divisions/bg/2021/06/08/world-ocean-day-2021/ and UiT websites https://www.youtube.com/watch?v=Y5x7YPzWyXw and in the The Ocean: Life and Livelihoods (https://unworldoceansday.org/)

The schools involved in the AKMA Polaroid project:

- TRINT, Tromsø International School, NO

https://www.trint.org

- Lycée sacré Coeur

111 rue de Lille
59200 Tourcoing FR

https://www.essc-lycee-sacrecoeur.fr

Blog post on AKMA on the school website: https://www.essc-lycee-sacrecoeur.fr/clubs/

- Liceo e Professionale Commerciale Giordano Bruno

Via Caduti di Cefalonia,57 40059 Medicina IT
https://www.iisgiordanobruno.edu.it/pagine/la-sede-di-medicina-liceo-e-professionale-commerciale

- 1 Istituto Europeo di Studi Superiori S.C.S. – Reggio Emilia, IT

https://www.iess.it/en/school/what-is-iess/

Blog post on AKMA on the school website: https://www.iess.it/notizie/news-home/akma-polaroid-project/

14. ACKNOWLEDGEMENT

We would like to thank Captain Johnny Peder Hansen, the Officers and Crew of the RV Kronprins Haakon for the valuable assistance at sea. This expedition was partially supported by the Research Council of Norway through AKMA Advancing Knowledge on Methane in the Arctic (project number 287869), an industry-funded research grant by Aker BP Norway and Centre of Excellence on Gas Hydrates, Environment and Climate (CAGE) (Norwegian Research Council (NFR) project number 223259/F5 at UiT the Arctic University of Norway.

15. REFERENCES

Argentino, C., Waghorn, K. A., Vadakkepuliyambatta, S., Polteau, S., Bünz, S. and Panieri, G.: Dynamic and history of methane seepage in the SW Barents Sea: new insights from Leirdjupet Fault Complex, Sci. Rep., 11(1), doi:10.1038/s41598-021-83542-0, 2021.

Bernhard, J. M., Ostermann, D. R., Williams, D. S., and Blanks,J. K.: Comparison of two methods to identify live benthicforaminifera: A test between Rose Bengal and CellTracker Greenwith implications for stable isotope paleoreconstructions, Paleoceanography, 21, 8 pp., doi:200610.1029/2006PA001290, 2006.

Boetius, A. et al. LOOME - Cruise No. MSM16/2 - September 24 - October 08, 2010 - Tromsø - Tromsø (Norway). Report No. 2195-8483, 1-46, doi.org/10.2312/cr_msm16_2, (DFG-Senatskommission für Ozeanographie;, Bremen, 2013).

Bünz, S., Polyanov, S., Vadakkepuliyambatta, S., Consolaro, C. and Mienert, J.: Active gas venting through hydrate-bearing sediments on the Vestnesa Ridge, offshore W-Svalbard, Mar. Geol., 332–334, 189–197, doi:10.1016/j.margeo.2012.09.012, 2012.

Crane, K., Sundvor, E., Buck, R. & Martinez, F. Rifting in the northern Norwegian-Greenland Sea: Thermal tests of asymmetric spreading. Journal of Geophysical Research: Solid Earth 96, 14529-14550, doi:https://doi.org/10.1029/91JB01231, 1991.

Engen, O., Faleide, J. I. & Dyreng, T. K. Opening of the Fram Strait gateway: A review of plate tectonic constraints. Tectonophysics 450, 51-69, doi:10.1016/j.tecto.2008.01.002, 2008.

Etiope, G. & Sherwood Lollar, B. Abiotic methane on earth. Reviews of Geophysics 51, 276-299, doi:https://doi.org/10.1002/rog.20011, 2013.

Faleide, J. I. et al. Late Cenozoic evolution of the western Barents Sea-Svalbard continental margin. Global and Planetary Change 12, 53-74, 1996.

Feseker, T. et al. Eruption of a deep-sea mud volcano triggers rapid sediment movement. Nat Commun 5, doi:10.1038/ncomms6385, 2014.

Hustoft, S., Bünz, S., Mienert, J. & Chand, S. Gas hydrate reservoir and active methane-venting province in sediments on <20Ma young oceanic crust in the Fram Strait, offshore NW-Svalbard. Earth and Planetary Science Letters 284, 12-24, 2009.

Johnson, J. E., Mienert, J., Plaza-faverola, A., Vadakkepuliyambatta, S., Knies, J., Bünz, S., Andreassen, K. and Ferré, B.: Abiotic methane from ultraslow-spreading ridges can charge Arctic gas hydrates, , (5), 371–374, doi:10.1130/G36440.1, 2015.

Kelley, D. S., Karson, J. A., Früh-Green, G. L., Yoerger, D. R., Shank, T. M., Butterfield, D. A., Hayes, J. M., Schrenk, M. O., Olson, E. J., Proskurowski, G., Jakuba, M., Bradley, A., Larson, B., Ludwig, K., Glickson, D., Buckman, K., Bradley, A. S., Brazelton, W. J., Roe, K., Elend, M. J., Delacour, A., Bernasconi, S. M., Lilley, M. D., Baross, J. A., Summons, R. E., and Sylva, S. P., A Serpentinite-Hosted Ecosystem: The Lost City Hydrothermal Field: Science, v. 307, no. 5714, p. 1428-1434, 2005.

Laberg, J. S. & Vorren, T. O. A Late Pleistocene Submarine Slide on the Bear Island Trough Mouth Fan. Geo-Marine Letters 13, 227-234, 1993.

Langlet, D., Baal, C., Geslin, E., Metzger, E., Zuschin, M., Riedel,B., Risgaard-Petersen, N., Stachowitsch, M., and Jorissen, F. J.:Foraminiferal species responses to in situ experimentally inducedanoxia in the Adriatic Sea, Biogeosciences. 11, 1775–1797, 2014

Langlet, D., Geslin, E., Baal, C., Metzger, E., Lejzerowicz, F., Riedel, B., Zuschin, M., Pawlowski, J., Stachowitsch, M., and Jorissen, F. J.: Foraminiferal survival after long-term in situ experimentallyinduced anoxia, Biogeosciences. 10, 7463–7480, 2013

Milkov, A. et al. Geological, geochemical, and microbial processes at the hydrate-bearing Hakon Mosby mud volcano: a review. Chemical Geology 205, 347-366, 2004.

Panieri, G., Bünz, S., Fornari, D. J., Escartin, J., Serov, P., Jansson, P., Torres, M. E., Johnson, J. E., Hong, W. L., Sauer, S., Garcia, R. and Gracias, N.: An integrated view of the methane system in the pockmarks at Vestnesa Ridge, 79°N, Mar. Geol., 390(June), 282–300, doi:10.1016/j.margeo.2017.06.006, 2017.

Pape, T., Feseker, T., Kasten, S., Fischer, D. and Bohrmann, G.: Distribution and abundance of gas hydrates in near-surface deposits of the Håkon Mosby Mud Volcano, SW Barents Sea, Geochemistry, Geophys. Geosystems, 12(9), doi:10.1029/2011GC003575, 2011.

Pucci, F., Geslin, E., Barras, C., Morigi, C., Sabbatini, A., Ne-gri, A., and Jorissen, F.: Survival of benthic foraminifera un-der hypoxic conditions: Results of an experimental study usingthe CellTracker Green method, Mar. Pollut. Bull., 59, 336–351,2009.

Serck, C. S., Faleide, J. I., Braathen, A., Kjølhamar, B. and Escalona, A.: Jurassic to Early Cretaceous basin configuration(s) in the Fingerdjupet Subbasin, SW Barents Sea, Mar. Pet. Geol., 86, 874–891, doi:10.1016/j.marpetgeo.2017.06.044, 2017.

Sultan, N., Plaza-Faverola, A., Vadakkepuliyambatta, S., Buenz, S. & Knies, J. Impact of tides and sea-level on deep-sea Arctic methane emissions. Nature Communications 11, 5087, doi:10.1038/s41467-020-18899-3, 2020.

Vogt, P. R., Crane, K., Sundvor, E., Max, M. D. & Pfirman, S. L. Methane-Generated(Questionable) Pockmarks on Young, Thickly Sedimented Oceanic-Crust in the Arctic - Vestnesa-Ridge, Fram Strait. Geology 22, 255-258, 1994.

Waghorn, K. A., Bünz, S., Plaza-Faverola, A. and Johnson, J. E.: 3-D Seismic Investigation of a Gas Hydrate and Fluid Flow System on an Active Mid-Ocean Ridge; Svyatogor Ridge, Fram Strait, Geochemistry, Geophys. Geosystems, 19(8), 2325–2341, doi:10.1029/2018GC007482, 2018.

Waghorn, K. A., Vadakkepuliyambatta, S., Bünz, S. and Waage, M.: Crustal processes sustain Arctic abiotic gas hydrate and fluid flow systems, Sci. Rep., (0123456789), 1–14, doi:10.1038/s41598-020-67426-3, 2020.

Appendix

Station List

Location	Station Id	Date	Time (UTC)	Lat. [N] Long. [E]	Filter in Column H or hide	Water Depth [m]	Notes
Prins Karls Forland	CAGE21-1-KH-01-OilS-01	24.05	09:28	78°29.193' 10°32.315'	0	109	
Prins Karls Forland	CAGE21-1-KH-01-OilS-02	24.05	09:30	78°29.193' 10°32.316'		109	
Prins Karls Forland	CAGE21-1-KH-01-OilS-03	24.05	09:32	78°29.193' 10°32.315'		109	
Prins Karls Forland	CAGE21-1-KH-216-CTD	24.05	10:17	78°29.578' 10°31.487'		115	
Prins Karls Forland	CAGE21-1-KH-01-Dive-01	24.05	10:53	78°29.578' 10°31.487'		116	
Prins Karls Forland	CAGE21-1-KH-01_Dive01-RocC-01	24.05	11:33	78°29.563' 10°31.402'		111	
Prins Karls Forland	CAGE21-1-KH-01_Dive01-RocC-02	24.05	12:44	78°29.592' 10°31.440'		109	
Prins Karls Forland	CAGE21-1-KH-01-Dive-02	24.05	17:12	78°29.532' 10°31.488'		115	
Prins Karls Forland	CAGE21-1-KH-01_Dive02-GasS-01	24.05	17:27	78°29.510' 10°31.429'		112	

Prins Karls Forland	CAGE21-1-KH-01_Dive02-PusC-01	24.05	17:57	78°29.594' 10°31.477'	29	108	
Prins Karls Forland	CAGE21-1-KH-01_Dive02-PusC-02	24.05	18:09	78°29.594' 10°31.477'	15	108	
Prins Karls Forland	CAGE21-1-KH-217-CTD	24.05	19:01	78°29.511' 10°31.424'	8	117	
Prins Karls Forland	CAGE21-1-KH-218-CTD	24.05	19:40	78°29.520' 10°29.448'	8	106	
Prins Karls Forland	CAGE21-1-KH-219-CTD	24.05	20:16	78°29.892' 10°31.410'	8	104	
Prins Karls Forland	CAGE21-1-KH-220-CTD	24.05	20:56	78°29.502' 10°33.276'	8	110	
Prins Karls Forland	CAGE21-1-KH-221-CTD	24.05	21:28	78°29.130' 10°31.308'	8	100	
Prins Karls Forland	CAGE21-1-KH-222-CTD	24.05	23:02	78°28.300' 09°37.636'	0	393	
North Knipovich Ridge	CAGE21-1-KH-1-HF-1	25.05	04:10	78°42.237' 08°17.790'		876	
North Knipovich Ridge	CAGE21-1-KH-02-Dive-03	25.05	07:48	78°41.052' 08°15.348'		888	
North Knipovich Ridge	CAGE21-1-KH-02_Dive03-CarC-01	25.05	11:30	78°41.451' 08°17.110'		873	
North Knipovich Ridge	CAGE21-1-KH-02_Dive03-CarC-02	25.05	11:32	78°41.451' 08°17.109'		873	

North Knipovich Ridge	CAGE21-1-KH-02_Dive03-CarC-03	25.05	11:34	78°41.451' 08°17.109'		873	
North Knipovich Ridge	CAGE21-1-KH-02_Dive03-CarC-04	25.05	12:06	78°41.449' 08°17.086'		874	
North Knipovich Ridge	CAGE21-1-KH-02_Dive03-CarC-05	25.05	12:10	78°41.450' 08°17.089'		874	
North Knipovich Ridge	CAGE21-1-KH-02_Dive03-PusC-01	25.05	14:09	78°41.438' 08°17.140'	empty	873	
North Knipovich Ridge	CAGE21-1-KH-02_Dive03-PusC-02	25.05	14:24	78°41.437' 08°17.140'	15	873	
North Knipovich Ridge	CAGE21-1-KH-02_Dive03-PusC-03	25.05	14:27	78°41.438' 08°17.138'	30	872	
North Knipovich Ridge	CAGE21-1-KH-02_Dive03-PusC-04	25.05	14:30	78°41.438' 08°17.135'	37	873	
North Knipovich Ridge	CAGE21-1-KH-02_Dive03-PusC-05	25.05	14:45	78°41.439' 08°17.129'	22	874	
North Knipovich Ridge	CAGE21-1-KH-02_Dive03-PusC-06	25.05	14:47	78°41.436' 08°17.131'	empty	874	
North Knipovich Ridge	CAGE21-1-KH-02_Dive03-PusC-07	25.05	14:52	78°41.437' 08°17.137'	40	873	
North Knipovich Ridge	CAGE21-1-KH-02_Dive03-PusC-08	25.05	14:55	78°41.437' 08°17.139'	18	873	
North Knipovich Ridge	CAGE21-1-KH-02_Dive03-BlaC-01	25.05	15:12	78°41.440' 08°17.136'	10	873	

North Knipovich Ridge	CAGE21-1-KH-02_Dive03-BlaC-02	25.05	15:35	78°41.437' 08°17.140'	15	872	
North Knipovich Ridge	CAGE21-1-KH-223-CTD	25.05	18:37	78°41.052' 08°15.347'	8	905	
North Knipovich Ridge	CAGE21-1-KH-02-BC-01	25.05	19:31	78°41.049' 08°15.321'		906	
North Knipovich Ridge	CAGE21-1-KH-2-HF-1	25.05	20:47	78°42.168' 08°17.895'		876	
North Knipovich Ridge	CAGE21-1-KH-2-HF-2	25.05	22:00	78°42.103' 08°17.997'		876	
Molloy Transform	CAGE21-1-KH-3-HF-1	26.05	01:40	78°39.676' 06°29.744'		1760	
Molloy Transform	CAGE21-1-KH-4-HF-1	26.05	03:54	78°35.632' 06°21.026'		2212	
Svyatogor Ridge	CAGE21-1-KH-04-Dive-04	26.05	07:13	78°28.451' 05°40.387'		1686	
Svyatogor Ridge	CAGE21-1-KH-04_Dive04-PusC-01	26.05	08:42	78°28.470' 05°40.742'	30	1660	
Svyatogor Ridge	CAGE21-1-KH-04_Dive04-Biol-01	26.05	08:52	78°28.486' 05°40.670'		1662	
Svyatogor Ridge	CAGE21-1-KH-04-Dive-05	26.05	14:25	78°23.628' 05°05.352'		1985	
Svyatogor Ridge	CAGE21-1-KH-04_Dive05-RocC-02	26.05	15:47	78°23.578' 05°05.249'		1955	

Svyatogor Ridge	CAGE21-1-KH-04_Dive05-RocC-03	26.05	16:42	78°23.552' 05°05.005'		1927	
Svyatogor Ridge	CAGE21-1-KH-04_Dive05-PusC-02	26.05	16:48	78°23.551' 05°05.011'	21	1928	
Svyatogor Ridge	CAGE21-1-KH-04_Dive05-PusC-03	26.05	16:57	78°23.552' 05°05.003'	40	1927	
Svyatogor Ridge	CAGE21-1-KH-04_Dive05-RocC-04	26.05	17:03	78°23.552' 05°04.967'		1923	
Svyatogor Ridge	CAGE21-1-KH-224-CTD	26.05	19:21	78°28.519' 05°13.899'	370	1972	
Svyatogor Ridge	CAGE21-1-KH-04-GC-01	27.05	00:24	78°28.519' 05°13.910'	discard	1974	
Svyatogor Ridge	CAGE21-1-KH-04-GC-02	27.05	02:49	78°28.427' 05°41.345'	313	1671	
Svyatogor Ridge	CAGE21-1-KH-04-Dive-06	27.05	06:34	78°23.629' 05°05.362'		1939	
Svyatogor Ridge	CAGE21-1-KH-04_Dive06-PusC-04	27.05	11:44	78°23.551' 05°05.002'	46	1929	
Svyatogor Ridge	CAGE21-1-KH-04_Dive06-PusC-05	27.05	11:46	78°23.551' 05°05.000'	32.5	1929	
Svyatogor Ridge	CAGE21-1-KH-04_Dive06-PusC-06	27.05	11:49	78°23.552' 05°05.000'	36.5	1929	
Svyatogor Ridge	CAGE21-1-KH-04_Dive06-PusC-07	27.05	11:51	78°23.553' 05°05.002'	37	1929	

Svyatogor Ridge	CAGE21-1-KH-04_Dive06-BlaC-01	27.05	11:56	78°23.551' 05°04.991'	30	1928	
Svyatogor Ridge	CAGE21-1-KH-04_Dive06-BlaC-02	27.05	12:05	78°23.551' 05°04.989'	22	1929	
Svyatogor Ridge	CAGE21-1-KH-04-Dive-07	27.05	14:05	78°19.452' 04°57.150'		1932	
Svyatogor Ridge	CAGE21-1-KH-5-HF-1	27.05	19:44	78°18.875' 04°54.130'		2055	
Svyatogor Ridge	CAGE21-1-KH-5-HF-2	27.05	21:31	78°19.116' 04°54.686'		2028	
Svyatogor Ridge	CAGE21-1-KH-5-HF-3	27.05	22:50	78°19.359' 04°55.245'		1992	
Svyatogor Ridge	CAGE21-1-KH-5-HF-4	27.05	23:46	78°19.599' 04°55.824'		1947	
Svyatogor Ridge	CAGE21-1-KH-5-HF-5	28.05	00:37	78°19.843' 04°56.385'		1929	
Svyatogor Ridge	CAGE21-1-KH-5-HF-6	28.05	01:49	78°20.087' 04°56.946'		1942	
Svyatogor Ridge	CAGE21-1-KH-5-HF-7	28.05	02:22	78°20.330' 04°57.508'		1960	
Svyatogor Ridge	CAGE21-1-KH-5-HF-8	28.05	03:10	78°20.574' 04°58.069'		1974	
Svyatogor Ridge	CAGE21-1-KH-6-HF-1	28.05	04:54	78°22.522' 05°02.602'		1971	

Svyatogor Ridge	CAGE21-1-KH-6-HF-2	28.05	05:52	78°22.763' 05°03.159'		1937	discard
Svyatogor Ridge	CAGE21-1-KH-6-HF-3	28.05	07:05	78°23.011' 05°03.708'		1880	
Svyatogor Ridge	CAGE21-1-KH-6-HF-4	28.05	08:03	78°23.253' 05°04.293'		1848	
Svyatogor Ridge	CAGE21-1-KH-6-HF-5	28.05	09:00	78°23.496' 05°04.858'		1947	
Svyatogor Ridge	CAGE21-1-KH-6-HF-6	28.05	10:18	78°23.741' 05°05.423'		2039	
Svyatogor Ridge	CAGE21-1-KH-6-HF-7	28.05	11:10	78°23.978' 05°06.000'		2052	
Svyatogor Ridge	CAGE21-1-KH-04-Dive-08	28.05	12:49	78°23.551' 05°05.010'		1893	
Svyatogor Ridge	CAGE21-1-KH-04_Dive08-VMap-01	28.05	13:57	78°23.556' 05°05.088'		1938	
Svyatogor Ridge	CAGE21-1-KH-04_Dive08-BlaC-03	28.05	18:15	78°23.550' 05°05.007'		1929	
Svyatogor Ridge	CAGE21-1-KH-04-GC-03	28.05	20:44	78°23.543' 05°04.952'		1893	
Svyatogor Ridge	CAGE21-1-KH-04-GC-04	28.05	22:27	78°23.543' 05°04.951'	298	1893	
Svyatogor Ridge	CAGE21-1-KH-7-HF-1	29.05	01:14	78°17.906' 04°51.921'		2248	

North Knipovich Ridge	CAGE21-1-KH-02-Dive-09	29.05	07:13	78°41.420' 08°17.184'		873	
North Knipovich Ridge	CAGE21-1-KH-02_Dive09-VMap-01	29.05	07:49	78°41.448' 08°17.118'		871	
North Knipovich Ridge	CAGE21-1-KH-02_Dive10-CarC-06	29.05	15:50	78°39.945' 08°14.903'		912	
North Knipovich Ridge	CAGE21-1-KH-02-Dive-10	29.05	16:40	78°39.888' 08°14.522'		922	
North Knipovich Ridge	CAGE21-1-KH-02_Dive10-CarC-08	29.05	16:51	78°39.937' 08°14.894'		914	ROV Carbonate Crust Collection - Bivalves
North Knipovich Ridge	CAGE21-1-KH-02_Dive10-CarC-09	29.05	17:08	78°39.939' 08°14.898'		914	
North Knipovich Ridge	CAGE21-1-KH-02_Dive10-CarC-10	29.05	17:24	78°39.943' 08°14.908'		911	
Prins Karls Forland	CAGE21-1-KH-01-GC-01	31.05	03:05	78°29.513' 10°31.434'	40	116	
Prins Karls Forland	CAGE21-1-KH-01-GC-02	31.05	03:42	78°29.513' 10°31.434'	105	116	
Prins Karls Forland	CAGE21-1-KH-01-GC-03	31.05	04:17	78°29.594' 10°31.477'	13	112	
Prins Karls Forland	CAGE21-1-KH-01-GC-04	31.05	04:48	78°29.575' 10°31.382'	Empty	114	
Prins Karls Forland	CAGE21-1-KH-01-Dive-11	31.05	07:08	78°29.513' 10°31.435'		116	

Prins Karls Forland	CAGE21-1-KH-01_Dive11-VMap-01	31.05	07:51	78°29.559' 10°31.369'		112	
Prins Karls Forland	CAGE21-1-KH-01-Dive-12	31.05	10:35	78°29.565' 10°31.373'		113	ROV Dive - First and second attempts unsuccessful. Microbial mat
Prins Karls Forland	CAGE21-1-KH-01_Dive12-PusC-03	31.05	11:19	78°29.563' 10°31.395'		113	ROV Push Core - Reference
Prins Karls Forland	CAGE21-1-KH-01_Dive12-PusC-04	31.05	11:24	78°29.563' 10°31.397'		113	ROV Push Core - Microbial mat
Prins Karls Forland	CAGE21-1-KH-01_Dive12-PusC-05	31.05	11:32	78°29.562' 10°31.404'		113	ROV Push Core - Microbial mat, intense bubbling
Prins Karls Forland	CAGE21-1-KH-01_Dive12-PusC-06	31.05	11:38	78°29.563' 10°31.398'		113	ROV Push Core - Reference
Prins Karls Forland	CAGE21-1-KH-01_Dive12-BlaC-01	31.05	11:49	78°29.562' 10°31.410'		113	
Prins Karls Forland	CAGE21-1-KH-01_Dive12-BlaC-02	31.05	11:59	78°29.563' 10°31.395'		113	
North Knipovich Ridge	CAGE21-1-KH-02-Dive-13	31.05	16:18	78°41.058' 08°16.861'		880	
North Knipovich Ridge	CAGE21-1-KH-02_Dive13-CarC-11	31.05	17:40	78°41.044' 08°16.892'		875	
North Knipovich Ridge	CAGE21-1-KH-02_Dive13-CarC-12	31.05	17:52	78°41.057' 08°16.942'		874	ROV Carbonate Crust Collection -

							On top of mound
North Knipovich Ridge	CAGE21-1-KH-02_Dive13-PusC-09	31.05	18:14	78°41.069' 08°16.733'		877	ROV Push Core - On top of bound
North Knipovich Ridge	CAGE21-1-KH-02_Dive13-PusC-10	31.05	18:20	78°41.071' 08°16.675'		877	ROV Push Core - Dense bacterial mat
North Knipovich Ridge	CAGE21-1-KH-02_Dive13-PusC-11	31.05	18:29	78°41.058' 08°16.625'		874	
North Knipovich Ridge	CAGE21-1-KH-02_Dive13-BlaC-03	31.05	18:42	78°41.045' 08°16.843'		872	
North Knipovich Ridge	CAGE21-1-KH-02_Dive13-BlaC-04	31.05	18:48	78°41.045' 08°16.845'		872	
Storfjorden	CAGE21-1-KH-01-Dive-14	02.06	01:21	77°09.716' 19°11.131'		157	
Storfjorden	CAGE21-1-KH-01-OBS-STOR2-Rec	02.06	02:11	77°09.692' 19°11.044'		153	
Sørkapp Basin	CAGE21-1-KH-225-CTD	02.06	17:14	75°31.179' 20°48.442'		50	
Leirdjupet Fault Complex	CAGE21-1-KH-226-CTD	03.06	05:03	73°54.805' 20°55.203'		346	
Leirdjupet Fault Complex	CAGE21-1-KH-05-Dive-15	03.06	06:40	73°54.804' 20°55.202'		347	
Leirdjupet Fault Complex	CAGE21-1-KH-05_Dive15-GasS-01	03.06	10:29	73°54.803' 20°55.176'		351	

Leirdjupet Fault Complex	CAGE21-1-KH-05_Dive15-PusC-01	03.06	11:05	73°54.801' 20°55.182'	27.5	351	
Leirdjupet Fault Complex	CAGE21-1-KH-05_Dive15-PusC-02	03.06	11:09	73°54.802' 20°55.182'	24	351	
Leirdjupet Fault Complex	CAGE21-1-KH-05_Dive15-PusC-03	03.06	11:17	73°54.800' 20°55.181'	5	350	
Leirdjupet Fault Complex	CAGE21-1-KH-05_Dive15-PusC-04	03.06	11:23	73°54.800' 20°55.179'	21	350	
Leirdjupet Fault Complex	CAGE21-1-KH-05-Dive-16	03.06	12:36	73°54.801' 20°55.177'		345	
Leirdjupet Fault Complex	CAGE21-1-KH-05_Dive16-VMap-01	03.06	13:02	73°54.804' 20°55.164'		349	
Leirdjupet Fault Complex	CAGE21-1-KH-05_Dive16-BlaC-01	03.06	14:41	73°54.803' 20°55.181'	15	351	
Leirdjupet Fault Complex	CAGE21-1-KH-05_Dive16-BlaC-02	03.06	14:50	73°54.803' 20°55.190'	21	352	
Leirdjupet Fault Complex	CAGE21-1-KH-05-Dive-17	03.06	16:25	74°00.856' 21°04.256'		291	
Leirdjupet Fault Complex	CAGE21-1-KH-05-GC-01	03.06	19:36	73°54.806' 20°55.178'	75	351	
Leirdjupet Fault Complex	CAGE21-1-KH-05-Dive-18	04.06	06:31	74°00.846' 21°04.676'		296	
Leirdjupet Fault Complex	CAGE21-1-KH-05_Dive18-VMap-02	04.06	08:20	74°00.879' 21°04.687'		297	

Leirdjupet Fault Complex	CAGE21-1-KH-05-Dive-19	04.06	12:40	74°00.847' 21°04.678'		296	
Leirdjupet Fault Complex	CAGE21-1-KH-05_Dive19-GasS-02	04.06	13:00	74°00.851' 21°04.666'		296	
Leirdjupet Fault Complex	CAGE21-1-KH-05_Dive19-CarC-01	04.06	13:07	74°00.850' 21°04.669'		296	
Leirdjupet Fault Complex	CAGE21-1-KH-05_Dive19-CarC-02	04.06	13:11	74°00.849' 21°04.671'		296	
Leirdjupet Fault Complex	CAGE21-1-KH-05_Dive19-CarC-03	04.06	13:23	74°00.852' 21°04.674'		297	
Leirdjupet Fault Complex	CAGE21-1-KH-05_Dive19-GasS-03	04.06	13:34	74°00.875' 21°04.696'		297	
Leirdjupet Fault Complex	CAGE21-1-KH-05_Dive19-CarC-04	04.06	13:37	74°00.873' 21°04.690'		297	
Leirdjupet Fault Complex	CAGE21-1-KH-05_Dive19-CarC-05	04.06	13:40	74°00.873' 21°04.691'		297	
Leirdjupet Fault Complex	CAGE21-1-KH-227-CTD	04.06	15:34	74°00.848' 21°04.974'	4	292	
Leirdjupet Fault Complex	CAGE21-1-KH-228-CTD	04.06	16:20	74°00.869' 21°04.790'	6	297	
Leirdjupet Fault Complex	CAGE21-1-KH-229-CTD	04.06	16:56	74°00.904' 21°04.726'	6	292	
Leirdjupet Fault Complex	CAGE21-1-KH-230-CTD	04.06	17:23	74°00.885' 21°04.606'	6	293	

Leirdjupet Fault Complex	CAGE21-1-KH-231-CTD	04.06	17:52	74°00.872' 21°04.697'	6	299	Over carbonate bank and bubbles
Leirdjupet Fault Complex	CAGE21-1-KH-232-CTD	04.06	18:21	74°00.847' 21°04.680'	6	294	Over carbonate bank and bubbles
Leirdjupet Fault Complex	CAGE21-1-KH-233-CTD	04.06	18:50	74°00.812' 21°04.650'	6	292	
Leirdjupet Fault Complex	CAGE21-1-KH-05-Dive-20	05.06	06:43	74°00.846' 21°04.681'		293	
Leirdjupet Fault Complex	CAGE21-1-KH-05_Dive20-BubQ-01	05.06	07:04	74°00.852' 21°04.670'		296	
Leirdjupet Fault Complex	CAGE21-1-KH-05_Dive20-BubQ-02	05.06	07:39	74°00.872' 21°04.691'		297	
Leirdjupet Fault Complex	CAGE21-1-KH-05_Dive20-BubQ-03	05.06	08:07	74°00.873' 21°04.690'		298	
Leirdjupet Fault Complex	CAGE21-1-KH-05-Dive-21	05.06	10:30	73°55.019' 20°56.123'		348	
Leirdjupet Fault Complex	CAGE21-1-KH-05_Dive21-PusC-05	05.06	12:58	73°55.033'	7	345	
Leirdjupet Fault Complex	CAGE21-1-KH-05_Dive21-PusC-06	05.06	13:02	73°55.034' 20°56.031'	33	345	
Leirdjupet Fault Complex	CAGE21-1-KH-05_Dive21-PusC-07	05.06	13:07	73°55.034' 20°56.030'	17	345	
Leirdjupet Fault Complex	CAGE21-1-KH-05_Dive21-PusC-08	05.06	13:14	73°55.031' 20°56.032'	37	344	

Leirdjupet Fault Complex	CAGE21-1-KH-05-Dive-22	05.06	13:40	73°55.032' 20°56.060'		345	
Leirdjupet Fault Complex	CAGE21-1-KH-05_DIve22-BlaC-03	05.06	14:04	73°55.033'	10	344	
Leirdjupet Fault Complex	CAGE21-1-KH-05_DIve22-BlaC-04	05.06	14:08	73°55.033' 20°56.045'	7	344	
Håkon Mosby Mud Volcano	CAGE21-1-KH-06-Dive-23	06.06	07:56	71°59.997' 14°43.592'	20	1266	
Håkon Mosby Mud Volcano	CAGE21-1-KH-06_Dive23-BlaC-01	06.06	13:10	72°00.054' 14°44.144'	39	1260	ROV Blade Core - Siboglinid field
Håkon Mosby Mud Volcano	CAGE21-1-KH-06_Dive23-PusC-01	06.06	13:17	72°00.054' 14°44.143'	24	1260	
Håkon Mosby Mud Volcano	CAGE21-1-KH-06_Dive23-BlaC-02	06.06	13:48	72°00.179' 14°43.820'	38	1256	
Håkon Mosby Mud Volcano	CAGE21-1-KH-06_Dive23-PusC-02	06.06	13:56	72°00.182' 14°43.807'	37	1255	
Håkon Mosby Mud Volcano	CAGE21-1-KH-06_Dive23-PusC-03	06.06	14:03	72°00.183' 14°43.814'	48	1255	
Håkon Mosby Mud Volcano	CAGE21-1-KH-06_Dive23-PusC-04	06.06	14:11	72°00.184' 14°43.806'	discard	1256	
Håkon Mosby Mud Volcano	CAGE21-1-KH-06_Dive23-BlaC-03	06.06	14:55	72°00.259' 14°43.471'	15	1254	

Håkon Mosby Mud Volcano	CAGE21-1-KH-06_Dive23-PusC-05	06.06	15:05	72°00.260' 14°43.471'	42	1254	
Håkon Mosby Mud Volcano	CAGE21-1-KH-06_Dive23-PusC-06	06.06	15:14	72°00.261' 14°43.469'	47	1252	
Håkon Mosby Mud Volcano	CAGE21-1-KH-06-BC-01	06.06	22:44	72°01.048' 14°42.222'		1266	
Håkon Mosby Mud Volcano	CAGE21-1-KH-234-CTD	06.06	23:48	72°01.074' 14°42.224'		1271	
Håkon Mosby Mud Volcano	CAGE21-1-KH-06-GC-01	07.06	00:46	72°01.068' 14°42.214'	513	1272	
Håkon Mosby Mud Volcano	CAGE21-1-KH-06-GC-02	07.06	02:24	72°00.170' 14°43.849'	320	1261	Soupy sediments, section #1 is in plastic bag
Håkon Mosby Mud Volcano	CAGE21-1-KH-06-GC-03	07.06	03:38	72°00.170' 14°43.849'	320	1261	Soupy sediments, section #1 is in plastic bag
Håkon Mosby Mud Volcano	CAGE21-1-KH-06-Dive-24	07.06	07:16	72°01.074' 14°42.200'		1271	
Håkon Mosby Mud Volcano	CAGE21-1-KH-06_Dive24-BlaC-04	07.06	08:14	72°01.079' 14°42.212'	15(?)	1262	ROV Blade Core - reference
Håkon Mosby Mud Volcano	CAGE21-1-KH-06_Dive24-PusC-07	07.06	08:18	72°01.078' 14°42.210'	46	1262	ROV Push Core - reference
Håkon Mosby Mud Volcano	CAGE21-1-KH-06_Dive24-PusC-08	07.06	08:22	72°01.078' 14°42.208'	29	1262	ROV Push Core - reference

Håkon Mosby Mud Volcano	CAGE21-1-KH-06_Dive24-PusC-09	07.06	08:26	72°01.077' 14°42.205'	18	1263	ROV Push Core - reference
Håkon Mosby Mud Volcano	CAGE21-1-KH-06-Dive-25	07.06	09:53	72°00.540' 14°43.060'		1272	
Håkon Mosby Mud Volcano	CAGE21-1-KH-06_Dive25-CarC-01	07.06	16:08	72°00.310' 14°43.920'		1249	
Håkon Mosby Mud Volcano	CAGE21-1-KH-06_Dive25-CarC-02	07.06	16:11	72°00.310' 14°43.922'		1250	
Håkon Mosby Mud Volcano	CAGE21-1-KH-06_Dive25-PusC-10	07.06	16:16	72°00.309' 14°43.920'	30	1250	
Håkon Mosby Mud Volcano	CAGE21-1-KH-06_Dive25-PusC-11	07.06	16:21	72°00.312' 14°43.917'	20	1251	ROV Push Core - mat
Håkon Mosby Mud Volcano	CAGE21-1-KH-06_Dive25-BlaC-05	07.06	16:32	72°00.312' 14°43.924'	15	1252	ROV Blade Core - mat
Håkon Mosby Mud Volcano	CAGE21-1-KH-06_Dive25-PusC-12	07.06	16:54	72°00.314' 14°43.923'	13	1252	ROV Push Core - mat
Håkon Mosby Mud Volcano	CAGE21-1-KH-06_Dive25-PusC-13	07.06	17:06	72°00.316' 14°43.941'	30	1252	ROV Push Core - tubeworms
Håkon Mosby Mud Volcano	CAGE21-1-KH-06-GC-04	07.06	18:22	72°00.331' 14°43.516'	Empty	1260	
Håkon Mosby Mud Volcano	CAGE21-1-KH-06-GC-05	07.06	19:54	72°00.395'	Not collected	1258	

Håkon Mosby Mud Volcano	CAGE21-1-KH-06-Dive-26	08.06	07:08	72°00.395' 14°43.730'		1257	
Håkon Mosby Mud Volcano	CAGE21-1-KH-06-VMap-01	08.06	09:10	72°00.390' 14°43.533'		1250	

Line List

Location	Line ID	Date	Time (UTC) START	Lat. [N] Long. [E] START	Time (UTC) STOP	Lat. [N] Long. [E] STOP	Comments
Leirdjupet Fault Complex	CAGE21-1-KH-001-CHIRP	04.06	20:39	07°48.060' 21°23.975'	21:44	74°13.265' 21°14.645'	file 20210604203926 and 20210604212711
Leirdjupet Fault Complex	CAGE21-1-KH-002-CHIRP	04.06	21:49	74°13.068' 21°13.799'	22:55	07°48.227' 21°22.533'	file 20210604214937 and 20210604224249
Leirdjupet Fault Complex	CAGE21-1-KH-003-CHIRP	04.06	23:00	07°48.152' 21°21.436'	00:04 +1 day	74°12.952' 21°12.558'	file 20210604230043 and 20210604235443
Leirdjupet Fault Complex	CAGE21-1-KH-004-CHIRP	05.06	00:10	74°12.746' 21°11.674'	01:14	07°48.137' 21°19.823'	file 20210605001035 and 20210605010840
Leirdjupet Fault Complex	CAGE21-1-KH-005-CHIRP	05.06	01:29	07°47.737' 21°16.548'	02:31	74°12.252' 02°17.807'	file 20210605012849
Leirdjupet Fault Complex	CAGE21-1-KH-006-CHIRP	05.06	02:38	74°12.152' 02°16.482'	03:33	07°47.610' 21°14.889'	File 20210605023246

Leirdjupet Fault Complex	CAGE21-1-KH-007-CHIRP	05.06	03:36	07°47.353' 21°14.175'	04:27	74°11.884' 02°15.315'	File 20210605033614
Leirdjupet Fault Complex	CAGE21-1-KH-008-CHIRP	05.06	04:31	74°11.928' 02°13.934'	05:22	07°47.125' 21°12.489'	File 20210605043027
Håkon Mosby Mud Volcano	CAGE21-1-KH-009-CHIRP	07.06	23:41	71°59.279' 14°57.144'	01:10	71°55.075' 14°37.767'	file 20210607234046
Håkon Mosby Mud Volcano	CAGE21-1-KH-010-CHIRP	08.06	01:23	71°55.783' 14°36.353'	02:46	71°59.815' 14°54.577'	File 20210608014906. Incomplete d/t eqpt. failure
Håkon Mosby Mud Volcano	CAGE21-1-KH-011-CHIRP	08.06	03:12	71°59.856' 14°50.148'	03:43	71°58.383' 14°43.391'	File 20210608031136

Details on processing and sub-sampling of sediment cores

	Superstation	ROV Dive No.	Local station	Activity	Latitude	Longitude	Water depth (m)	Recovery (cm)	Comments	Pore water	Headspace gas	Sliced	frozen blade core (half or whole)	Micropalaeont olgy	Meiofauna	Macrofauna	Microbiology	Frozen
LEG 1	**1**	2	1	PusC1	78,4932	10,5246	107,9	29	Microbial mat	x	x	x		x			x	
	1	2	2	PusC2	78,4932	10,5246	108,15	15	Microbial mat	x	x	x		x			x	
	2	3	1	PusC1	78,6906	8,2857	872,8	empty	Microbial mat								x	
	2	3	2	PusC2	78,6906	8,2856	872,65	15	Microbial mat	x	x	x		x			x	
	2	3	3	PusC3	78,6906	8,2856	871,6	30	Microbial mat	x		x		x			x	
	2	3	4	PusC4	78,6906	8,2856	873,53	37	background/tubeworms?	x	x			x			x	
	2	3	5	PusC5	78,6906	8,2855	874,2	22	background/tubeworms?	x								
	2	3	6	PusC6	78,6906	8,2855	874,27	empty	background/tubeworms?									
	2	3	7	PusC7	78,6906	8,2856	873,41	40	tubeworms	x		x					x	
	2	3	8	PusC8	78,6906	8,2856	873,02	18	tubeworms+mat	x		x					x	
	2	3	1	BlaC1	78,6907	8,2856	872,65	10	Microbial mat			x mixed						
	2	3	2	BlaC2	78,6906	8,2857	872	15	Microbial mat, pebbles	x				x				x
	2		1	Box Core	78,68414	8,2553	906											
	4	4	1	PusC1	78,4745	5,679	1660	30	reference	x								
	4	5	2	PusC2	78,3925	5,0835	1927	21	Microbial mat	x	x	x					x	
	4	5	3	PusC3	78,3925	5,0834	1925,67	40	Microbial mat	x	x	x		x			x	
	4		1	GC1	78,4753	5,2318	1974	370		x	x							x

	4		2	GC2	78,4738	5,6891	1671	313		x	x						
	4	6	4	PusC4	78,3925	5,0834	1928	46	Microbial mat	x	x	x		x		x	x
	4	6	5	PusC5	78,3925	5,0833	1928	32,5	tubeworms		x	x		x		x	x
	4	6	6	PusC6	78,3925	5,0833	1927,55	36,5	tubeworms	x	x						
	4	6	7	PusC7	78,3925	5,0834	1928	37	reference	x	x	x		x		x	x
	4	6	1	BlaC1	78,3925	5,0832	1927,6	30	Microbial mat				x			x	
	4	6	2	BlaC2	78,3925	5,0831	1927,46	22	tubeworms				x	x		x	
	4	8	3	BlaC3	78,3925	5,083455	1929	21,5		x			x	x		x	
	4		3	GC3	78,3924	5,0825	1893	208	PW, gas, Sr isotopes, 4C	x	x						
	4		4	GC4	78,3924	5,0825	1893	298	no samples, kept frozen								x
LEG 2	**1**		1	GC1	78,49189	10,52391	116	40	0-14 interval in a ziplock bag at -20C.Shells on top.								x
	1		2	GC2	78,49188	10,52391	116	105	0-5 interval in a ziplock bag at -20C. Collected pore water. Shells on top.	x							
	1		3	GC3	78,49323	10,52462	112	13	in ziplock bag at -20C. Shells on top.	x							
	1	12	3	Pusc3	78,4927	10,5232	111,81	48	Microbial mat			x			x		
	1	12	4	Pusc4	78,4927	10,5233	111,7	6	reference								
	1	12	5	Pusc 5	78,4927	10,5234	112,13	39	Microbial mat			x			x		
	1	12	6	Pusc 6	78,4927	10,5233	111,88	40	Microbial mat, intense bubbling	x	x	x			x		

1	12	1	BlaC1	78,4927	10,5235	111,55	14	reference						x		
1	12	2	BlaC2	78,4927	10,5233	112	30	reference	x		x	x		x		
2	13	9	Pusc9	78,6845	8,2789	877	53	ref			x			x		
2	13	10	Pusc10	78,6845	8,2779	877	44	ref	x		x			x		
2	13	11	Pusc 11	78,6843	8,2771	874	24	mat			x			x	x	
2	13	3	BlaC3	78,6841	8,2807	872	7	mat	x		x		x	x	x	
2	13	4	BlaC4	78,6841	8,2807	872	27	mat			x		x	x		
5	15	1	Pusc1	73,9134	20,9197	349,9	27,5	mat	x		x					
5	15	2	Pusc2	73,9134	20,9197	349,66	24	mat	x		x			x		
5	15	3	Pusc3	73,9133	20,9197	349,51	5	mat. Put in a ziplock bag and frozen.			x			x		
5	15	4	Pusc4	73,9133	20,9196	348,21	21	reference	x		x			x		
5	16	1	Blac1	73,9134	20,9197	349,82	15	mat	x		x	x	x	x		
5	16	2	Blac2	73,9134	20,9198	350,19	21	reference	x		x		x	x		
5		1	GC1	73,91344	20,91964	351	75	0-5 cm in a ziplock bag and frozen.	x	x						x
5	21	5	PusC5	73,9134	20,9197	349,92	7	mat	x		x			x		
5	21	6	PusC6	73,9134	20,9197	349,66	33	mat	x		x			x		
5	21	7	PusC7	73,9133	20,9197	349,51	17	mat	x		x			x		
5	21	8	PusC8	73,9133	20,9196	348	37	reference	x		x			x		
5	22	3	Blac3	73,9134	20,9197	349,82	10	no PW			x		x	x		
5	22	4	Blac4	73,9134	20,9198	350,19	7	7 to 17 cm, asymmetric. No PW			x			x		
6	23	1	Blac1	72,0009	14,7357	1260	20	reference				x	x	x	x	

6	23	1	PusC1	72,0009	14,7357	1260	39	reference	x		x						
6	23	2	BlaC2	72,0030	14,7303	1256	24	Microbial mat			x mixed	x	x	x	x	x	
6	23	2	PusC2	72,0030	14,7301	1255	38	Microbial mat	x		x			x			
6	23	3	PusC3	72,0030	14,7302	1255	37	Microbial mat	x		x			x			
6	23	4	PusC4	72,0031	14,7301	1256	48	Microbial mat	x		x			x			
6	23	3	BlaC3	72,0043	14,7245	1254	15	Microbial mat					x	x	x	x	
6	23	5	PusC5	72,0043	14,7245	1254	42	Microbial mat									
6	23	6	PusC6	72,0044	14,7245	1252	47	Microbial mat	x		x						
6		1	box core	72,0175	14,7037	1266		reference					x				
6		1	GC1	72,0178	14,70357	1272	513	reference	x	x							
6		2	GC2	72,00283	14,73081	1261	300	gassy, soupy sediment due to hydrate destabilization		x							x
6		3	GC3	72,00283	14,73082	1261	320	no PW. Frozen									x
6	24	4	BlaC4	72,01798	14,70353	1262	15(?)	reference			x		x	x	x		
6	24	7	PusC7	72,01797	14,7035	1262	46	reference	x		x			x			
6	24	8	PusC8	72,01797	14,70347	1262	29	reference			x			x	x		
6	24	9	PusC9	72,01795	14,70342	1263	18	reference	x		x			x			
6	25	10	Pusc10	72,00515	14,73201	1250	30	tubeworms, next to MDAC slab	x		x						
6	25	11	PusC11	72,00521	14,73196	1251	20	Microbial mat	x		x			x			
6	25	5	BlaC5	72,00521	14,73206	1252	15	Microbial mat			x mixed		x		x		
6	25	12	PusC12	72,00523	14,73204	1252	13	Microbial mat			x			x			
6	25	13	PusC13	72,00527	14,73235	1252	30	tubeworms	x		x						